UNIVERSIDADE FEDERAL DE SANTA CATARINA
CENTRO TECNOLÓGICO
PROGRAMA DE PÓS-GRADUAÇÃO EM ENGENHARIA QUÍMICA

Heloísa Bremm Madalosso

Modification of commercial polymeric membranes via electrospraying for membrane distillation applications aiming to water recovery from textile wastewater

Florianópolis, SC, Brasil
2021

Heloísa Bremm Madalosso

Modification of commercial polymeric membranes via electrospraying for membrane distillation applications aiming to water recovery from textile wastewater

Dissertação submetida ao Programa de Pós-Graduação em Engenharia Química da Universidade Federal de Santa Catarina para a obtenção do título de Mestre em Engenharia Química.
Orientadora: Prof.ª Dr.ª Cintia Marangoni
Coorientador: Prof. Dr. Ricardo Antonio Francisco Machado

Florianópolis, SC, Brazil
2021

Ficha de identificação da obra elaborada pelo autor,
através do Programa de Geração Automática da Biblioteca Universitária da UFSC.

Madalosso, Heloísa Bremm
Modification of commercial polymeric membranes via electrospraying for membrane distillation applications aiming to water recovery from textile wastewater / Heloísa Bremm Madalosso ; orientadora, Cintia Marangoni, coorientador, Ricardo Antonio Francisco Machado, 2021.
166 p.

Dissertação (mestrado) - Universidade Federal de Santa Catarina, Centro Tecnológico, Programa de Pós-Graduação em Engenharia Química, Florianópolis, 2021.

Inclui referências.

1. Engenharia Química. 2. Modificação de membranas poliméricas. 3. Electrospraying. 4. Efluente têxtil. 5. Destilação por Membranas por Contato Direto. I. Marangoni, Cintia . II. Machado, Ricardo Antonio Francisco. III. Universidade Federal de Santa Catarina. Programa de Pós Graduação em Engenharia Química. IV. Título.

Heloísa Bremm Madalosso

Modification of commercial polymeric membranes via electrospraying for membrane distillation applications aiming to water recovery from textile wastewater

O presente trabalho em nível de Mestrado foi avaliado e aprovado por banca examinadora composta pelos seguintes membros:

Prof. Luiz Fernando Belchior, Dr.
Universidade Federal de Santa Catarina - UFSC

Prof. Dachamir Hotza, Dr.
Universidade Federal de Santa Catarina - UFSC

Certificamos que esta é a **versão original e final** do trabalho de conclusão que foi julgado adequado para obtenção do título de Mestre em Engenharia Química.

Documento assinado digitalmente
Debora de Oliveira
Data: 19/04/2021 11:09:58-0300
CPF: 728.453.929-15
Verifique as assinaturas em https://v.ufsc.br

Coordenação do Programa de Pós-Graduação

Documento assinado digitalmente
Cintia Marangoni
Data: 19/04/2021 10:48:40-0300
CPF: 947.521.849-15
Verifique as assinaturas em https://v.ufsc.br

Prof.ª Cintia Marangoni, Dr.ª
Orientadora

Florianópolis, SC, Brasil.
2021

Para Inacio Madalosso (*in memoriam*), que certamente amaria ver sua filha se tornar mestra.

ACKNOWLEDGEMENTS

Esta dissertação foi uma caminhada construída em meio à um período de severos problemas sanitários e políticos no Brasil. Não foi, de forma alguma, uma caminhada solitária. Por essa razão, eu agradeço:

À minha mãe Cleusa, minha maior incentivadora na busca de conhecimentos e de superações como ser humano; a pessoa que mais acredita em mim neste mundo.

Ao meu pai Inácio, minha grande inspiração na busca por mim mesma nas caminhadas que assumo nesta vida. Queria poder ter tido mais tempo pra poder compartilhar esta contigo.

À minha vó, Estanislava Madalosso, de quem me despedi durante esta caminhada, por todo amor e fé.

Ao Maurício, por tanta doação, compreensão e amor compartilhados mesmo nos momentos mais difíceis.

Aos meus orientadores Prof.ª Dr.ª Cintia e Prof. Dr. Ricardo, pelos conhecimentos partilhados, e principalmente pela confiança a mim concedida.

Aos meus tios, Clair e Rui, pelo zelo e amor de sempre.

Aos meus amigos Thiago Ouriques, Camila Guindani e Jeovandro Beltrame, pelas inúmeras contribuições e partilhas, principalmente durante nossos cafés na Copa do LCP1. Agradeço pela amizade, parceria e pela inspiração.

Às colegas Bianca, Regilene e Heloisa, pela amizade e por toda a ajuda concedida.

À Joceane, a grande amiga que fiz nessa caminhada.

À Central de Análises do Departamento de Engenharia Química e Alimentos da UFSC, pela estrutura concedida, e especialmente, ao Leandro e à Fernanda, pela agilidade nas análises, eficiência e prestatividade.

Ao Laboratório de Materiais do Departamento de Engenharia de Materiais da UFSC, pela estrutura concedida e pela parceria gerada para realização deste trabalho. Em especial, ao Prof. Dr. Cristiano Binder, pelas análises de MEV concedidas, e à Patrícia, pela execução das mesmas com grande prestatividade. Ao Gabriel Araújo, pela grande disponibilidade em realizar as análises de ângulo de contato.

Ao Laboratório de Processamento de Cerâmicas (PROCER), pela estrutura concedida para a execução deste trabalho.

Ao Prof. Dr. Marco di Luccio e ao Guilherme, pela doação de reagentes.

À Catiane, Leopoldo, Vicente e Ana Clara, por serem também a minha família em Florianópolis.

À Flávia, por ter transformado esta caminhada em uma experiência para dentro de mim mesma.

Ao Departamento de Engenharia Química e Alimentos da UFSC, pela estrutura e suporte, essenciais para a realização deste trabalho.

Aos membros da banca, pelas contribuições de melhoria para este trabalho.

À Coordenação de Aperfeiçoamento de Pessoal de Nível Superior (CAPES), pelo apoio financeiro.

RESUMO

A complexidade do efluente têxtil, relacionada a grande quantidade de solutos em sua composição, faz com que processos convencionais de tratamento não apresentem completa degradação e gerem um volume crítico de lama, além de baixa qualidade da água resultante. O processo de Destilação por Membranas (DM) apresenta-se como uma alternativa promissora para a recuperação e reinserção da água deste efluente no processo, visto que possibilita a utilização de calor residual do processo de tingimento, resultando em um permeado de alta qualidade. Entretanto, alguns desafios para a consolidação desta tecnologia persistem, relacionados a fenômenos do processo, como a incrustação e o molhamento. A baixa resistência ao molhamento das membranas comerciais faz com que a DM ainda não seja capaz de ser aplicada à totalidade de componentes dos efluentes têxteis, como algumas classes de corantes e aditivos utilizados, como surfactantes. Neste contexto, este trabalho visou a modificação de membranas comerciais de poliamida (PA) e polipropileno (PP) utilizando a técnica de electrospraying, com blendas poliméricas contendo PVDF, PDMS com ou sem agente de cura e nanopartículas de sílica, em solução de THF:DMF 1:1, com o intuito de aumentar a hidrofobicidade e a resistência ao molhamento. A influência da concentração de polímero, cura do polímero, tempo de exposição sob o spray e concentração de nanopartículas de sílica na hidrofobicidade das membranas foram avaliadas. Ângulos de contato de 167,13º e 144,07º foram obtidos para as membranas de PA e PP, respectivamente, e estas foram caracterizadas em termos de estrutura morfológica e química (FTIR, MEV, EDX), estudo térmico (DSC), espessura, porosidade, ângulo de contato com diferentes soluções e Potencial Zeta. O potencial de remoção das membranas modificadas foi avaliado em operações de Destilação por Membranas por Contato Direto (DCDM), durante 4 h, em condições operacionais fixas. A membrana modificada de PP com a solução de porcentagem mássica 2% PVDF e 6% Sylgard (PDMS curado) foi testada com quatro diferentes classes de corantes utilizados industrialmente (reativo, disperso, direto e ácido), e apresentou fluxos de 29,7, 44,85, 29,79 e 35,41 kg m^{-2} h^{-1}, respectivamente, com redução máxima de 11,6% em relação ao fluxo da membrana de PP pura. As taxas de rejeição obtidas para a membrana modificada foram maiores que 95%, e maiores que as taxas de rejeição da membrana pura com as diferentes classes de corantes. A cura do polímero PDMS, combinada com a estrutura rugosa obtida através do electrospraying, diminuiu o potencial zeta da membrana modificada na faixa de pH das soluções testadas, contribuindo para uma maior resistência ao molhamento e maior potencial de remoção de corantes. A membrana modificada de PA com a solução de porcentagem mássica 2% PVDF, 10% PDMS e 20% de nanopartículas de sílica apresentou fluxos mais baixos devido sua estrutura densa. Foi testada com os componentes do banho de tingimento de algodão (corante preto reativo e surfactante), resultando em fluxo de 0,6 e 0,39 kg m^{-2} h^{-1}, respectivamente, e em taxas de rejeição superiores ao da PA pura. Este aspecto foi observado principalmente com a solução de surfactante, onde o início do molhamento foi evidenciado na membrana de PA pura. A membrana modificada de PA apresentou uma propriedade anti-incrustante mediante à deposição de corante em sua superfície. A modificação de membranas comerciais visando a criação de estruturas mais hidrofóbicas viabilizou a operação DCMD com diferentes classes de corantes e soluções de baixa tensão superficial (surfactante), com maior resistência ao molhamento e maior potencial de remoção de corante, sem comprometer a estrutura química e morfológica das membranas. Neste trabalho, a modificação das membranas comprovou a potencialidade do processo DCMD para recuperação de água de soluções contendo solutos do efluente têxtil.

Palavras-chave: Modificação de membranas poliméricas. Electrospraying. Efluente têxtil. Destilação por membranas por contato direto. Anti-molhamento.

RESUMO EXPANDIDO

Introdução

O aumento crescente da demanda global de água, relacionada ao aumento da população, urbanização, aumento das atividades agrícolas e industrialização, faz com que se busque métodos cada vez mais eficazes para sua recuperação e reúso (CETESB - COMPANHIA AMBIENTAL DO ESTADO DE SÃO PAULO, 2020). A indústria têxtil ocupa segunda posição dentre as atividades industriais mais poluentes, consumindo mais de 2,5 bilhões de toneladas de água por ano (SINTEX, [s.d.]). Os métodos convencionais para tratamento da água residual deste processo, como rotas físicas e biológicas, apresentam uma degradação não completa de poluentes, com alta geração de lodo residual (KUNZ *et al*., 2002). Para garantir a sustentabilidade deste processo industrial, alternativas para recuperação da água são necessárias. Neste contexto, a Destilação por Membranas (DM) apresenta-se como uma estratégia eficiente e promissora, visto que permite a utilização do calor residual do processo têxtil, bem como apresenta grande potencial de recuperação de água com alta qualidade.

Entretanto, os materiais convencionais utilizados para o uso de membranas no processo de DM (como PTFE, PP, PVDF) são suscetíveis à fenômenos inerentes do processo, como a incrustação e o molhamento, potencialmente aumentados devido à complexidade dos efluentes têxteis. Neste sentido, este trabalho propõe uma modificação superficial em membranas comerciais poliméricas via *electrospraying*, visando aumentar sua hidrofobicidade, resistência ao molhamento e garantir separações mais eficientes na DM mediante à diferentes classes de corantes e surfactantes utilizados no processo têxtil.

Objetivo

Este trabalho propõe a modificação de membranas comerciais de polipropileno (PP) e poliamida (PA) por meio da técnica de *electrospraying,* com o intuito de aumentar a hidrofobicidade destas membranas e potencializar seu desempenho para aplicação em Destilação por Membranas por Contato Direto (DMCD) visando a recuperação de água de soluções contendo componentes do efluente têxtil (diferentes classes de corantes e um surfactante). Compara-se o desempenho entre as membranas puras e modificadas para avaliar os resultados em termos de fluxo de permeado, taxa de rejeição e resistência ao molhamento.

Metodologia

Para a modificação das membranas poliméricas foi utilizada a técnica de *electrospraying*, com condições operacionais fixas: tensão de 15 kV, distância da entre a agulha e o coletor de 10 cm, e vazão de spray de 1,75 mL h^{-1}. O tempo sob spray foi avaliado na primeira modificação proposta na membrana de PP, sendo variado de 30, 60 e 90 min. Soluções poliméricas contendo porcentagens mássicas de 2% PVDF, 6 ou 10% de PDMS não curado e 0, 10, 20 e 30% de nanopartículas de sílica (porcentagem de Si NPs em relação à massa de polímero) em solução de THF:DMF (1:1) foram utilizadas para confeccionar 24 diferentes membranas modificadas. Estas foram avaliadas em termos de ângulo de contato e porosidade, a fim de selecionar as melhores, correspondentes àquelas com os maiores valores para estas propriedades. As membranas selecionadas foram caracterizadas em termos de análise química e morfológica da superfície e análise térmica. Em seguida, a modificação das melhores membranas foi reproduzida em uma membrana hidrofílica de poliamida, onde foram determinadas a hidrofobicidade, porosidade, análises térmica, química e morfológica. Nesta

matriz, a concentração de nanopartículas de sílica foi novamente avaliada em termos de ângulo de contato.

Visando avaliar a cura do polímero PDMS na hidrofobicidade da membrana de PP, uma nova solução polimérica foi preparada para o electrospraying. O polímero curado teve sua concentração variada entre 6 e 10% na solução, com 2% de PVDF e 0, 10 ou 20% de nanopartículas de sílica. As membranas resultantes foram avaliadas em termos de ângulo de contato e porosidade. As com melhores ângulos de contato foram caracterizadas com as demais técnicas mencionadas anteriormente.

Quatro diferentes classes de corantes (ácido, direto, reativo e disperso) e um aditivo de banho de tingimento de algodão (surfactante aniônico) foram testados em operação de DMCD em condições operacionais fixas. As membranas utilizadas em cada operação foram selecionadas com base no maior ângulo de contato obtido para cada solução e avaliadas em termos de grau de inchamento e potencial zeta. O desempenho das membranas modificadas na operação DMCD foi comparada com as comerciais, em termos de taxa de rejeição e fluxo de permeado visando selecionar as melhores membranas para cada operação. Por fim, todas as membranas contaminadas após a operação foram caracterizadas, a fim de verificar o mantimento da modificação proposta, e fenômenos de incrustação e molhamento.

Resultados e Discussão

As modificações propostas na membrana de PP contendo PDMS não curado (6 e 10%), PVDF (2%) e nanopartículas de sílica (0, 10, 20 e 30%), em tempos sob o spray de 30, 60 e 90 min, não ocasionaram aumento significativo ($p < 0,05$) na hidrofobicidade da membrana. O maior ângulo de contato obtido para as modificações propostas com estas soluções foi correspondente à membrana modificada utilizando 2% PVDF, 10% PDMS não curado e 20% de nanopartículas de sílica, onde verificou-se um aumento no ângulo de contato de 6,5 %. Observou-se que tempo sob o spray não influenciou significativamente a hidrofobicidade das membranas resultante. Não foi possível estabelecer relação entre o aumento da concentração de nanopartículas de sílica na superfície da membrana com o aumento do ângulo de contato. Por esta razão, a membrana correspondente ao maior ângulo de contato foi selecionada para novas avaliações, juntamente com a membrana modificada contendo 2% PVDF, 10% PDMS e 0% de nanopartículas de sílica. A análise morfológica destas membranas evidenciou a formação de estrutura rugosa e homogênea para a modificação contendo sílica, em detrimento à cobertura não-homogênea para a membrana sem sílica, que também não apresentou variações na estrutura química, comparando-se com a membrana pura.

Para as modificações seguintes, o tempo sob spray foi fixado em 90 min, a fim de garantir uma completa cobertura da superfície. As modificações propostas reproduzidas na membrana de PA, por sua vez, aumentaram gradativamente o ângulo de contato da membrana pura em relação à inclusão de nanopartículas de sílica. A membrana modificada com 2% PVDF, 10% PDMS e 20% de sílica ativou ângulo de contato de 167,13º. Este aumento foi relacionado à baixa energia superficial dos polímeros empregados, combinada com a matriz densa da membrana, onde a incorporação das nanopartículas promoveu um aumento da rugosidade da superfície. Ainda, diferenças na estrutura química da membrana foram verificadas a partir das técnicas de FTIR e EDX. A modificação aumentou a temperatura de fusão da membrana em apenas aproximadamente 1ºC, concluindo-se que a resistência térmica da membrana pura não foi afetada pela modificação.

A cura do polímero PDMS foi realizada com o intuito de avaliar a reticulação da cadeia polimérica no aumento da hidrofobicidade da membrana. Por meio das novas modificações propostas para a membrana de PP com o polímero curado (Sylgard 184), um ângulo de contato de 142.07º foi obtido para a solução de 2% PVDF, 6% Sylgard. A membrana resultante

apresentou estruturas química e morfológica alteradas pelo electrospraying, com superfície homogênea e rugosa, sem perdas em resistência térmica em relação à membrana pura.

As membranas selecionadas tiveram seus ângulos de contato medidos para 4 diferentes soluções de corantes têxteis (preto reativo, preto disperso, preto direto e preto ácido) a 30 mg L^{-1} e para solução de surfactante (Colorswet 30 mg L^{-1}), a fim de selecionar as melhores membranas para cada solução. Estes reagentes foram definidos com base nos corantes e auxiliares mais utilizados no processo de tingimento têxtil, e remanescentes no efluente gerado. A membrana de PP 2% PVDF e 6% Sylgard foi selecionada para operação DMCD com as classes de corantes, enquanto a membrana de PA 2% PVDF, 10% PDMS e 20% Si NPs foi selecionada para a operação com componentes do banho de tingimento de algodão (corante preto reativo e solução de surfactante). As membranas modificadas foram avaliadas em termos de grau de inchamento com as soluções de corantes selecionadas, e apresentaram redução do mesmo comparando-se com a membrana pura, com exceção do corante preto reativo para a membrana modificada de PP.

A operação de DMCD ocorreu em condições operacionais fixas. Os testes com a membrana modificada de PP mostraram, de forma geral, uma queda no valor de fluxo de permeado (ao máximo de 11,6% para o corante preto reativo). Em contrapartida, a membrana modificada apresentou taxa de rejeição superior em todos os testes com corantes. O aumento máximo da taxa de rejeição foi obtido para o corante direto (6%). O parâmetro de Incremento de Ângulo de Contato (IAC) foi avaliado para as membranas pós DCMD, onde observou-se um aumento para a membrana de PP para todos os corantes ($11,61 < ICA < 16,27$ %), indicando a adsorção de sólidos em sua superfície, o que também foi verificado na análise morfológica (MEV/EDX). Para a membrana modificada, observou-se inalteração no ângulo de contato após a operação, o que demostra a não deposição de solutos, bem como infere sobre a estabilidade da modificação proposta.

Os testes com as membranas modificadas de PA (2% PVDF, 10% PDMS, 0 e 20% Si NPs) para o corante preto reativo revelaram um alto potencial anti-incrustante para a modificação, que aumentou conforme aumentou-se a concentração de sílica na superfície da membrana. Os fluxos de permeado com o corante preto reativo diminuíram conforme o aumento da concentração de sílica (2,45 kg $m^{-2}h^{-1}$ para PA pura, 0,67 kg $m^{-2}h^{-1}$ para 0% Si NPs e 0.59 kg $m^{-2}h^{-1}$ para 20% Si NPs), devido à mais negativa carga superficial da membrana obtida na faixa de pH do corante. A alta negatividade da superfície promoveu forças de repulsão entre o corante e a membrana, reduzindo as interações físico-químicas, e, portanto, o fluxo de permeado. Além disso, o aumento da resistência para transferência de massa ocorreu conforme o aumento de sílica, devido ao aumento da espessura da membrana resultante. Os experimentos com a solução de surfactante evidenciaram um provável molhamento da membrana de PA pura após as 4 h de operação, devido ao alto valor de fluxo de permeado obtido (2,71 kg $m^{-2}h^{-1}$) e baixa taxa de rejeição (<91%). Em contrapartida, a membrana modificada com a solução polimérica contendo sílica apresentou rejeição de ~98% para a operação, demonstrando o potencial para recuperação de água de soluções de baixa tensão superficial. O alto ângulo de contato desta membrana foi mantido após a operação, indicando o mantimento da modificação proposta a partir da análise química e morfológica.

Considerações finais

A modificação proposta para a membrana de PP contendo 2% PVDF e 6% Sylgard, bem como a modificação da membrana de PA com 2% PVDF, 10% PDMS e 20% Si NPs aumentaram satisfatoriamente a hidrofobicidade das membranas e o desempenho no processo DMCD. A membrana modificada de PP apresentou superior ângulo de contato para água e para as diversas classes de corantes, especialmente para o corante preto ácido. Este aumento pode

ser relacionado à superfície homogênea e alta rugosidade, que possibilitou a operação DMCD com altas taxas de rejeição (aumentadas em até 6%). O aumento da taxa de rejeição para os corantes foi vinculado a uma diminuição do potencial zeta oriundo da modificação proposta, na faixa de pH dos corantes. Este aumento intensificou as forças repulsivas entre os corantes e a membrana, diminuindo suas interações físico-químicas, e desta forma, aumentando o potencial de rejeição da membrana. A diminuição do potencial zeta, combinado com o incremento de resistência à transferência de massa devido ao aumento de espessura da membrana, diminuiu os fluxos de permeado obtidos para a membrana modificada em até 11,6%. A manutenção da modificação após a operação foi evidenciada através das análises química e morfológica, bem como pela avaliação do incremento de ângulo de contato.

As modificações para a membrana de PA contendo 2% PVDF 10% PDMS e 20% Si NPs originou uma membrana super hidrofóbica mesmo em soluções de baixa tensão superficial (surfactantes). Além disso, apresentou propriedade anti-incrustante para as operações DMCD com o corante preto reativo, que foi aumentado conforme o aumento da concentração de Si NPs. Esta propriedade foi vinculada com a diminuição do potencial zeta ocorrido de forma proporcional ao aumento de Si NPs, na faixa de pH do corante. A diminuição do potencial zeta aumentou as forças repulsivas entre a membrana e a solução, diminuindo suas interações físico-químicas e a deposição de corante. As taxas de rejeição obtidas para o corante preto reativo foram superiores a 99%, e o fluxo diminui de acordo com o aumento da concentração de Si NPs, principalmente relacionado ao aumento da resistência à transferência de massa ocasionado pela adição da modificação proposta. Esta membrana apresentou fluxo de permeado inferior ao da membrana pura em operação com surfactante, mas uma taxa de rejeição aumentada em 7%. O molhamento da membrana pura na operação com surfactante foi iniciado durante as 4h de experimentos, evidenciados pelo alto fluxo de permeado, o que não foi evidenciado na membrana modificada.

As modificações propostas aumentaram a hidrofobicidade das membranas, sem grandes perdas na porosidade ou grande aumento de espessura, não comprometendo o fenômeno de transferência de massa. Ainda, as modificações alteraram a estrutura química e morfológica das membranas, concebendo estruturas rugosas e de potenciais zetas negativos em solução. Desta forma, as modificações viabilizaram a operação de DM com diferentes solutos presentes no efluente têxtil, resultando em maiores taxas de rejeição, propriedades anti-incrustante e anti-molhante para as membranas modificadas. Desta forma, este trabalho comprovou a potencialidade do processo DCMD para recuperação de água de soluções contendo solutos do efluente têxtil, através da modificação superficial de membranas comerciais via *electrospraying.* Contribui-se, portanto, para a mitigação de problemas envolvendo a operação da DM com soluções de baixa tensão superficial (surfactantes), e diferentes classes de corantes.

ABSTRACT

The conventional processes of textile wastewater treatment show a not-completely effluent degradation and generates high sludge-volume, due to the high complexity of this effluent, related to the great number of solutes in its composition. The process of Membrane Distillation (MD) consists of a promisor alternative to water recuperation from textile wastewater and its reinsertion in the process. It enables the utilization of waste heat from the dyeing process and results in a high-quality permeate. However, some challenges to the consolidation of this technique persist, related to the fouling and wetting phenomena. The low wetting resistance of the commercial membranes makes the DM process not applicable to the whole textile effluents compounds, such as some classes of dyes and additives employed in the process, i.e., surfactants. In this context, this work aimed at the membrane modification of polyamide (PA) and polypropylene (PP) membranes, using electrospraying technique through the incorporation of polymeric blends on the membrane surface, with PVDF, cured or not-cured PDMS, and silica nanoparticles (Si NPs) in THF: DMF (1:1) solutions. The main goal of modifications was the hydrophobicity improvement and achievement of anti-wetting property. The influence of polymer and Si NPs concentration, polymer curing, and time under the spray were evaluated. Water contact angles of 167.13º and 144.07º were obtained to PA and PP membranes, respectively. These membranes were characterized in chemical and morphological structures (FTIR, SEM, and EDX), thermal analysis (DSC), membrane thickness and porosity, contact angle against different solutions, and Zeta Potential. The removal potential of modified membranes was evaluated in a Direct Contact Membrane Distillation (DCMD) operation, during four hours, in a fixed operational condition. The modified PP membrane using 2% PVDF and 6% Sylgard (cured PDMS) was tested with four different industrial dye classes (Reactive, Disperse, Direct, and Acid) and presented permeate fluxes of 29.7, 44.85, 29.79 e 35.41 kg m^{-2} h^{-1}, respectively. The flux was reduced at most 11.9% comparing to the pristine PP membrane. The rejection rates reached more than 95%, and they were higher than the rejection rates of pristine PP against the different classes of dyes. The polymer curing, combined with the high roughness and hydrophobic structure obtained through electrospraying, decreased the zeta potential of the modified membrane in the pH range of dye solutions, contributing to a high wetting resistance and high rejection rates without loses in membrane porosity. The PA modified membrane using 2% PVDF, 10% PDMS, and 20% Si NPs showed lower permeate fluxes due to its dense structure. It was tested with a cotton dyeing bath compounds (reactive black dye and surfactant), resulting in permeate fluxes of 0.6 and 0.39 kg m^{-2} h^{-1}. Higher rejection rates than the pristine PA membrane were achieved, mainly dealing with the surfactant solution, where the PA membrane has been beginning wetted. The PA modified membrane achieved an antifouling property against the deposition of dye particles. The modification of commercial membranes aiming to create more hydrophobic structures enabled the DCMD operation with different dye classes and low surface tension solutions (detergent), with higher wetting resistance and higher removal potential, without compromising the chemical and morphological structure of the membranes. In this work, the membrane modification proved the DCMD process's potentiality in water recuperation from solutions containing textile wastewater solutes.

Keywords: Membrane modification. Electrospraying. Textile effluent. Direct Contact Membrane Distillation. Anti-wetting.

LIST OF FIGURES

LIST OF TABLES

TABLE OF CONTENTS

1 INTRODUCTION

The global scarcity of water is worsening due to social inequality and the lack of management and sustainable uses of natural resources. The growing demand for this non-renewable resource is related to population growth, urbanization, increased agricultural production, and industrialization (CETESB - COMPANHIA AMBIENTAL DO ESTADO DE SÃO PAULO, 2020). It is estimated that the global use of water for industry presently accounts for 20% of the world's total water consumption (BORETTI; ROSA, 2019).

Among the industrial activities with the highest water consumption level, the textile industry consists of the second most polluting industrial activity globally. It is estimated that the average annual consumption of this sector is about 93 trillion liters. The textile industry ranked third overall in the discharge of wastewater in the amount of 2.5 billion tons of wastewater per year, which is equivalent to 20% of industrial water pollution in the world (AMDA, 2018). The industrial stages that generate more effluents are dyeing and finishing.

The textile industry is evolving in applying sophisticated water treatment technologies to design more sustainable processes and reduce the harmful effect of releasing wastewater into the environment. However, it involves multi-stage processes, combining biological, electrochemical, psychic-chemical pre-treatment, coagulation, filtration, and membrane processes, aiming to the zero-liquid discharge. In many cases, the multi-stages involving these operations become expansive, mainly due to the operational problems involving the traditional membrane processes employed in these methods, such as reverse osmosis, ultrafiltration, and nanofiltration. Among these problems, it can be cited the membrane fouling, harsh requirements of pressure and temperature, and concentration polarization effect (LEAPER *et al.*, 2019). In this context, the search for an alternative and feasible method to water recovery from textile wastewater consists of a need for textile process sustainability.

Membrane Distillation (MD) appears as a promisor alternative to water recuperation from textile wastewater due to the high process efficiency, purely physical nature of the separation principle, and the possibility of using the residual heat from the dyeing bath process (RAMLOW; MACHADO; MARANGONI, 2017). The MD is a thermally-driven process separation, where a hydrophobic and microporous membrane is employed. This operation uses the difference of vapor pressure across the membrane as a driving force to the mass transfer. The membranes employed in this process are selective to the vapor passage, avoiding the liquid and solute penetration into their pores (CAMACHO *et al.*, 2013a; GONZÁLEZ; AMIGO;

SUÁREZ, 2017). Compared to other membrane processes, MD is less prone to membrane fouling and requires milder conditions of pressure and temperature.

The MD is a consolidated process to water desalination, where polymer membranes made of PP, PVDF, and PTFE are usually employed. These materials present good performance in membrane modules and low cost comparing to ceramic membranes (CAMACHO *et al.*, 2013a). These membranes also meet MD separation requirements, such as hydrophobicity, thickness, porosity, chemical stability, etc.

However, the MD process is inherent to operating phenomena, such as wetting and fouling, that can be avoided by choosing a specific membrane. Singularly, the wetting phenomenon consists of the loss of membrane hydrophobicity, allowing the passage of contaminants and non-volatile compounds from the feed solution to the permeate side, affecting the permeate quality and the efficiency of the MD process (GARCÍA *et al.*, 2018). The presence of organic solutes in the solutions to be treated by MD can harshly affect the membrane hydrophobicity due to decreasing the surface tension of solutions. The textile dyes and auxiliaries to the dyeing process are examples of solutes that decrease the solutions' surface tension.

For this reason, the MD operation using conventional polymeric membranes is compromised when it comes to separations with some classes of dyes or dyeing auxiliaries, as surfactants (TOLENTINO FILHO, 2019). Thereby, developing resistant membranes against these kinds of substances becomes a need to consolidate MD technology in water recuperation from textile wastewater.

Due to environmental concerns and MD operation problems, this work aims to modify PA and PP commercial membranes using the electrospraying technique, aiming for hydrophobicity improvement and enhancing the DCMD performance against the textile solutes. Different polymers (PVDF and PDMS) were tested to design the modification, along with silica nanoparticles; the polymer cure, polymer concentration and the time under the spray, were evaluated affecting the membrane hydrophobicity. Also, the use of silica nanoparticles was studied in terms of membrane roughness, porosity, and droplet size. The modifications were carried out in a hydrophobic and a hydrophilic commercial membrane. The modified membranes were tested in a Direct Contact Membrane Distillation (DCDM) unit, and their performances were compared with the pristine membranes. The solutions consisted of four different textile dyes and one surfactant. All the experiments were carried out at Polymer Design and Process Control Laboratory (LCP) and at Laboratory of Ceramic Processing (PROCER), of Federal University of Santa Catarina (UFSC).

The choice of the commercial membranes used to support membrane modification is made based on the membranes' availability and based on the type of structure required for a modification (porous and dense, hydrophobic and hydrophilic). The polymers employed in the doping solutions are selected based on their chemical characteristics, such as their non-polar chains and viscosity, and based on results from the available literature, reported in the state-of-the-art. The use of silica nanoparticles was supported by previous studies, where the development of antifouling and wetting resistance against low surface tension solutions was achieved. The electrospraying technique was selected to develop the present study due to its easy fabrication, quick capability of cover surfaces, high roughness created, low losses on membrane porosity, and its high-control of membrane properties. (MADALOSSO *et al*., 2021)

Operational problems involving commercial polymeric membranes reveal a high fragility when dealing with low surface tension solutions, due to the wetting phenomenon, oily solutions, due to poor oleophobicity, and inorganic scaling, for the separations involving salts or solid particles. Although this work only comprised the application of the modified membranes in textile compounds, their application is not limited to this kind of separation.

Regarding academic publications of membrane modification via electrospinning or electrospraying, a search in the database CAPES resulted in 18 works to MD applications during the last five years. Among them, only 3 embraced membrane modification applied to surfactant solutions. There are no reports about the study of a modified membrane using electrospraying to solutions with textile dyes. For this reason, new research is fundamental and necessary for this application.

This work's development contributes to mitigating problems involving membranes operating with dyes and textile auxiliaries in the MD process. In this way, progress is gradually made towards the consolidation of membrane distillation technology in the recovery of water from textile effluents.

1.1 OBJECTIVES

1.1.1 General Objectives

This work aimed to modify commercial polymeric membranes via electrospraying to improve their performance in Direct Contact Membrane Distillation to water recovery from dyes and surfactant solutions, through the improvement of their hydrophobicity and wetting resistance.

1.1.2 Specific Objectives

The specific objectives of this work are:

a) Improve the hydrophobicity of polypropylene (PP) and polyamide (PA) membranes, using electrospraying technique to design the membrane modification;
b) Evaluate the influence of the time under the spray affecting the membrane hydrophobicity;
c) Evaluate the influence of polymer curing (PDMS) in the hydrophobicity improvement of modified membrane;
d) Evaluate the incorporation of silica nanoparticles in membrane hydrophobicity, as well as its relation with droplets size and membrane porosity;
e) Apply the PP modified membrane in a DCMD process with synthetic solutions of Reactive Black Dye, Disperse Black Dye, Direct Black Dye, and Acid Black Dye, aiming the investigation of membrane performance against different classes of dyes;
f) Apply the PA modified membrane in a DCMD process with synthetic solutions compounded by the auxiliaries of cotton dyeing bath (Reactive Black Dye and anionic surfactant solutions) to determine the performance of modified membrane against low surface tension solutions;
g) Evaluate the modified membranes in terms of wetting and fouling resistance.

2 LITERATURE REVIEW

In this section, a literature review about the followed main topics will be presented:

a) The process involved in the textile industry, the dyes and chemical additives employed in this process, and the amount of water required in each stage.
b) The membrane distillation process and the principle of operation, applying this technology in an experimental process, their advantages, and configurations are commonly used.
c) The usually commercial membranes employed in this process, their classification, the permeation modules, the desirable characteristics for these membranes, and their main properties.
d) Phenomena involving the MD operation.
e) The main kinds of modification employed to achieve desirable properties in polymeric membranes.
f) Electrospraying technique applied to modify polymeric membranes to their applications in MD processes.

The chronological order in which the information is presented follows the explanation of the textile industry's wastewater generation and the potentialities and difficulties of the membrane distillation technology to water recovery from this residual water. Finally, the importance of modifying membranes in overcoming operational problems for this application is justified.

2.1 THE TEXTILE INDUSTRY

The textile industry consists of an essential manufacturing process, which harshly contributes to the world’s economy. Moreover, it was known as one of the biggest consumers of freshwater and chemical products, discharging much wastewater in the environment (RAMLOW *et al*., 2019a). Brazilian textiles industries occupy the fifth position in the more prominent textile industries globally, where the South Region stands out with 29% of this sector’s entire enterprises. The region of “Vale do Itajaí”, in the state of Santa Catarina, accounts for a significant share of companies and employees, with about 60% of the total state of the textile and garment industry. The municipalities as Blumenau, Gaspar, and Indaial concentrate together more than 62% of the companies (MILNITZ; LUNA, 2017).

The textile process can be divided into three main stages: wiring, weaving, and finishing. There is no generation of wastewater in the two first stages since only mechanical operations are employed. Hence, the total wastewater generation occurs in the finishing stage (BELTRAME, 2000), which comprises washing, softening, dyeing, stamping, and finishing woven (BASTIAN *et al*., 2009).

Dyeing is a chemical process that involves the color modification of textile fibers by the application of colored materials, which may be pigments or dyes, involving a solution or dispersion. Pigments and dyes differ from each other by particle size and solubility. Dyes are soluble, while pigments are insoluble in water. Besides, more than the proposal of coloration, the pigments can give coverage and opacity for the fabric while the dyes maintain their transparency (VELOSO, 2012).

The dyeing process is divided into three main stages: assembly, fixation, and final treatment. The dye fixation is carried out through chemical reactions, such as solubilization of the dye or derivatives, which occurs in several steps during the assembly and fixation phases. The dyeing process's final step consists of washing the fabric in sequential baths to remove the excess concentration of dyes not fixed to the fiber in the preceding steps (FÊNIX - FABRIL INDÚSTRIA E COMÉRCIO, 2019).

When the fiber is immersed in the dye bath, the dyeing process took place in three main steps:

i. Dye transfer to bath, in direction to fiber surface;
ii. Dye adsorption by the surface;
iii. Dye diffusion from the fiber surface into the fiber.

The attraction forces are responsible for dye absorption, and they can be ionic connections, hydrogen bonds, covalent bonding, or Van der Waals forces (LADCHUMANANANDASIVAM, 2008).

2.1.1 Dyes and chemical auxiliaries used in the dyeing process

The dyes classification is provided by Color Index, published by The Society of Dyers and Colorists, in a partner of the Association of Textile Chemists and Colorists. This classification and its relation with fixation, dye applications, and related pollutants are presented in Table 1.

Table 1 – Dyes classification, fixation percentage, and pollutants associated

(to be continued)

Dyes Class	Description	Fiber types	Fixation (%)	Pollutants associated
Acid	Anionic compounds are soluble in water.	Wool and Polyamide.	80 - 93	Color, organic acids and unfixed dyes.
Basic	Cationic compounds, soluble in water, applicable in bath weakly acidic.	Acrylic and some types of polyester.	97 – 98	Almost total fixation in the fiber. Salt, organic acids, retardants, dispersants, etc.
Direct	Soluble in water, Anionic compounds. It can be applied directly into cellulose without cheek (or metals as chrome and copper).	Cotton, Rayon, and cellulosic fibers.	70 - 95	Color, salt, non-coloring fixed, fixed; agents cationic surfactants, defoamer, retarding agents and equalizers, etc.
Scattered	Insoluble in water, nonionic compounds.	Polyester, Acetate, and other synthetic fibers.	80 - 90	Color, organic acids, equalization agents, phosphates, antifoams, lubricants, dispersants, etc.
Reactive	Soluble in water, Anionic compounds, a most important class of dyes.	Cotton, Wool and other cellulosic fibers.	60 - 90	Color, salt, alkalis, dyes hydrolyzates, surfactants, anti-theft organic, antifoams, etc.

Table 1 – Dyes classification, fixation percentage, and pollutants associated

(conclusion)

Dyes Class	Description	Fiber types	Fixation (%)	Pollutants associated
Sulfur gases	Mercapto dyes. Organic compounds containing sulfur and polysulfides in their formulation.	Cotton and others cellulosic fibers.	60 - 70	Color, salt, alkalis, agents oxidants, reducing agents and non-dyestuffs fixed, etc.
Cuba	Redox type dyes, insoluble in water. The "Nobler" class of dyes.	Cotton and others cellulosic fibers	80 - 95	Color, Alkalis, Agents oxidants, reducing agents, etc.

Font: Bastian *et al*., (2009)

The chemical dyes are constituted of (1) chromogenic groups which are responsible for the dye color; (2) auxocrome groups which intensify the colors and provide the dyeing quality; (3) solubilizes groups that provide the permanent solubility (acid, direct and reactive dyes) or temporary solubility (enolic and ketolic groups). The chromogenic groups include the chemical structures as C=C, C≡C, C=O, C≡N, N=N, NO_2, while the auxochrome groups comprehend structures as $–NH_2$, -NHR, $-NR_2$, -COOH, -OH. (TWARDOKUS, 2004). The auxocrome groups are responsible for donating or accept the electrons.

Natural fibers as cotton and wool majorly dominate fiber consumption in the world. Because of their higher price and difficulties of production, the demand for new synthetic fibers, as cellulose fibers, is increasing around the world in recent years. The scenario leads to polyester and cotton as the most fabricated fibers in the textile industry (ALAM; CHRISTOPHER, 2017). In the face of fiber consumption, the reactive, disperse, direct, and acid dyes classes are the most employed in the textile industry.

The reactive dyes are represented by the bond C-R, where C is the chromogenic group, and R is the reactive group. These groups react with the hydroxyl groups of the fiber, forming a covalent bond. The main chemical groups susceptible to react with reactive dyes consist of amino and hydroxyl groups. The covalent bond shows high resistance, resulting in high solidity to washing. High reactivity allows the dyeing process in low temperatures. The dyeing process using the reactive dyes generally occurs by exhaustion (GOMES, [s.d.]). The chromogenic

groups of reactive dyes are mostly azo and anthraquinone groups, while the reactive groups are chlorotriazinyl and sulfatoethylsulfonyl. This dye involves a chemical reaction where the hydroxyl groups substitute the nucleophilic groups from cellulose (GUARATINI; ZANONI, 2000).

Reactive dyes show high water solubility, and its covalent established bond results in high color stability and high intensity. The chemical structure of a reactive dye can be illustrated in Figure 1.

Figure 1 – Reactive Dye molecules

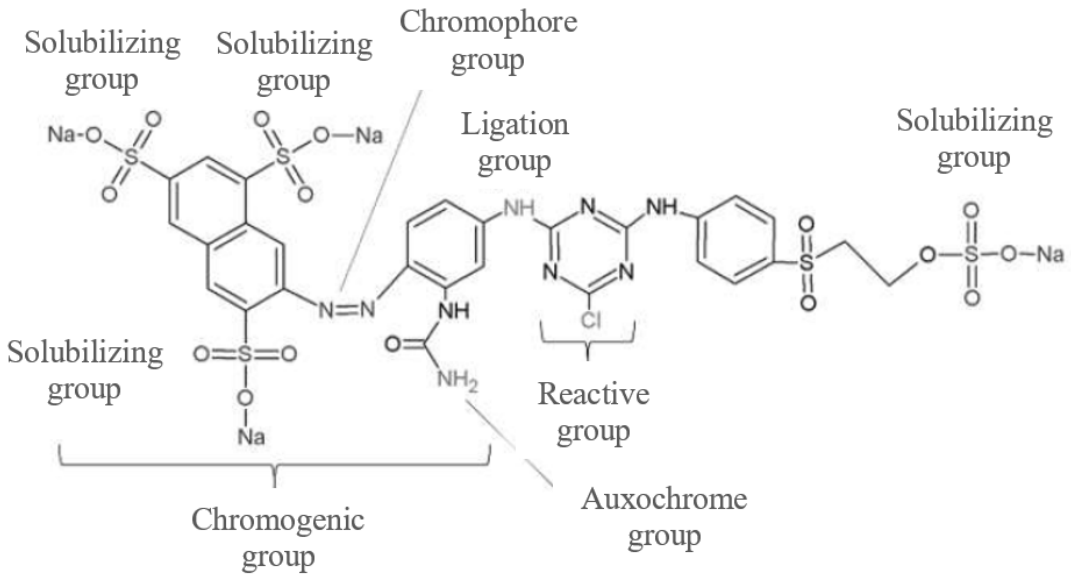

Font: Adapted from Ramlow (2018)

High water solubility is also characteristic of direct dyes targeted to dyeing processes of cellulosic fibers, such as cotton and viscose. They present more than one azo group and can be pre-transformed in metal complexes. The dyeing process occurs through Van der Waals interactions between the dye and the fiber. Its affinity is increased by electrolytes' insertion or the dye's double bond (GUARATINI; ZANONI, 2000).

On the other hand, disperse dyes are insoluble in water and generally applied in hydrophobic and synthetic fibers – such as cellulose, nylon, and polyester - by particle suspension in high pressures and temperatures. The solubility degree should be small, and it directly influences the process and dyeing quality. In the dyeing process, disperse dyes suffers hydrolysis, where precipitates in a disperse phase. This process requires dispersant agents that act as suspension stabilizers and intensify the contact between the dye and the hydrophobic

fiber (TWARDOKUS, 2004). The reaction involving dispersed dyes can be illustrated in Figure 2.

Figure 2 – Temporary solubilization of dispersed dye.

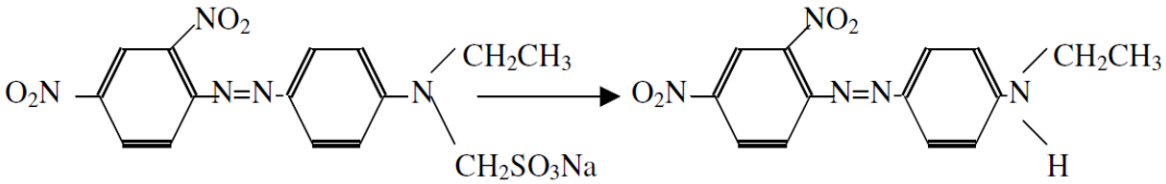

Font: Adapted from Twardokus (2004)

In this turn, the acid dyes consist of anionic dyes containing at least one and up to three sulfonic groups, which are ionizable and result in high water solubility. The acid dyes are used to dye protein fibers such as wool and silk and synthetic fibers, such as polyamide. They are characterized by the presence of azo, anthraquinone, triarylmethane, azine, xanthene, ketonimine, nitro, and nitrous groups and present a high fixation degree. The dye process involving acid dyes requires a previous dye neutralization, usually done with chloride, acetate, hydrogen sulfate, etc. The dye bonding with the fiber through an ionic change involving the carboxyl or amino groups of protein fibers (GUARATINI; ZANONI, 2000).

Beyond the dyes, dyeing processes require auxiliaries for several applications, such as to improve the stabilization of the dye, facilitate the dispersion, homogenize the solution, decrease time to the humectation, and improve the quality of the final product (BELTRAME, 2000). These auxiliaries vary according to the dye employed in the dyeing process and the fiber to be dyed. The main additives used in the dyeing process are presented in Table 2.

Table 2 – Auxiliaries used in the dyeing process

(to be continued)

Auxiliaries	**Composition**	**Function in the Dyeing Process**
Acids	Acetic and sulfuric	pH control
Bases	Sodium hydroxide and sodium carbonate	pH control
Oxidizing agents	Hydrogen peroxide and sodium nitrite	Avoid the dye solubilization
Reductor agents	Sodium sulfate and sodium hydrosulfite	Removal of unreacted dyes; solubilization
Defoamers	Silicon emulsions	Avoid the foam formation
Carriers	Methyl-naftene	Improve the dye fixation

Table 2 – Auxiliaries used in the dyeing process

(conclusion)

Auxiliaries	Composition	Function in the Dyeing Process
Dispersants and surfactants	Anionic, cationic and non-ionic	Softener and dye dispersant
Salts	Sodium chloride, sodium sulfate	Retardants
Kidnappers	EDTA, acrylates	Avoid the precipitation of dyes by the presence of high metals concentration in water
Humectants	Ethoxylated nonylphenol	Homogenization and fiber hydrophilization

Font: Adapted from (RAMLOW, 2018)

2.1.2 Water consumption and wastewater generation in the textile industry

In recent years, environmental issues are becoming increasingly worrying and critical, mostly linked to population growth and increased industrial activity, which causes several alterations in the air, water, and ground. In this sense, water contamination is a critical consequence of human action through industrial activities (KUNZ *et al*., 2002).

The textile industry deserves special attention from the industrial sectors due to the high volume of wastewater generation and water consumption. According to Amda (2018), the textile industry consumes 93 billion cubic meters of water per year. It is responsible for 20% of industrial water pollution globally, which becomes this industry as the third most consumer of water in the world.

Water is a non-renewable resource, mostly found in the saline form (97%, approximately). Moreover, 2% of the total freshwater is presented in ice form. Brazil concentrates 8% of the total superficial freshwater in the world. Agriculture and industry activities are the biggest consumer globally, where the textile industry is responsible per 15%, generating effluents with high levels of contaminants (WEILER, 2005). The textile industry uses about 100 m³ of water to produce 1 t of fabric (BERGNA; BIANCHI; MALPEI, 1999).

The water consumption and wastewater generation in the textile process can be illustrated in Figure 3.

Figure 3 – Steps of processing of wool and synthetic fibers

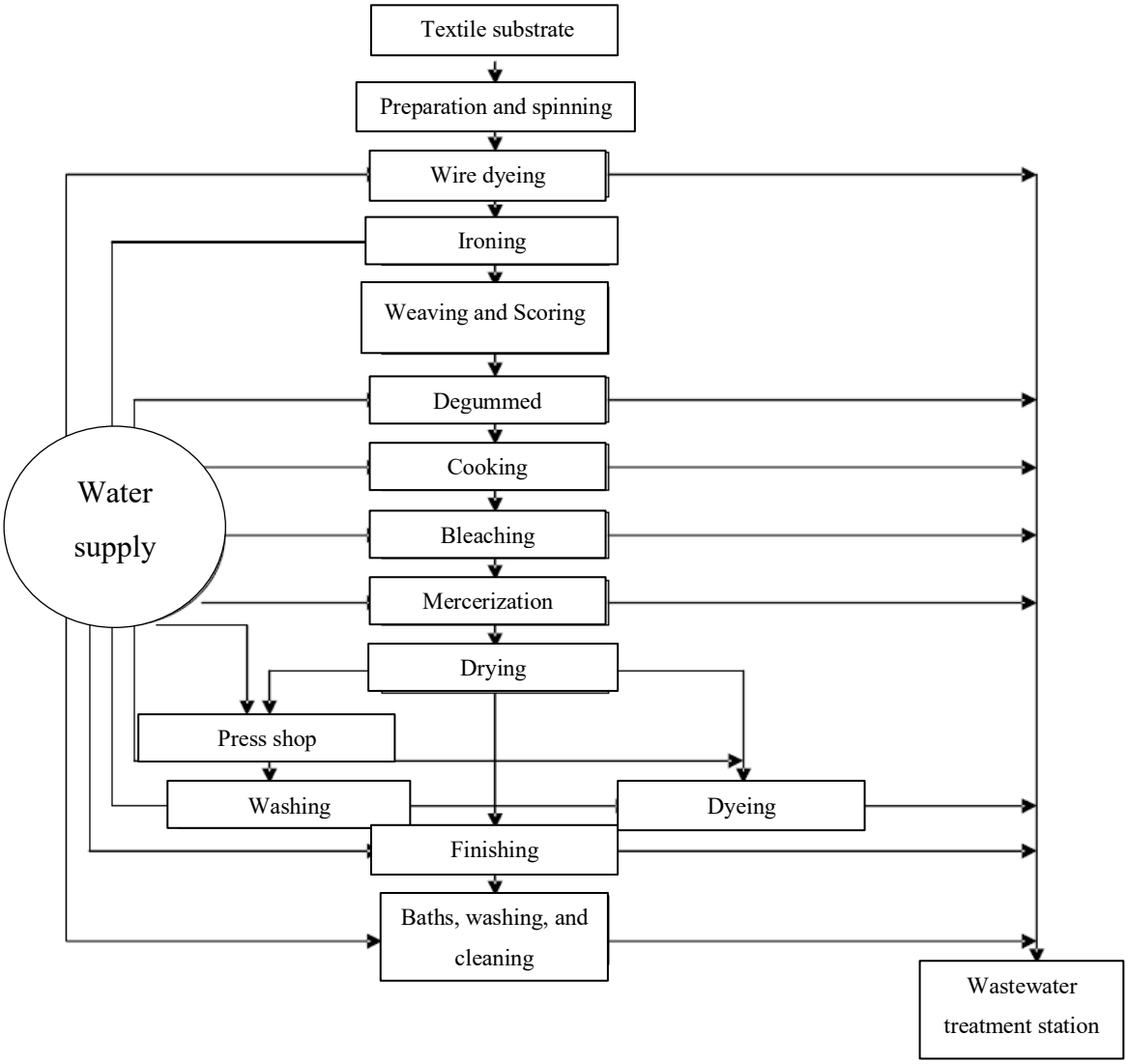

Font: Braile; Cavalcanti (1993)

Wastewater generation in the textile industry occurs mainly in the dyeing and finishing processes due to the high water consumption in these stages. The residual water generally has a color presence due to the dye's poor fixation on the fabric, and organic charge, due to the auxiliaries and dyes employed in the textile process (WEILER, 2005). The main characteristics of textile wastewater are presented in Table 3.

Table 3 – Wastewater characteristics of the textile industry

(to be continued)

Parameters	**Range**
pH	4.7 – 11.8
Total Organic Carbon (TOC)	140 – 170 mg/L
Biochemical Oxygen Demand (BOD)	9 – 2580 mg/L

Table 3 – Wastewater characteristics of the textile industry

(conclusion)

Parameters	Range
Conductivity	0.2 – 11.9 mS/cm
Chemical Oxygen Demand (COD)	102 – 170 mg/L
Total of Suspense Solids	<3 – 2500 mg/L
Nitrogen	0.3 – 73 mg/L
Chlorides	19.5 – 3800 mg/L
Sulfates	18 – 38 mg/L

Font: Adapted from Batista (2015)

The water pollution resulted from inadequate discharge of textile wastewater alters the biological cycles, mainly the photosynthesis process. Some dyes classes and their sub-products can be carcinogenic and mutagenic (KUNZ *et al*., 2002). In this context, the search for new technologies to treat the textile wastewater, focus on the recovery and reuse of water used in the textile process are an urgent need to conserve water resources and guarantee sustainable processes.

2.1.3 Recent advances to treatment of textile wastewater

The treatment process conventionally applied to textile wastewater can be classified into three main groups: biological, oxidational, and physical processes, subdivided in general form according to Figure 4.

Figure 4 – Treatment methods for the degradation of dyes in textile wastewater

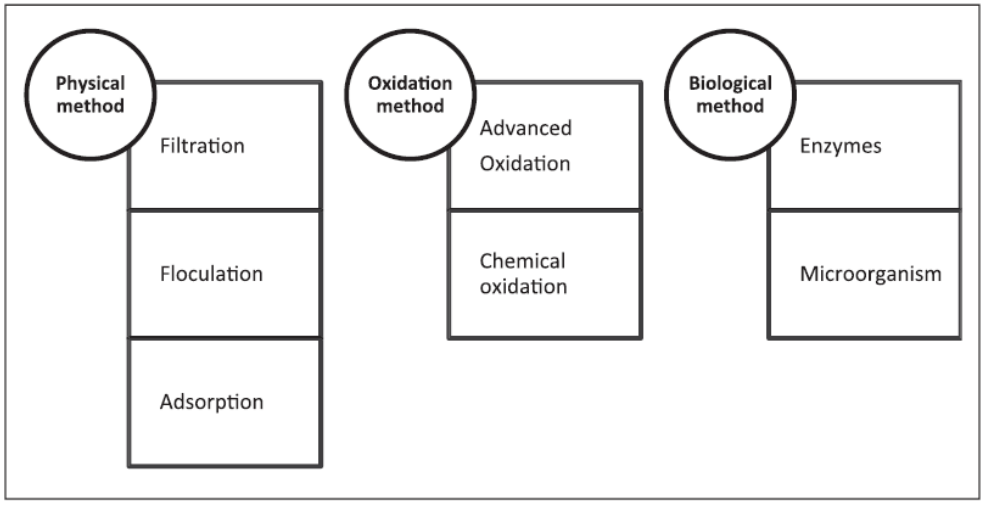

Font: Holkar *et al*. (2016)

The usual process employed in most textile industries is the physical separation, followed by biological treatment, with activated sludge. In this process, firstly occurs the flocculation and coagulation of organic compounds. After the physical step, the effluent is stirring in the presence of air and microorganisms several times to metabolize a considerable part of organic material. The process efficiency corresponds to 80% of the dye's charge, although it generates a critical sludge volume, hardly reused. The water resulted from this treatment is sent back to the river without reuse and may still contain traces of organic matter (KUNZ *et al*., 2002). The conventional treatment process is generally insufficient to obtain the required water quality to reuse (VAN DER BRUGGEN; CURCIO; DRIOLI, 2004).

To improve the treatment process and find an alternative to water reuse, innovative technologies for textile wastewater treatment and water recuperation are widely studying. The mainly recent innovations on this issue are presented in Table 4.

Table 4 – Some innovative technologies to treat textile wastewater

Dye	**Treatment**	**Propose to reuse of water?**	**Reference**
Foron Blue-2RN, Azul Dianix K-2GLS, and Brilliant Red	Electrochemical treatment	Yes	(BATISTA, 2015)
Gray and Dark Blue	Electrocoagulation	Yes	(NÚÑEZ *et al*., 2019)
Dark Blue	Membrane photocatalytic reactor (ZnO-PEG) + Ultrafiltration	No	(DESA *et al*., 2019)
Reactive Black 5	Electrocoagulation + Ozone treatment	No	(BILIŃSKA *et al*., 2019)
Real effluent	Adsorption on alkali-activated sand	No	(SHARMA *et al*., 2019)
Real effluent	Membrane Bioreactor + Nanofiltration + RO	Yes	(CINPERI *et al*., 2019)
Real effluent	Hybrid anaerobic-aerobic biological treatment	No	(SHOUKAT; KHAN; JAMAL, 2019)
Real effluent	Ultrafiltration + Electrodialysis	No	(LAFI *et al*., 2018)
Real effluent	Electrocoagulation + electrochemical advanced oxidation process	Yes	(ZAZOU *et al*., 2019)

Font: The Author (2021)

Table 4 evidenced the focus of the recent studies under treatment to discharge to the detriment of potential technologies to reuse or recovery the water from this effluent. In this scenario, membrane technology could be a key in the recycling and reusing water, enabling combined operations with other treatment processes (VAN DER BRUGGEN; CURCIO; DRIOLI, 2004). It is important to emphasize that the membrane processes do not replace the textile wastewater's traditional treatment once they only enable the water reuse from the final treatment stage or the final stage of the dyeing process. The water reuse allows a more sustainable production and generates a smaller volume of effluent to be treated.

Among the membrane processes, the Membrane Distillation (MD) technology arises as a promising alternative to water recuperation from textile wastewater. The main advantage linked to the MD process to textile wastewater is the possibility of using the waste heat present in the residual water, which comes from the dyeing bath at approximately 100ºC (RAMLOW, 2018). According to Figure 3, the MD could be employed in the final stages of textile processes, such as dyeing, finishing, and washing, or after the wastewater treatment station.

2.2 THE PROCESS OF MEMBRANE DISTILLATION

Membrane Distillation (MD) is a thermal, membrane-based separation process that uses the vapor pressure difference across the membrane as a driving force to the occurrence of the mass transfer (CAMACHO *et al*., 2013b). The gradient of vapor pressure is achieved through the difference of temperature between the both sides of the hydrophobic membrane.

In this process, a feed solution's volatile compounds evaporate by warming the feed, crossing the microporous hydrophobic membrane, and condense in a distillate solution at a lower temperature than the feed (GONZÁLEZ; AMIGO; SUÁREZ, 2017). The membrane works as a physical barrier that only allows the vapor's passage through the pores while rejects the liquid, the non-volatile compounds, and dissolved salts (DUONG *et al.*, 2017a).

The hydrophobic nature of the membrane, related to its high surface tension, prevents the liquid from the feed solution to penetrate membrane pores (WANG; CHUNG, 2015). The separation results in a highly pure distillate solution and a concentrated feed solution where the non-volatile solutes are retained (GONZÁLEZ; AMIGO; SUÁREZ, 2017).

2.2.1 Main advantages of the MD process

Comparing with other methods of membrane separation, the main advantages of the MD process are:

a) The complete removal of non-volatiles, salts, and ions (100% of rejection), resulting in an almost pure distillate;
b) Operation in lower temperatures and lower pressure-driven in comparison with other membrane-separation methods (WANG; CHUNG, 2015);
c) The salt separation is relatively constant in the process course;
d) The rejection of the salts, ions, and non-volatile compounds is practically independent of its concentrations in the feed;
e) Wide sources of low-grade heat can be employed to create the gradient of temperature in this operation, as solar heat or industrial waste heat;
f) Generally, the feed does not require extensive pretreatment (YE *et al*., 2019);
g) This operation presents fewer requirements on membrane mechanical properties (WANG; CHUNG, 2015).

Compared to the traditional distillation method, the MD operates at lower temperatures and demands a reduced vapor space, which implies smaller equipment. The solutions also do not be warmed until their boiling points (DUONG *et al*., 2017a).

Because of these advantages, the MD process is an emerging and attractive method that can be considered an alternative solution for conventional desalination processes and for treating a wide range of industrial effluents (BOUBAKRI; HAFIANE; BOUGUECHA, 2017).

2.2.2 Membrane Distillation Configurations

Depending on the condensation in the membrane cold side, the MD systems can be classified into four mainly configurations: Air-Gap Membrane Distillation (AGMD), Direct Contact Membrane Distillation (DCMD), Sweep Gas Membrane Distillation (SGMD), and Vacuum Membrane Distillation (VMD) (GONZÁLEZ; AMIGO; SUÁREZ, 2017), briefly described below and illustrated by Figure 5.

Figure 5 – MD configurations

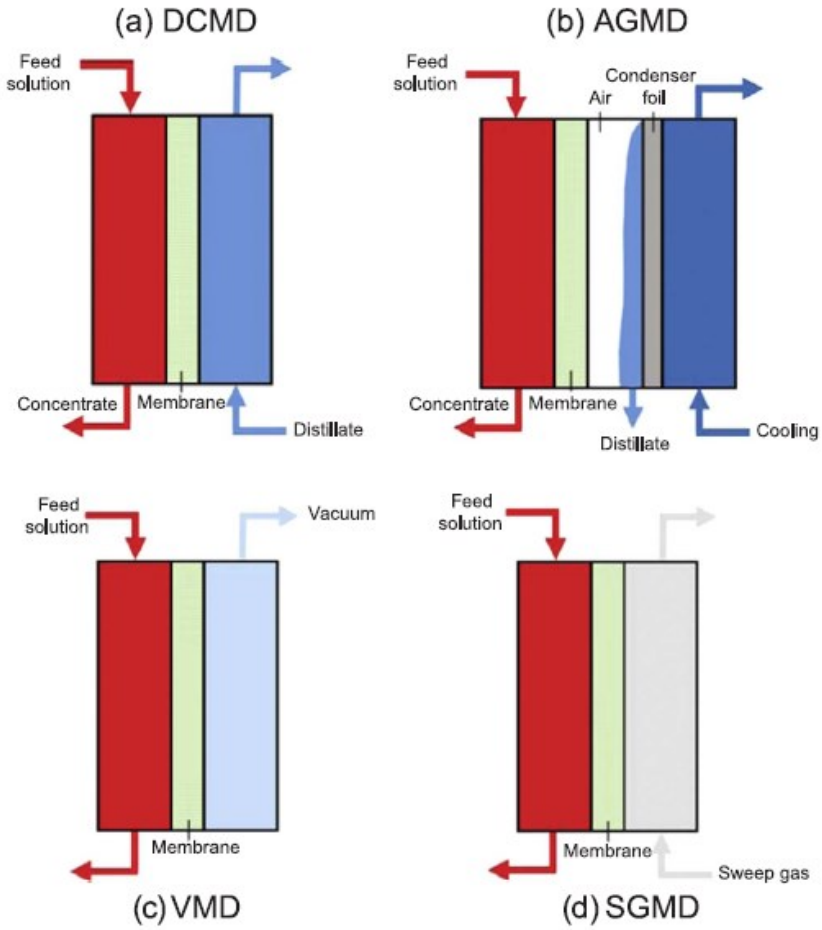

Font: Adapted from Gonzalez; Amigo; Suárez (2017)

i. AGMD: This configuration induces the permeate's condensation by inserting an air gap between the membrane and the condensation surface, which operates as a heat insulation layer. For this reason, AGMD presents the highest thermal efficiency comparing to other configurations. However, the air gap increases the mass transfer resistance, resulting in a lower flux than DCMD (DUONG *et al.*, 2017a). As a significant advantage of AGMD, there is no danger of membrane wetting at the distillate side (GONZÁLEZ; AMIGO; SUÁREZ, 2017).

ii. DCMD: In this configuration, the membrane and the liquid phase of permeate solution are in direct contact. The vapor condensation occurs in the permeate side, where the cold water circulates tangentially to the membrane surface, inducing a driving force for this process. DCMD is the simplest and most suitable configuration of the MD process and consists of the configuration where the biggest heat losses occur during the operation. Therefore, the DCMD configuration exhibit lower thermal efficiency

compared to other configurations (DUONG *et al*., 2017a; GONZÁLEZ; AMIGO; SUÁREZ, 2017)

iii. SGMD: A stripping gas, which consists of inert, cold gas, is employed to transfer water vapor to an external condenser, where the condensation occurs (CAMACHO *et al*., 2013b). This module has a lower thermal polarization effect, and the wetting in the permeate side is avoided. However, heat recovery is difficult due to this configuration's complexity (GONZÁLEZ; AMIGO; SUÁREZ, 2017).

iv. VMD: Vacuum is applied in the membrane's permeate side, generating the operation's driving force. The condensation occurs outside of the module once the pressure applied is lower than the evaporation components' saturation pressure, so the water vapor is transported. This configuration presents low heat losses by conduction and high permeate flux, which consists of critical operational advantages. However, because of the high flux, the membrane is more prone to wetting than other configurations (GONZÁLEZ; AMIGO; SUÁREZ, 2017). The VMD configuration requires more equipment, like vacuum pumps and condensers, and presents as more costly than DCMD and AGMD.

2.2.3 Principal applications of the MD process

The MD process was patented in the late 1960s. At this time, this technology was rarely applied in commercial processes (i.e., desalination), mainly because of the poor access to membranes with suitable characteristics, such as low liquid permeability, high resistance to heat flow, ideal thickness, high porosity, and viable cost (ALKLAIBI; LIOR, 2005).

Nowadays, the MD process consists of emerging technology for separation processes because of the evolution in membrane fabrication. Its applications are widely varying at the different processes, from the most typical, as desalination (GUAN *et al*., 2015; LI *et al*., 2019c; MENDEZ *et al*., 2019), to the most robust process, as a radioactive wastewater treatment (CHEN *et al.*, 2019).

Boubakri; Hafiane; Bouguecha (2017), for example, studied the potentialities of this technology to desalt raw waters, using the direct contact as a module configuration and flat sheet polypropylene membranes. Khumalo *et al*. (2019) used a modified PVDF/PTFE membrane to remove Congo red dye from water, with 99% removal efficiency achieved. Silva *et al*. (2018) applied MD to desalination, removing organic micropollutants and microorganisms of river water, seawater, and municipal wastewater. Dong *et al*. (2019) studied

the separation of oil-water using a hybrid and porous membrane. Furthermore, Criscuoli; Drioli (2019) used Vacuum Membrane Distillation to treat coffee products. Loulergue *et al*. (2019) studied the separation of bioethanol from algal-based fermentation broths using the AGMD configuration. Couto *et al*. (2019) evaluated the effect of humic acid concentration on pharmaceutically active compounds rejections by DCMD.

2.3 MEMBRANES USED IN THE MD PROCESS

As previously mentioned, the membrane can be defined as a restriction barrier that only allows the vapor passage to the permeate side (HABERT; BORGES; NOBREGA, 2006). The classification, permeation modules, and requested characteristics for membranes to application in the MD process will be mentioned in this section.

2.3.1 Membrane Classification

In terms of morphology, the membranes can be classified into two large groups: porous and dense membranes. The dense membranes present the transport of the components via dilution and diffusion through the membrane material. On the other hand, the porous membrane shows the transport of the components preferentially occurring in a fluid phase that fills the porous.

In some cases, the membrane can present both morphologies, and the classification considers the predominant transport mechanism. When the membrane presents a thin layer dense, sustained by a porous structure, the membrane can be considered dense once the permeant compounds' transport occurs via dissolution and diffusion.

Moreover, the classification extends to the composition of the membrane. If the membrane's material is the same in all membrane structures, it may be considered integral. Conversely, if the membrane's constitution is mixed (more than one component), it is classified as a composite membrane.

Porous membranes can be classified into two groups: the anisotropic (asymmetric) and the isotropic (symmetric). The membrane is isotropic when the porous density is the same along the membrane and anisotropic when the density varies throughout the membrane length (HABERT; BORGES; NOBREGA, 2006).

Figure 6 shows the main variations in membrane morphology, previously classified.

Figure 6 – The morphology of the membrane transversal section.

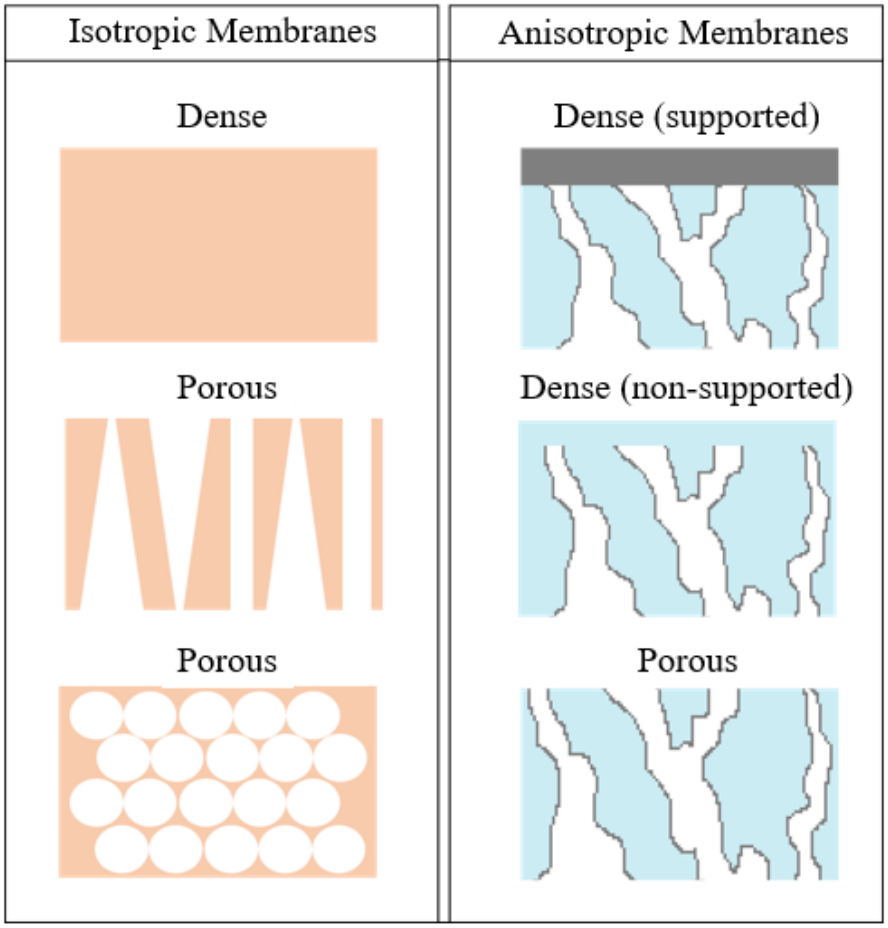

Font: The Author (2021)

2.3.2 Membrane modules

Different module configurations can be used in the MD process. The most common modules will be described below and illustrated in Figure 7.

i. Hollow Fiber: This module consists of a hollow fiber packaged and plugged inside a shell tube. The feed passes through the hollow fiber, and the permeate is outside of the membrane. The inverse flux can also be used. The feed flows from outside of the membrane, and the permeate is retracted inside the membrane. Hollow fiber membranes present the highest packing density (high as 9000 m^2/m^3) compared to other modules, increasing the compactness and reducing the physical requirement of the MD process.

ii. Plate and Frame: The flat sheet membrane module is the easiest to clean and replace, which becomes this module the most used in the laboratory scale. It

consists of a membrane layer allocated between two plates. This configuration, as the spiral-wound module, offers higher mixing and turbulence than other modules, which turns the membrane lesser prone to fouling and polarization effects than the hollow fiber modules;

iii. Tubular Membrane: In this module, the membrane is inserted between hot and cold cylindrical chambers. Because of this structure, the module is easy to clean, has a low fouling tendency, and presents a high effective area, which increases its economic attractiveness;

iv. Spiral Wound Membrane: This module offers high mixing and turbulence, such as the plate-and-frame module, which results in less effect of temperature polarization and fouling. It consists of a flat-sheet membrane covering a perforated tube that functions as a collection tube. The feed passes through the membrane surface in an axial direction. The permeation flows in a radial direction, conducting the permeate to the collection tube (ALKHUDHIRI; DARWISH; HILAL, 2012; DUONG *et al*., 2017b).

Figure 7 – MD modules configuration

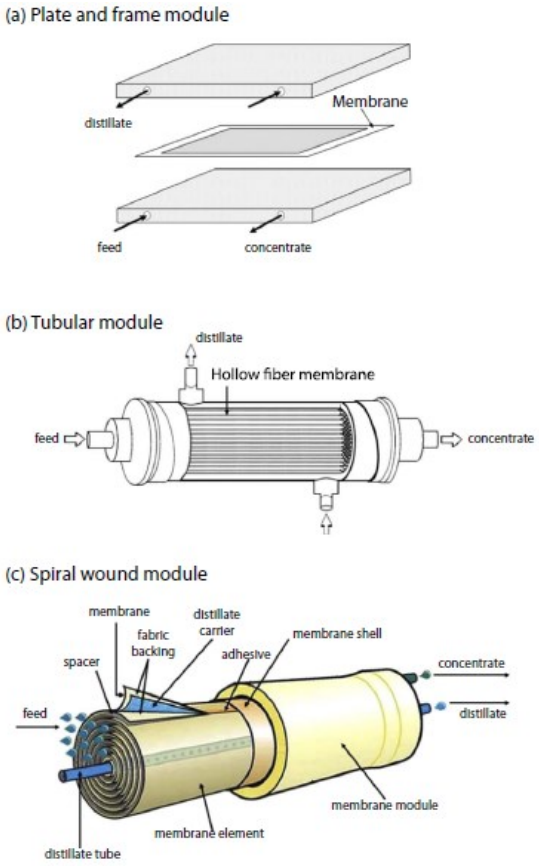

Font: Adapted from González, Amigo, Suarez (2017)

2.3.3 Membrane properties and desirable feature to the membranes used in the MD process

Firstly, the MD applications' preferred membranes should be hydrophobic (non-wetting) and microporous (GONZÁLEZ; AMIGO; SUÁREZ, 2017). The pores in the membrane are needed to establish a vapor flux. Simultaneously, the hydrophobicity prevents the liquid entrance into membrane pores, avoiding the liquid from the feed in the permeate side of the membrane (MENDEZ *et al*., 2019). Besides, to prevent wetting, the membrane has to have a reasonably small pore diameter, low surface energy on the membrane material, high roughness, high contact angle, high surface tension (ALKLAIBI; LIOR, 2005), and hence, high Liquid Entry Pressure.

The Liquid Entry Pressure (LEP) is the minimum hydrostatic pressure required on the feed solution to penetrate the membrane pores. It is a singular and specific characteristic of each membrane. High LEP values avoid the wetting in the membrane pores and, therefore, the unity's failure. Thus, a high LEP is required to the membranes for application in the MD process (DRIOLI; ALI; MACEDONIO, 2015).

In terms of high permeate flux, the membrane should have high porosity, low tortuosity, and a specific and small thickness (MENDEZ *et al*., 2019), besides a low resistance to mass transfer. The flux is linearly proportional to the porosity, which means that the flux increases with the membrane's high permeability (EYKENS *et al*., 2017a).

The tortuosity expresses how the pore of the membrane resembles a cylinder. It indicates the effective length that vapors must pass through, from the feed side to the permeate side.

Some possible reactions between the solvent and the membrane material may occur in operation and then affect the surface structure; acid gases or corrosive compounds of the feed solution can affect unit operation. For this reason, it is expected to membranes a high resistance to chemical attack.

In terms of thermal stability, a high temperature of operation may degrade, decompose, or change the nature of the membrane components, as well as the specific properties. For this reason, high thermal stability is required for the membrane materials (DRIOLI; ALI; MACEDONIO, 2015).

The membrane thickness influences the mass transfer phenomena, heat loss, and wetting phenomenon. The greater is the thickness, the greater is the mass transfer resistance, which is harmful to the MD process once it decreases the permeate flux. On the other hand, a higher

thickness improves the heat resistance, preventing heat losses (EYKENS *et al*., 2017a). An optimization between these two important points should be done to improve the MD operation.

Beyond that, the porosity results in a low thermal conductivity. This point is essential to prevent heat losses related to the heat conduction throughout the membrane, which would cause a low thermal efficiency in the MD process (EYKENS *et al*., 2017a). The polymer thermal conductivities are dependent on temperature and crystallization degree. Besides, the porosity dictates the mechanical stability of the membrane; Not only the overall porosity but also the mechanism of achieving the porosity.

Concerning pore size, the membrane should not have a single pore size. It should exhibit a range of pore size distribution, enabling different mass transport mechanisms and increasing the mass transfer through the membrane. The pore size, as well as the pore size distribution, is critical for the MD process. Big pores allow high permeate fluxes while makes the membrane susceptible to wetting. For this reason, the operation should be optimized between stable performance and high flux (DRIOLI; ALI; MACEDONIO, 2015). The desired values to the properties mentioned above are presented in Table 5.

Table 5 – Desired values to the properties of the membranes used in the MD process

Property	**Affects**	**Typical Values (Commercial Membranes)**	**Recommendation**
Porosity (ε)	Flux, energy efficiency, strength	39 – 90%	>80%
Contact Angle (θ)	Wetting resistance	80 – 160°	>90º, as high as possible
LEP	Wetting resistance	0.5 – 4.6	>2.5 bar
Pore diameter (d_p) (μm)	Wetting resistance, flux, and energy efficiency	0.012 – 1.2	0.1 – 1
Thickness (δ) (μm)	Flux, energy efficiency, strength	20 - 400	Low salinity: 30-60 High salinity: 2-700
Tortuosity (τ)	Flux, energy efficiency	1.1 – 3.9	As low as possible
Thermal conductivity (k_m) ($Wm^{-1}k^{-1}$)	Flux, energy efficiency	0.031 – 0.057	As low as possible
Tensile Strength (MPa)	Strength	3.4 – 57.9	As high as possible
Compaction (bar)	Flux and energy efficiency as a full scale, strength	PTFE: 22% at 0.6	Not compressible

Font: Eynkens *et al*., (2017); Mendez *et al*., (2019)

2.3.4 Membrane Materials for the MD Process

The polymeric membranes have been processed since 1990, and they are mainly manufactured from polytetrafluoroethylene (PTFE), polypropylene (PP), polyethylene (PE), or polyvinylidene fluoride (PVDF), which consist of hydrophobic materials (CAMACHO *et al*., 2013b). PTFE membranes are commonly manufactured by stretching and heating process. PP is fabricated by thermally induced phase separation or melt-spinning and cold-stretching. PVDF is made by non-solvent induced phase separation (HOU *et al*., 2017).

PTFE membranes show a superior permeate flux in terms of MD performances, followed by PP and PVDF membranes. It is attributed to differences in molecular configuration and the kinetics of polymer crystallization in the manufacturing production process that affects the pore opening, electrostatic repulsions between the molecules, and hydrophobicity. For this reason, PTFE presents a higher contact angle and hence, higher hydrophobicity and higher LEP than PVDF and PP membranes. This condition enables a higher vapor transport, higher mass transfer, and a higher permeate flux. The reason for these advantages is the larger pore size than the other materials and higher porosity, which eventually can result in a higher wetting tendency (DAMTIE *et al*., 2018).

Polymeric membranes can present hydrophilic behavior, such as cellulose acetate (CA) and polyamide (PA) membranes. The hydrophilic substrate acts as a support for the deposition of hydrophobic materials through membrane modification. In this case, this material functions as a dual-layer membrane, presenting opposite water wetting behaviors, leading to great performances in MD membranes. The hydrophobic layer is maintained in contact with the feed, while the hydrophilic layer is in contact with the permeate, which reduces the thermal polarization effects (CAMACHO *et al*., 2013b).

Polymers that present low hydrophobicity or non-desirable properties are susceptible to surface modification, commonly designed to enhance a specific MD process's desirable characteristic. The main goals of membrane modification are obtaining a higher primary flux and reduction of the pore wetting. To enhance hydrophobicity or reduce pore diameters, technologies such as blending the membrane materials with other polymers, incorporating hydrophobic groups, increasing membrane thickness, and designing dual or triple membrane structures are employed (HOU *et al*., 2017).

Nevertheless, polymeric membranes demonstrate several disadvantages in terms of thermal and chemical stabilities, which affect their lifetime. In this context, the ceramic membranes, made from metal oxides like alumina, titania, and zirconia (HUBADILLAH *et al.*,

2019), show higher mechanical strength, chemical and thermal stabilities, higher permeate flux. Its asymmetric structure of the pores minimizes the wetting effect in the MD operation compared to polymeric membranes. These characteristics play a key role in the MD process (CHEN *et al*., 2018). However, ceramic membranes require a hydrophobic surface modification once hydroxyl groups make the membrane water behavior naturally hydrophilic. For this reason, the organic-based membranes show a better promise to application in the MD process like desalination, because of their better performance in the modules, the ability to cast thinner polymeric membranes, which enhance the flux performance, and the lower cost, comparing to the ceramic membranes (CAMACHO *et al*., 2013b).

2.4 PHENOMENA INVOLVING THE OPERATION OF THE MD PROCESS

In this section, the main phenomena that occur in the MD process will be presented and discussed.

2.4.1 Temperature and Concentration Polarization

In the MD process, the heat and mass transfer phenomena are correlated. Heat is transferred from the feed to the permeate side by the phase change and conductive heat through the membrane. Because of the temperature difference between the feed and the permeate, the membrane acquires different temperatures on both sides, creating a temperature gradient through the membrane, where the thermal polarization phenomena appear (SANTORO *et al*., 2017).

This phenomenon develops in the non-isothermal MD process, decreasing the system driving force and reducing the permeate flux. For this reason, it is considered as a heat transfer limitation. It is explained by the exponential behavior of the vapor pressure with the temperature. The mitigation of a thermal polarization effect involves the creation of turbulence in the MD system through aeration. In this way, the membrane structure does not control the heat transfer (ALSAADI *et al*., 2014). The thermal polarization phenomenon can be illustrated in Figure 8.

On the other hand, the concentration polarization occurs both in isothermal and non-isothermal MD processes. This phenomenon is related to the concentration gradient between the two sides of the membrane that is originated in the MD process. In this case, a fractional

reduction in MD flux is related to an increase in feed concentration near the membrane surface. This effect is lower for diluted solutions (ALSAADI *et al*., 2014) because the effect of solute in the feed alters the fluid-dynamics, reducing the vapor pressure (MARTÍNEZ-DÍEZ; VÁZQUEZ-GONZÁLEZ, 1999).

In other words, concentration polarization is defined as the increase of solute concentration on the membrane surface compared to the solute concentration in the bulk solution. The solute accumulated on the membrane surface creates a diffusive flow back to the feed, making the properties of the boundary layer different from bulk solution properties (ALKHUDHIRI; DARWISH; HILAL, 2012).

Figure 8 – Thermal Polarization phenomenon

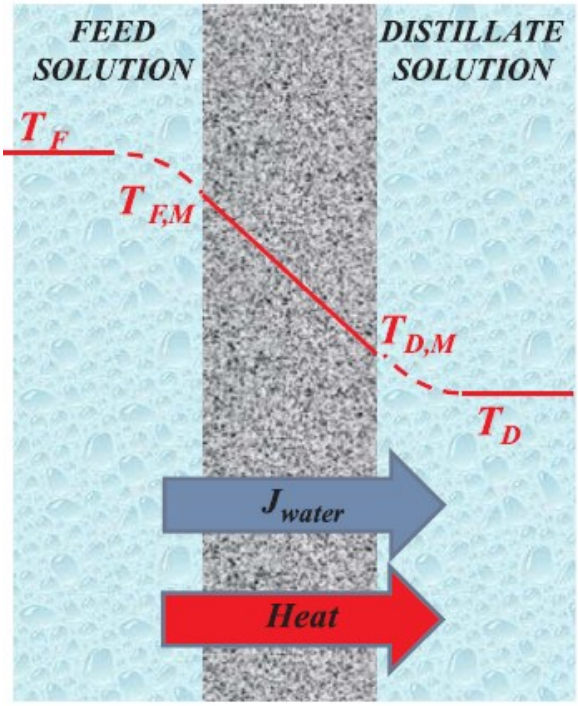

Font: Santoro *et al*. (2017).

Concentration polarization has been linked to membrane scaling and fouling and harshly influences the separation process's performance (LOKARE *et al*., 2019). This phenomenon reduces the process driving force and hence, reduces the mass flux. The reduction of mass flux is more significantly affected by the thermal polarization effect than the concentration polarization (MARTÍNEZ-DÍEZ; VÁZQUEZ-GONZÁLEZ, 1999).

2.4.2 Fouling

The membrane fouling consists of the biggest concern to the commercialization of the MD process focused on the water treatment and desalination. This phenomenon reduces the membrane permeability, the membrane lifetime and increases the energy cost. The fouling is the accumulation of unwanted deposits on the membrane surface or into the membrane pores, which reduces the membrane efficiency due to the increase in the mass transfer resistance (DUONG *et al.*, 2017a). The porous deposit layer increases the heat resistance through the membrane, while the non-porous increases the mass transfer resistance (TIJING *et al*., 2015).

Compared with other separation processes using membranes, such as Nanofiltration (NF) and Reverse Osmosis (RO), the MD process is lesser prone to membrane fouling. This fact is attributed to the lower hydrostatic pressures employed in this process, with the liquid phase's discontinuity (DUONG *et al*., 2017a).

Several factors can induce the fouling formation, such as the low hydrophobicity of the material, degradation of the membrane, presence of inorganic solutes in the feed, inadequate thickness, and organic or colloidal molecules on the feed solution. Fouling is a time-dependent process, and its long-term effect cannot be easily predicted. Its mechanism depends on the interaction forces between the particles and the membrane (TIJING *et al*., 2015).

The fouling can be classified according to its source. For example, the inorganic scale is the deposition of alkaline, non-alkaline, or basic salts on the membrane, such as $CaCO_3$, $CaSO_4$, $MgCl_2$, and $Mg(OH)_2$, originating a cake-layer. Its formations depend on solution temperature and pH. On the other hand, the fouling can be shown as particulate or colloidal formation, as clay, silt, particulate humic substances, silica, and iron oxides. Biofouling is the deposits of microorganisms on the membrane and occurs mainly in the food, beverage, and wastewater industries. Besides, materials such as proteins, amino sugars, polysaccharides, and humic substances can be deposited on the membrane, characterizing the natural organic fouling (WARSINGER *et al.*, 2015). Hydrophobic MD membranes are more prone to organic fouling due to their capacity to adsorption organic materials (DUONG *et al*., 2017a).

The fouling is the main contributor to membrane wetting, remarkable by foulant adsorption, pore blockage, and cake formation. It is affected by temperature, which influences the scaling solubility and flow velocity (GONZÁLEZ; AMIGO; SUÁREZ, 2017).

Concerning water recuperation from textile wastewater using the MD process, dye molecules adsorb on the membrane due to the polar interactions, hydrophobic interactions, and hydrogen bonding between the molecules and the membrane. This adsorption leads to pore

blockage and affects the membrane wettability. The deposit of the dye molecule can occur on the membrane surface and also inside the membrane pores. The fouling caused by the dye decreases the contact angle, which turns the membrane more prone to the wetting phenomenon (LAQBAQBI *et al.*, 2019a).

To minimize the fouling phenomenon, the particles and the membrane surface should be repulsive to each other. Fouling increases the thermal polarization effect, which results in a decrease of driving force to the separation (TIJING *et al*., 2015). Besides, the use of pretreatments as filtration, coagulation, boiling water, membrane flushing, gas bubble, reverse flow, antiscalants, and chemical cleaning are good alternatives to prevent and treat the fouling (WARSINGER *et al*., 2015).

2.4.3 Wetting

The wetting phenomenon is the loss of membrane hydrophobicity, allowing the passage of contaminants and non-volatile compounds from the feed solution into the permeate side. The wetting affects the permeate quality and the MD process's overall efficiency (GARCÍA *et al*., 2018). The liquid penetration into the membrane pores occurs if the transmembrane hydrostatic pressure is higher than Liquid Entry Pressure (LEP) or if the solution contains organic or inorganic compounds capable of adsorbing/deposit on the membrane surface (REZAEI *et al*., 2018).

The wetting is affected by three primary parameters: Liquid Entry Pressure, surface wettability, and membrane surface free energy. Many membranes and process conditions directly affect the LEP, including operation temperature, porosity, roughness, solution composition, pore shape, and liquid surface tension. As higher the LEP, the higher is the membrane wetting resistance. The membrane surface free energy is the energy difference between the bulk and the surface of the membrane. It depends on the receding contact angle and advancing contact angle of two liquids on the membrane surface. It directly affects the surface wettability, which also depends on the contact angle (REZAEI *et al.*, 2018).

When the wetting occurs, water evaporation's active surface area is reduced on the membrane, reducing the vapor flux. Besides, the wetted membrane pores reduce the membrane's rejection rate, decreasing the permeate quality (DUONG *et al.*, 2017a). Many process conditions lead to pore flooding and decrease the product quality, such as membrane aging, membrane fouling, and feed water contamination by surfactants or organic compounds (ALKLAIBI; LIOR, 2005).

The membrane wettability is classified as non-wetted, surface wetted, partially wetted, and fully wetted. The non-wetted corresponds to a membrane that allows the maximum vapor transport through the pores, achieving the highest flux and rejection rate. A surface-wetted membrane presents a gap for vapor transport, but there is no penetration of feed water into the pores. A partially wetted membrane allows the feed water to penetrate the pores, while vapor transport decrease in other pores. The fully wetted membrane allows the complete penetration of the feed water into the pores (CHOUDHURY *et al.*, 2019). Figure 9 illustrates this classification. Partial wetting under specific conditions leads to a reduction in the permeate flux due to decreased mass transfer (solid blue line). On the other hand, if the feed solution contains some foulant, the partial wetting can increase the permeate flux, related to overtaken liquid transport than vapor transport, followed by a rapid decrease due to the pore blockage occasioned by the foulants (blue dash line) (REZAEI *et al.*, 2018).

Figure 9 – Wetting Degrees

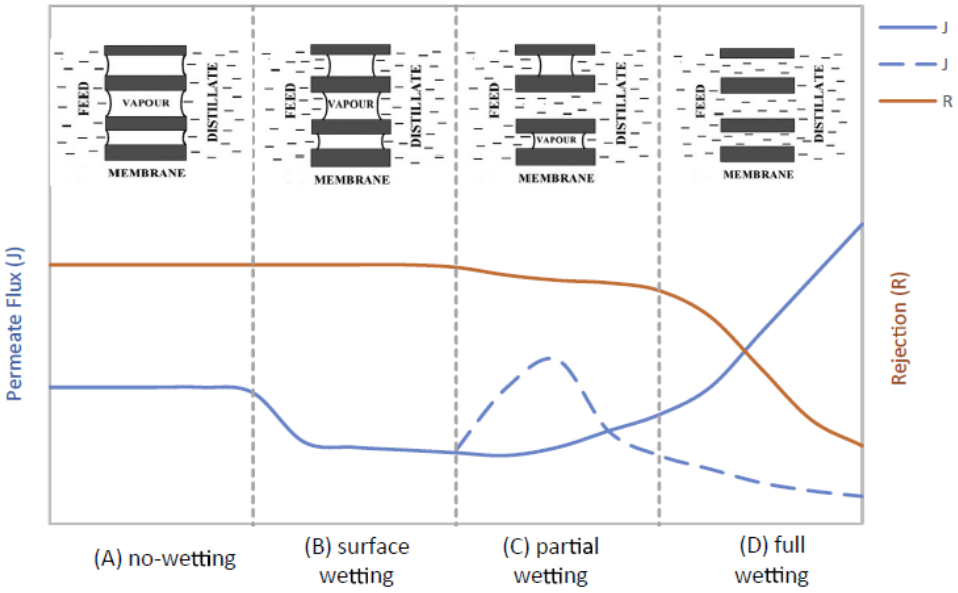

Font: Rezaei *et al.* (2018)

PTFE shows the highest wetting resistance regarding polymeric membranes applied to the MD process once it presents high porosity and high hydrophobicity compared to other commercial membranes (RAMLOW; MACHADO; MARANGONI, 2017). However, all the commercial membranes used in MD, such as PP, PTFE, and PVDF, showed a partial wettability after a specific time, which compromises the shelf life of these membranes (REZAEI *et al.*, 2018).

Some techniques such as rinsing and drying the membrane with water or chemical products and backwashing to remove crystals and scales are employed to mitigate the wetting and restore the membrane. However, this restoration is still a challenger. In many cases, fouling is associated with the wettability or an irreversible structural change induced by the liquid into the pores occurred. (REZAEI *et al*., 2018).

Concerning the water recovery from textile wastewater, some auxiliaries employed in the dyeing process and present in the effluent can affect the membrane wettability. The wetting phenomenon's main concern is the high concentrations of surfactants, directly affecting the membrane performance. Surfactants in textile wastewater reduce the membrane hydrophobicity once they exhibit amphiphilic properties and reduce the feed solutions' surface tension. Detergents and dispersants employed in cotton and polyester's dyeing process show a hydrophilic head and a hydrophobic tail. In this case, the membrane wetting is caused by physical and chemical interactions between the polymeric membrane and the foulant. The hydrophobic tails of surfactants interact with the hydrophobic membrane surface, creating a hydrophilic channel. Besides, it can be caused by the adsorption of surfactants into the membrane pores (MOKHTAR *et al.*, 2016).

The improvement of wetting resistance can be hit by surface modification using advanced materials (MOKHTAR *et al.*, 2016). For example, García *et al*. (2018) added hydrophilic coatings on the membrane surface, such as polyurethane. The hydrophilic polyurethane is selectively permeable to water vapor. It is allied to a hydrophobic surface, preventing the wetting phenomena, which turns this material into an ideal candidate for the textile wastewaters treatment. On the other hand, Lin *et al*. (2015) made a thin layer of agarose hydrogel attached to the hydrophobic porous Teflon membrane's surface, which avoids the surfactant penetration into the hydrogel layer.

In this sense, the study of surface modification to improve membrane hydrophobicity plays a crucial role in consolidating the MD technology to water recovery from textile wastewater.

2.5 MODIFICATION OF COMMERCIAL MEMBRANES

Several methods are employed to modify membranes to improve their characteristics, such as hydrophobicity, oleophobicity, and anti-fouling properties. Some of these methods will be described in this section. The focus of membrane modification is enhancing the hydrophobicity of polymeric membranes to mitigate wetting phenomena to this research.

A wetting resistance is obtained by the construction of superhydrophobic and omniphobic surfaces to the membranes. Superhydrophobic membranes can be formed by the employed inorganic nanoparticle or micro-particle coating, as fluorographite, silica, and titanium oxide. These nanoparticles develop rough and hydrophobic surfaces and decrease the surface energy of the pristine membrane. On the other hand, omniphobic membranes repel low surface tension contaminants, water, and oil. Its obtention involves single/multi-level re-entrant structures that show low surface energy, ensuring wetting resistance (CHOUDHURY *et al*., 2019).

Simultaneously increase the LEP value and the contact angle is the main challenge of superhydrophobic layer construction in a hydrophobic membrane. The LEP is affected both by surface wettability and wettability inside the pores. The addition of layers to the membrane surface can reduce the permeability once it increases the membrane thickness. In terms of the fabrication of omniphobic membranes, the main attached problems control the faultless surface. (REZAEI *et al.*, 2018).

2.5.1 Strategies of membrane modification

The methods usually employed to modify membranes include superficial and microstructural modifications or modifications in the membrane matrix (REZAEI *et al.*, 2018). The requirements of membrane application determine the type of modification used (FENG *et al.*, 2018). The most common types of membrane modification consist of wet-chemical modification, plasma treatment, irradiation, atomic layer deposition, high-temperature melting, and pore filling, briefly described below.

i. *Wet-chemical modification*: This method is widely employed due to its easy operation and mild reaction conditions. Chemical solutions are used in this process to obtain membranes with specific surface functionalities (FENG *et al.*, 2018). In this method, fluorinated surfaces with modified macromolecules can be incorporated to enhance the pristine membrane's hydrophobicity.

ii. *Plasma treatment:* In this method, monomer molecules are ionized and form free active radicals, which are aggregate on the membrane surface by adsorption, condensation, and polymerization, resulting in dense hydrophobic coating layers (TAI *et al.*, 2018). The particles employed in plasma treatment are used in material surface cleaning, sterilization, activation, and grafting. Plasma surface activation results in a hydrophilic structure. On the other hand, plasma-assisted grafting changes both surface morphology

and chemical groups of the polymeric membrane. The radicals initiate the polymerization reactions, forming grafted copolymers on the membrane surface (FENG *et al*., 2018).

iii. *Irradiation:* This technique includes ultraviolet, gamma rays, laser, ion beam, and electrons, and it is employed to modify polymers, changing the morphology structure, surface properties, and membranes chemical composition. Irradiation using ions can change the physical properties of thin films, making irreversible changes. Besides, it can modify the near-surface characteristics of the bulk polymer. Gamma irradiation is employed for polymerization and grafting processes. The UV irradiation requires a pre-treatment method to break the covalent bonds once it is a low-energy process (FENG *et al*., 2018).

iv. *Pore filling*: This process involves employing inorganic particles or liquids into polymeric porous membranes by filling, which modify membrane properties and induce pH-sensitive membranes. This technique is used to fabricate membranes to use in fuel cells and lithium-ion batteries (CUI; DRIOLI; LEE, 2014).

v. *Atomic layer deposition*: This technique involves metal depositions on internal pores of the coated membrane. This reaction occurs on a binary sequence, with the deposition of a binary compound film and substrate functionalization. There is an incongruity to apply this technique once many polymers decompose at the temperatures required for this reaction (FENG *et al*., 2018).

vi. *High temperature melting*: The melting point's irradiation can heal polymer defects, decrease porosity and improve mechanical properties. Besides, it can decrease the crystallinity value, which reduces the surface free energy of the membrane. The dendrites formed by heating improve the surface roughness and affect the contact angle (FENG *et al*., 2018).

2.5.2 Electrospinning/Electrospraying

The electrospinning technique is one of the most common methods to synthesize porous membranes. In 2008, electrospinning was employed for the first time to fabricate membranes for membrane distillation applications (FENG *et al*., 2008). In contrast, the membrane surface modification for MD application is a recent issue once it has been studied only since 2011. Thorugh electrospinning, nanofibers can be obtained with high porosity (above 80%) and roughness. This characteristic positively affects the membrane's mass flux and thermal

efficiency (EYKENS *et al.*, 2017b). Its high versatility leads to design membrane modifications without losses in membrane porosity, and its reentrant formed structure achieves high hydrophobicities.

The electrospinning technique is governed by self-assembly processes induced by electric charges (AGARWAL; GREINER; WENDORFF, 2013). When dealing with membrane modification, the fiber-collector is recovered by the pristine membrane, which will receive the fibers or drops on its surface. The materials to membrane modification compound a dope solution submitted to a high voltage electric field. A syringe pump is employed to flow the dope solution, occasioning a micro jet on the pristine membrane at the collector. An electric field is created by the high voltage supplier between the metallic needle and the collector. The charged droplet is formed when the applied tension increases up to the hemispherical surface tension, which is lower than the repulsive force. The solvent evaporates before forming the fibers on the membrane surface (FENG *et al.*, 2018; LIU *et al.*, 2018). When solutions with low polymer concentration – and low viscosities – are employed in the electrospinning system, the droplet formation replaced the fibers, where the technique is called electrospraying. The electrospinning/electrospraying apparatus used for membrane modification is illustrated in Figure 10.

Figure 10 – Electrospinning (a)/ Electrospraying (b) apparatus

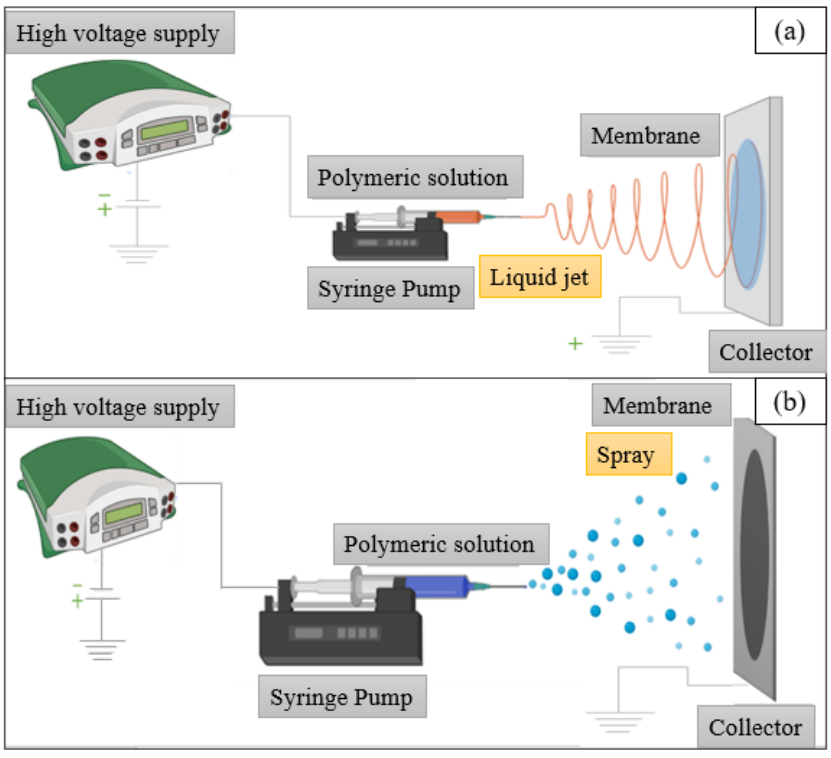

Font: The Author (2021)

2.5.2.1 Parameters that influence the electrospinning process

Operational conditions that could affect the electrospinning consisted of the high voltage supplier's tension, the distance tip-to-collector, and the dope solution's flow. Moreover, it could be affected by the solution viscosity, time under the jet, and environmental parameters.

i. *Viscosity*: The viscosity of the polymeric dope solution affects the fiber diameter. Low viscosities result in the formation of microdroplets, where the technique is called electrospraying. The formation of fibers or droplets is also affected by the concentration and nature of the polymer. For the electrospraying, the high viscosity of the solution leads to the formation of smaller drops.
ii. *Voltage of the high voltage supplier*: The droplets become more prolate, extending in the electric field's direction. The fiber diameter decreases as the electric field increases. (AGARWAL; GREINER; WENDORFF, 2013; LIU *et al*., 2013).
iii. *Distance tip-to-collector*: A minimum distance between the tip and the collector is required to create uniform fibers. Too small or too large distance leads to the beads generation, causing defects on the membrane surface.
iv. *Feed flow rate*: Beads are also formed with a high flow rate, and the fiber diameter decreases with a decrease in the feed flow rate. (BHARDWAJ; KUNDU, 2010).
v. *Environmental conditions*: temperature and humidity also affect the formation of drops/fibers (JUNG *et al.*, 2016). The increase in temperature results in a fiber diameter decrease. On the other hand, high humidity creates circular pores on the fibers. In a general way, humidity of 50-60% and temperature of 20-25°C are the ideal environmental conditions for the electrospinning process.
vi. *Time under the jet*: Poor times under the jet can originate a low cover on the membrane surface, being harmful to achieve desirable membrane characteristics through this technique.

Although the electrospinning parameters play a key role in membrane modification, they are not widely studied in the research involving membrane modification, especially regarding the jet/spray time.

2.6 STATE OF THE ART OF ELECTROSPINNING APPLIED TO MEMBRANE MODIFICATION TO MEMBRANE DISTILLATION APPLICATION

A state-of-the-art investigation was carried out in the CAPES database concerning the environmental research about membrane modification using the electrospinning technique for membrane distillation applications. The words ("electrospinning" OR "electrospraying") AND "membrane distillation" were employed in the search terms, where 360 results were found. Refining the search to the period from 2015 until the moment, 315 academic papers were found. The articles' dynamic analysis was performed, excluding review papers, papers focusing on the membrane fabrication via electrospinning, and papers that do not apply the modified membranes in membrane distillation. These filters resulted in 19 works. A more precise search term was not applied to avoid excluding some works that do not have "membrane modification" in their titles or keywords. Table 6 summarizes the main information about the state-of-art of this topic.

The electrospinning produces membranes with higher porosity and higher interconnected open structures than other membrane modification techniques. This fact is attributed to a high surface roughness originated from overlapping the fibers – in the case of electrospinning – or drops regarding electrospraying. Among the investigated studies, there is an exploration of several kinds of substrates, such as polymeric membranes (PET, PP, PSF, PTFE, PA, and PVDF), natural substances, such as cellulose filter paper. All the modified membranes were applied in DCDM, except one that applied the modified membrane in AGMD (ATTIA *et al*., 2018a) and another in VMD (LI *et al*., 2019b). It was noted a clear preference of tested solutions with electrospun modified membranes, where 57.9% of the studies employed NaCl solutions, simulating a desalination process; 26.3% employed mixtures of NaCl with crude oil, where the electrospinning modification achieved oleophobic properties. Only 15.8% of the investigated studies applied the modified membranes against low surface tension solutions, such as surfactants. There were no reports about the electrospun modified membranes applied in MD operation to water recovery from textile wastewater, highlighting innovation for the topic embraced by this work.

In a general way, the electrospinning or electrospraying to modify membranes focused on achieving super-hydrophobic, oleophobic, or omniphobic surfaces, on designing membranes capable of long-term operations, with flux enhanced or with anti-fouling properties.

Table 6 – State-of-art of electrospinning modified membranes to membrane distillation applications, since 2015

(to be continued)

Reference	Membrane/ Substrate	Material of modification	Contact Angle	Feed composition	Permeate Flux (J)	Property achieved
(KHAYET; GARCÍA-PAYO; MATSUURA, 2019a)	Polysulfone (PSF)	Fluorinated Polyurethane additive (FPA)	150º	NaCl aqueous solution (12, 30, 60 g L^{-1})	53.8 kg m^{-2} h^{-1}	30 – 32 h without wetting
(WANG *et al*., 2019a)	PVDF	Polyetherimide (PEI)/Ethane diamine (EDA)	145º for oil	NaCl (35 g L^{-1}) + crude oil (1 g L^{-1}) aqueous solution	4.5 L m^{-2} h^{-1}	Oleophobicity
(DENG *et al*., 2019)	PVDF	PVDF + aPP	156º	NaCl aqueous solution (35 g L^{-1})	135.3 kg m^{-2} h^{-1}	50 h tested without wetting
(ATTIA *et al*., 2018a)	PVDF	PVDF + Al2O3 NPs	154º	NaCl aqueous solution (35 g L^{-1})	18.6 L m^{-2} h^{-1}	30 h tested without wetting
(ZHAO *et al*., 2018a)	Biodyne-A Nylon 6,6	PVDF - HFP + AC (activated carbon)	142.7º	NaCl aqueous solution (35 g L^{-1})	45.6 L m^{-2} h^{-1}	Improve in the permeate flux
(HOU *et al*., 2018a)	PTFE	Cellulose acetate (CA)+ SiNPs	154.2º for oil	NaCl (600 mM) + crude oil (1 g L^{-1}) aqueous solution	19.92 L m^{-2} h^{-1}	Fouling resistance
(WANG *et al*., 2018)	PTFE	Poly (Vinyl Alcohol) (PVA)	148.7º for oil	NaCl (35 g L^{-1}) + crude oil (1 g L^{-1}) aqueous solution	15 kg m^{-2} h^{-1}	Fouling resistance
(HAMMAMI *et al*., 2017)	Polyester (PE)	PEI + PMO NPs	142º	NaCl aqueous solution (35 g L^{-1})	31 L m^{-2} h^{-1}	Flux increase (140%) and biofouling resistance
(HOU *et al*., 2018b)	PTFE	Poly (Vinyl Alcohol) (PVA) + SiNPs	156.5º for oil	NaCl (600 mM) + crude oil (1 g L^{-1}) aqueous solution	17.53 kg m^{-2} h^{-1}	Fouling resistance

Table 6 – State-of-art of electrospinning modified membranes to membrane distillation applications, since 2015

(to be continued)

Reference	Membrane/ Substrate	Material of modification	Contact Angle	Feed composition	Permeate Flux (J)	Property achieved
(RAY *et al.*, 2018)	PP	Cera Flava + Polysulfone (PSF)	162º	NaCl aqueous solution (30 g L^{-1})	6.4 L m^{-2} h^{-1}	Superhydrophobicity and long-term operation
(RAY *et al.*, 2017a)	PP	Poly (Vinyl Alcohol) (PVA) + Triton X-100	-	NaCl aqueous solution (10 g L^{-1})	6.9 L m^{-2} h^{-1}	High permeate flux (2 times higher than PP), long-term operation, higher mechanical stability
(HOU *et al.*, 2019a)	Polyester (PET)	Cellulose acetate (CA)+ SiNPs + PDTS	155.6º for water and 95.3º for decane	NaCl (35 g L^{-1}) + SDS (0.1 - 0.5 mM) aqueous solution	13.6 kg m^{-2} h^{-1}	Omniphobic behavior, anti-wetting performance (120 h without wetting in solution with 0.2 mM of SDS)
(LI *et al.*, 2019b)	Polyester (PE) and Polypropylene (PP) fabrics	PVDF	140º	NaCl aqueous solution (35 g L^{-1})	49.3 kg m^{-2} h^{-1}	Long-term operation, wetting and scaling resistance, high permeate flux
(LEE; DEKA; AN, 2019a)	PVDF	PVDF + PDMS + Silica Aerogel	162.1º for water and 156.1º for SDS solution	NaCl (35 g L^{-1}) + SDS (0.1 mM) aqueous solution	20 L m^{-2} h^{-1}	Long term operation, anti-wetting performance, operation in low-surface tension solution
(AL-FURAIJI *et al.*, 2019)	Polyether sulfone (PES)	PVDF	130.2º	NaCl aqueous solution (5 M)	~9 kg m^{-2} h^{-1}	High mechanical strength, higher performances than pristine membranes
(RAY *et al.*, 2017b)	Cellulose Filter Paper (CFP)	Polysulfone (PSF) + SDS	128.4º	NaCl aqueous solution (30 g L^{-1})	9 L m^{-2} h^{-1}	Mechanical and chemical durability, long-term operation

Table 6 – State-of-art of electrospinning modified membranes to membrane distillation applications, since 2015

(conclusion)

Reference	Membrane/ Substrate	Material of modification	Contact Angle	Feed composition	Permeate Flux (J)	Property achieved
(DEKA *et al.*, 2019)	PVDF	Organosilane + 30% ZnO	159º for water, 129.6º for SDS saline solution, 130.4º for ethanol and 126º for vegetable oil	NaCl (0.015 v/v) + SDS (0.4 mM) aqueous solution	22.17 L m^{-2} h^{-1}	High anti-wetting/ antifouling performance and high salt rejection operating with a surfactant solution
(LI *et al.*, 2019a)	PP nonwoven fabric	PVDF + FTES+GO	140.5º	NaCl aqueous solution (35 g L^{-1})	36.4 kg m^{-2} h^{-1}	Improvement of 2 times on the permeate flux. Anti-wetting property, long term operation (60h)
(TANG *et al.*, 2019)	PTFE membrane	PAN hydrolyzed with EDA and NaOH	155º for oil (EDA) and 161.7º for oil (NaOH)	NaCl (35 g L^{-1}) + crude oil (1 g L^{-1}) aqueous solution	16.7 kg m^{-2} h^{-1}	Anti-oil-fouling and superoleophobic performance

Font: The author (2021)

Super-hydrophobic membranes via electrospinning modifications were obtained mainly in three different ways: using fluoropolymers (CHEW *et al.*, 2017; DENG *et al*., 2019; KHAYET; GARCÍA-PAYO; MATSUURA, 2019b; LEE; DEKA; AN, 2019b; LI *et al*., 2019a; ZHAO *et al.*, 2018b); using nanoparticles in the dope solution (ATTIA *et al*., 2018a; HAMMAMI *et al.,* 2017; HOU *et al.,* 2019a; LEE; DEKA; AN, 2019b); and using natural hydrophobic materials (RAY *et al.*, 2018), where the highest water contact angle among the electrospinning modified membranes was achieved (162.5º) using Cera Flava in the dope solution. The main nanoparticles employed in the dope solutions among the evaluated studies were Al_2O_3 (ATTIA *et al.*, 2018a), PMO nanoparticles (HAMMAMI *et al*., 2017), and silica aerogel (LEE; DEKA; AN, 2019b).

The oleophobic membranes were obtained combining hydrophobic and hydrophilic layers, that presented antifouling properties in most cases. The membrane oleophobicity is obtained in two main ways: when a cross-link is employed after electrospinning modification (LIN *et al*., 2018; TANG *et al.*, 2019; WANG *et al*., 2019b); or via one-step electrospinning modifications using hydrophilic agents in the dope solution (HOU *et al.*, 2018a).

The anti-fouling behavior can be related to the repellence properties against the inorganic particle depositions (scaling) or against organic depositions, which means repellence against organic and oily foulants. Among the investigated studies, 37.5% reported the anti-fouling related to inorganic depositions (HAMMAMI *et al*., 2017; LI *et al*., 2019b; RAY *et al*., 2018), where anti-biofouling behaviors were also noticed. The anti-oil fouling property consisted of 50% of the anti-fouling electrospun modified membranes (HOU *et al.*, 2018a; TANG *et al.*, 2019; WANG *et al.*, 2018, 2019a), and it was obtained combining hydrophobic and hydrophilic layers with or without cross-linking, or through the incorporation of the nanoparticles.

An omniphobic behavior is related to the repellence of water, oil, and low surface tension solutions, such as the surfactants. These membranes are attractive to water recuperation from complex wastewater because of their asymmetric wettability. Among the evaluated studies, omniphobic behaviors were achieved combining organosilanes and zinc oxide nanoparticles (DEKA *et al*., 2019), cellulose acetate with silica nanoparticles followed by fluorination (HOU *et al.*, 2019a), and silica aerogel with PVDF and PDMS (LEE; DEKA; AN, 2019b).

Long-term operations with the modified membranes were reported by 47.4% of the evaluated studies. The influence of the hydrophobicity improvement on the anti-wetting behavior was studied along the time (ATTIA *et al.*, 2018b; DENG *et al.*, 2019; KHAYET;

GARCÍA-PAYO; MATSUURA, 2019a; LEE; DEKA; AN, 2019b; LI *et al*., 2019a, 2019b; RAY *et al.*, 2017b, 2018). Among these studies, only 9.2% performed DCMD tests with solutions differing from the typical desalination. The maximum operation time was achieved by Hou *et al*. (2019), where the modified membrane performed with stable rejection during 120 h, even in a concentration of 0.2 mM of Sodium Dodecyl Sulfate (SDS).

Electrospinning seems to be a promising technique to obtain membranes with enhanced permeate fluxes in MD operations once it achieves high membrane porosities. The high flux obtained among the evaluated studies corresponded to an increase of 140% comparing with the pristine membrane (HAMMAMI *et al*., 2017). In this work, organosilica nanoparticles were incorporated into the dope solution.

The scientific scenario analysis led to observe the persistence of problems involving membranes to MD applications, even for the separations where this technique is already consolidated (i.e., desalination), explaining the increasing research about the membrane modifications. Moreover, it shows a gap in the applications of electrospinning modified membranes beyond traditional desalination, combined or not with traditional surfactants, such as SDS. The background proposed in this state-of-the-art guided the present study in choosing the substrate and materials of the dope solution to achieve the membrane's necessary characteristics to operate against components from textile wastewater.

2.6.1 Membrane Distillation applied to water recovery from solutions containing textile solutes

Concerning the water recovery from textile effluents, some research has been developing, from the MD separations using dyes solutions to separations involving low surface tension solutions, such as dyeing bath additives. Ramlow *et al*. (2019a, 2019b, 2019c) employed the DCMD and VMD configurations to water recovery from different classes of dyes (reactive and disperse), different chromogenic groups, and real wastewater from the dyeing process of polyester, cotton, and viscose. High rejection rates were obtained for the dye solutions (>95.9%) using PTFE and PP membranes. However, a wetting phenomenon was evidenced in operation with the real effluents due to surfactants' presence. Higher fluxes were obtained for the VMD configuration than DCMD since the mass transfer was enhanced due to the permeate side's vacuum application. Ramlow; Tolentino Filho; Andrade (2019) reported MD's potential for water recovery from solutions containing textile dyes (disperse and reactive classes) using a

PVDF membrane in a DCMD configuration. Rejection rates of 100% were obtained for the disperse dye solutions.

The operating conditions for the DCMD applications in water recovery from textile wastewater were determined by De Sousa Silva *et al.* (2021), where synthetic solutions of reactive and disperse black dyes are tested. The feed flow rate, permeate flow rate, and feed temperature was varied. Tests with residual waters from laboratory dyeing baths of cotton and polyester evidenced the PTFE membrane's wetting. The determination of the operational conditions in DCMD application with textile dyes was also reported by Tolentino Filho *et al*. (2020) at high dye concentration. Simulating the DCMD operation with textile compounds in MATLAB, Madalosso *et al.* (2020) determined the singular influence of each MD variable in the permeate flux and evidenced the harsh effect of feed temperature.

Tolentino Filho (2019) studied the influence of the dye concentration in the DCMD performance and the singular influence of each additive of the cotton and polyester dyeing bath in the overall DCMD performance at fixed operational conditions. Excellent results were obtained in the rejection rate for the salts employed in the dyeing baths. Wetting was also reported operating with surfactants, which mainly consisted of detergent and dispersant. The formic acid was not well separated by the DCMD process, demonstrated by the low rejection rates obtained for this additive. The permeate flux of DCMD was decreased as much the dye concentration increased.

Regarding the recent studies, it is possible to infer that the research about this topic is moving forward to the mitigation of operational problems, such as the fouling and wetting, related to the presence of low surface tension solutions, and foulant agents, such as salts and some classes of dyes. Moreover, strategies to improve the total of water produced from DCMD operation, such as innovative configurations using parallel or series units, are also an emerging need.

The recent studies evidenced the wetting caused by the surfactant presence as the biggest concern to the MD operation to recuperate water from textile wastewater. Moreover, the behavior study of this membrane process with other dye classes beyond the reactive and disperse is still unknown. These facts justify the objective of the present study, moving forward to the consolidation of MD to water recovery from textile wastewater.

3. MATERIALS AND METHODS

This section will present the materials employed in membrane modification, the analytical equipment, the experimental units of electrospinning and direct contact membrane distillation, and methods employed in this work. A schematic flowchart is presented (Figure 11) to better visualization of the experimental procedure.

Figure 11– Schematic methods flowchart

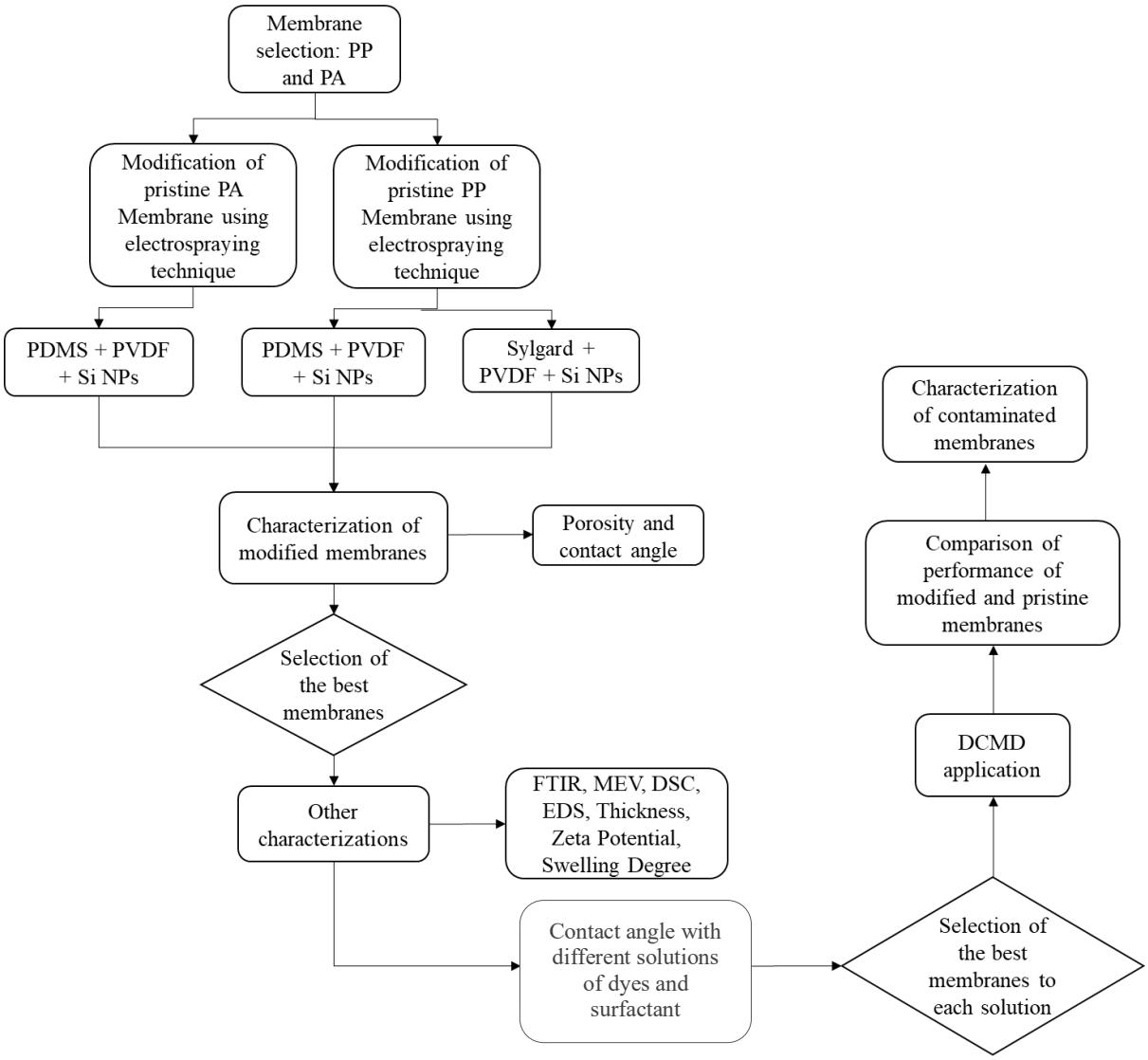

3.1 MATERIALS

3.1.1 Materials to membrane modification

Two different membranes were selected to design a membrane modification based on their cost and performance in the MD process. The polypropylene (PP) (PP023001 Sterlitech Corporation) membrane was selected as a hydrophobic substrate. This membrane has not any material support. According to the supplier, the volumetric porosity of the membrane varies between 65 and 85%, and the pore size is about 0.22 μm. The selection of the PP membrane was based on a lesser report of membrane modification using this substrate, and based on the availability. The polyamide membrane (PA) (NF-90 DOW FILMTECTM Membranes) was chosen as a hydrophilic substrate. This membrane is supported in PET and shows a 17% porosity and pore size of 0.68 nm. The PA membrane was selected due to their distinct water behavior and its lesser cost comparing to the PP membrane. The chemical structures of the constituted membrane polymers are shown in Figure 12. The reagents employed in the experimental procedure for membrane modification are listed in Table 7, and they were not submitted to any purification.

Figure 12 – Membrane polymers

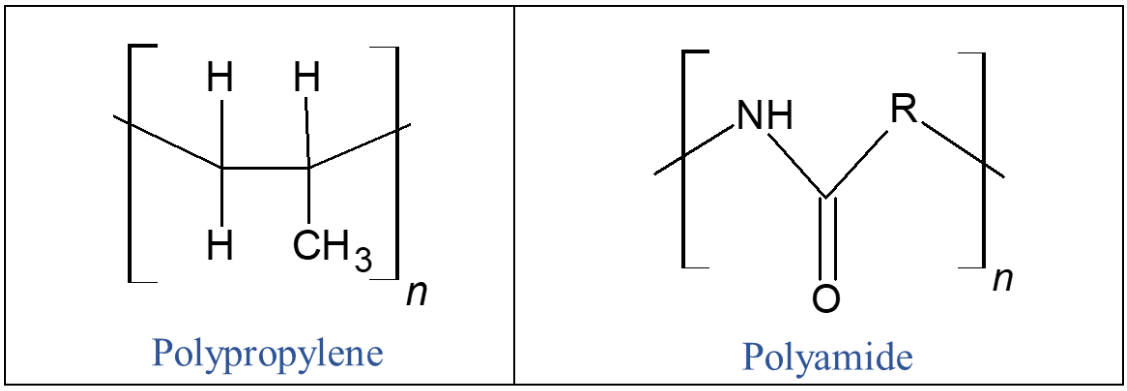

Font: The Author (2021)

Table 7 – Reagents used in membrane modification

Reagent	Supplier	Additional information
Tetrahydrofuran (THF)	Neon Comercial	P.A/ACS
Dimethylformamide (DMF)	Neon Comercial	P.A/ACS
Polyvinylidene Fluoride (PVDF)	Sigma Aldrich	Mw ~534,000 by GPC, powder
Polydimethylsiloxane (PDMS) vinyl terminated	Sigma Aldrich	Mw ~25,000
Sylgard 184	X5K Rayden	Polydimethylsiloxane (PDMS) vinyl terminated + curing agent
Silica Nanoparticles HDK N20	Wacker Chemical Corporation	Refraction Index = 1.46

Font: The Author (2021)

The Tetrahydrofuran (THF) consists of a cyclic ether usually employed as a solvent, represented by the molecular formula C_4H_8O. Its molecular weight is 72.11 $g.mol^{-1}$, and its viscosity is 0.48 cP at 25ºC. Dimethylformamide (DMF) is a solvent with molecular formula $(CH_3)_2NC(O)H$, weighed 73.09 $g.mol^{-1}$, with the viscosity of 0.92 cP at 20ºC. Both solvents consist of polar aprotic solvents, which have bonds between atoms with different electronegativities and cannot make hydrogen bonds with themselves due to their lack of O-H and N-H bonds.

3.1.2 Materials to DCMD tests

The reagents employed as a feed solution in DCMD tests are listed in Table 8.

Table 8 – Reagents used to design the feed solution in DCMD unit

Reagent	Supplier	Additional information
Distilled Water	-	-
Reactive Black Dye	Aupicor Química Ltda	Tiafix RBL 133% (CI 20505), Molecular formula: $C_{26}H_{21}N_5Na_4OS$, Mw = 991.82
Disperse Black Dye	TMX Corporation	Trillon KCR, mixture of dyes
Acid Black Dye	TMX Corporation	Trimacid CP, Molecular formula: $C_{20}H_{12}N_3NaO_7S$, Mw = 461.38
Direct Black Dye	TMX Corporation	Tricel NG-LBR, Molecular formula: $C_{44}H_{32}N_{13}Na_3O_{11}S_3$, Mw = 1087.01
Detergent Colorswet DTU-M	Color Química do Brasil	Anionic characteristic

Font: Author (2021)

3.1.3 Equipment

This section presents the analytical and experimental equipment used to design the membrane modification and the DCMD tests.

3.1.3.1 Electrospinning apparatus

The electrospinning apparatus used in this work was installed in the PROCER Laboratory b at EQA – UFSC. It was illustrated in Figure 13 and comprised a high voltage supplier (a), an injection syringe pump (b), and a fixed collector (c). The 5 mL syringes were made by polymer and replaced in each new batch of electrospinning because of the harsh attack of the dope solution's solvents. The needle attached to the syringe has a size of 25 x 0.7 mm, and it had its tip cut to favor the formation of the desired speed profile.

Figure 13 – Electrospinning equipment

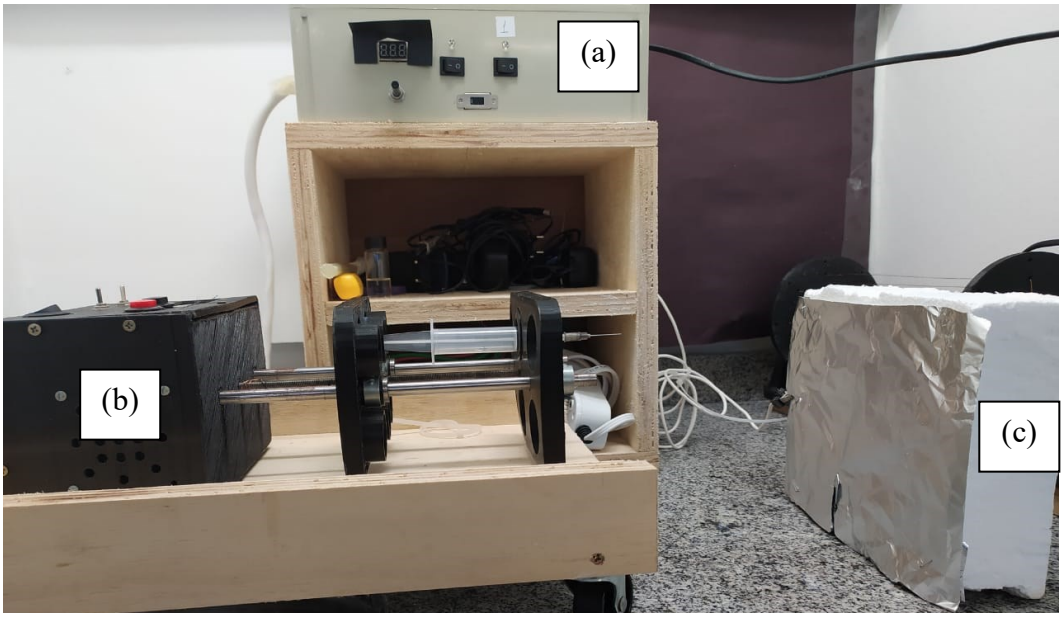

Font: The Author (2021)

3.1.3.2 Direct Contact Membrane Distillation Unit

The experimental unit of DCMD was installed in the LCP laboratory at EQA – UFSC. This unit comprised two reservoirs, one for the feed solution and another to collect the permeate. A thermal resistance and a thermostatic bath (MS Tecnopon, MQBTC 99-20 model)

were employed to the heat supply. A submersible pump and a centrifugal pump (BOMMOTOR, BM-05 model) were employed to maintain the feed and permeate flux. The membrane module consists of a plate and frame configuration, made by "Hidrix Soluções Sustentáveis", in stainless steel, as shown in Figure 14. The module's diameter is 5.1 cm, while the useful diameter of the membrane inside the module is 4.2 cm. The useful diameter is measured according to the membrane's useful area, where the permeate and feed solutions circulate. The useful area is equivalent to 13.85 cm^2.

Figure 14– Membrane module (a) opened and (b) closed

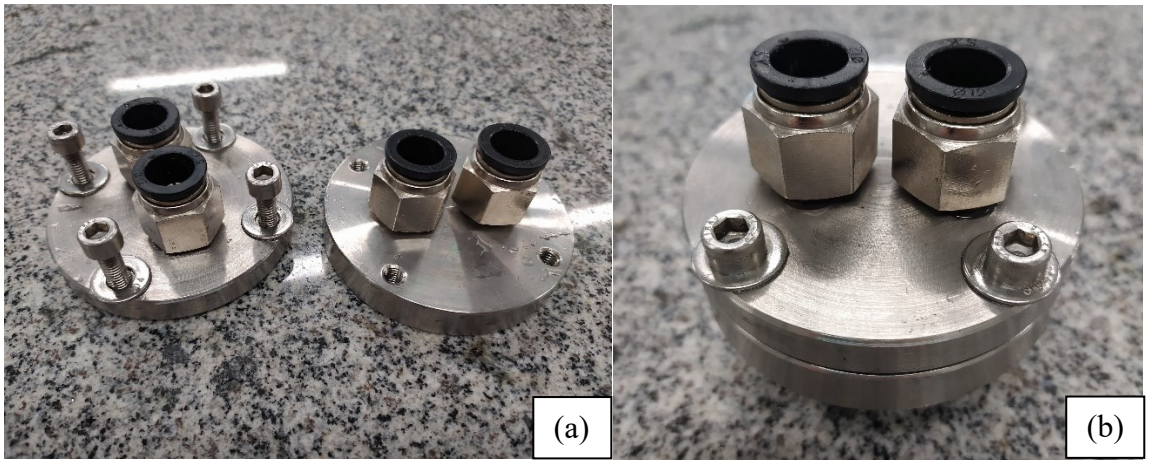

Font: The author (2021)

3.1.3.3 Equipment and software

The design of membrane modification, their application in a DCMD unit, and the results' measurements involved several analytical equipment and software. All the equipment and software employed in this work are listed in Table 9.

Table 9 – Analytical equipment and software

(to be continued)

Equipment/Software	**Model/Brand**
Analyzer of Differential Scanning Calorimetry	Jade-DSC Perkin Elmer
Digital Micrometer	MDC-25P Mitutoyo
Digital pHmeter	MB10 Marte
Digital Tensiometer	Sigma 702
Electrokinetic analyzer of Zeta Potential measurements and software Attract 1.1	Surpass Anton Paar GmbH
Electrospinning equipment	-

Table 9 – Analytical equipment and software

(conclusion)

Equipment/Software	Model/Brand
Goniometer and software DSA4	DSA25E Krüss
Magnetic Stirrer with heating	HS7 IKA C-MAG
MD Experimental Unit	-
Microscope for electron microscopy of scanning and Jeol Scanning Electron software	VEGA3 TESCAN
Precision electronic balance	ATX224 Shimadzu
Rheometer	Haake Mars 379-0200 (006-0572), Thermo Electron (Karlsruhe) GmbH
Software ACD/ChemSketch 2016.2.2	-
Software ImageJ	-
Software Microsoft Visio Professional 2016	-
Software OriginPro 2016	-
Spectrometer for spectroscopy of total attenuated reflection in the infrared with Fourier transform	Tensor 27 Bruker
Spectrometer of UV/visible and software UV-Professional	US-M51 BEL Photonics

Font: The Author (2021)

3.2 METHODS

The methods employed to design the membrane modification, apply the modified membranes in an MD unit and analyze the results will be presented.

3.2.1 Membrane modification

This section will present two different ways to modify the commercial PP membrane, using PDMS with and without the cross-linking agent, aiming to evaluate the influence of the elongation of the non-polar chain in membrane hydrophobicity. The PA commercial membrane

was modified using PDMS without curing agent only. The presentation of the sections follows the chronological order in which the experiments were carried out.

3.2.1.1 PP modification using PDMS vinyl terminated, without curing agent

The membrane modification was carried out using the electrospraying technique, which consisted of a variation of electrospinning. Depending on the solution's viscosity, the electric field's action can result in the formation of fibers or drops. The drop formation occurs when the solution viscosity is low, generally when a low concentration of polymers is employed.

The preparation of the polymer´s solution to modify the membrane employed a mixture of THF and DMF as solvents (1:1). As polymers were used: 2 wt% of PVDF and two different concentration of PDMS: 6 and 10 wt%. A Silica Nanoparticles concentration was inserted, varying in 0, 10, 20, and 30 wt% to the total polymer concentration. As a result, 8 solutions were made. All the reagents were inserted together in a vial, submitted to magnetic stirring for 14 h, at 80 ºC. The chemical structures of PVDF and PDMS vinyl terminated are shown in Figure 15.

Figure 15 – Chemical structures of polymers that constitute the doping solution

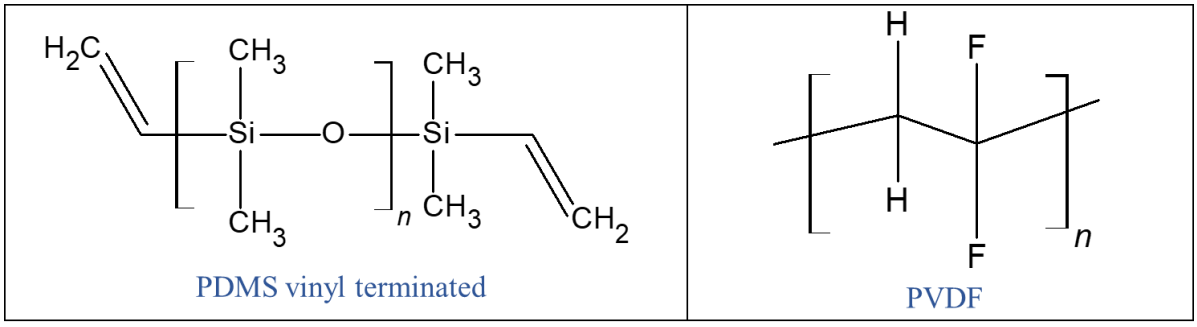

Font: The Author (2021)

After the stirring, all the solutions were inserted in an ultrasonic bath for 1 h to homogenize the polymers completely. Immediately before each electrospraying batch, the solutions were submitted to an ultrasonic tip for 10 min, at 40% amplitude, in an ice bath.

The electrospraying procedure was made at PROCER, using a fixed collector rather than a rotation drum, where the PP membrane was fixed. The polymer solution was inserted in a 5 mL volume syringe. The used voltage was fixed in 15 kV, the distance tip-collector was 10 cm, and the solution flow rate was 1.75 mL/h. These parameters were selected based on the apparatus limitations and follow the based methodology (LEE; DEKA; AN, 2019a).

The experimental procedure employed in this modification can be visualized in Figure 16. Besides the variation on polymer and silica concentration, the spray's exposition time varied in 30, 60, and 90 min, resulting in 24 different modified membranes. After the electrospraying, the modified membranes were dried in an oven for 24 h, to evaporate the remaining solvents. Table 10 shows the approached variables of the 24 modified membranes.

Table 10 – Modified PP membranes varying the time under the spray and the PDMS and Si NPs concentration

wt% of PVDF	wt% of PDMS	wt% of Si NPs	Time under the spray (min)
2	6	0	30
2	6	0	60
2	6	0	90
2	6	10	30
2	6	10	60
2	6	10	90
2	6	20	30
2	6	20	60
2	6	20	90
2	6	30	30
2	6	30	60
2	6	30	90
2	10	0	30
2	10	0	60
2	10	0	90
2	10	10	30
2	10	10	60
2	10	10	90
2	10	20	30
2	10	20	60
2	10	20	90
2	10	30	30
2	10	30	60
2	10	30	90

Font: The Author (2021)

Figure 16 – Schematic experimental procedure to membrane modification using PDMS vinyl terminated

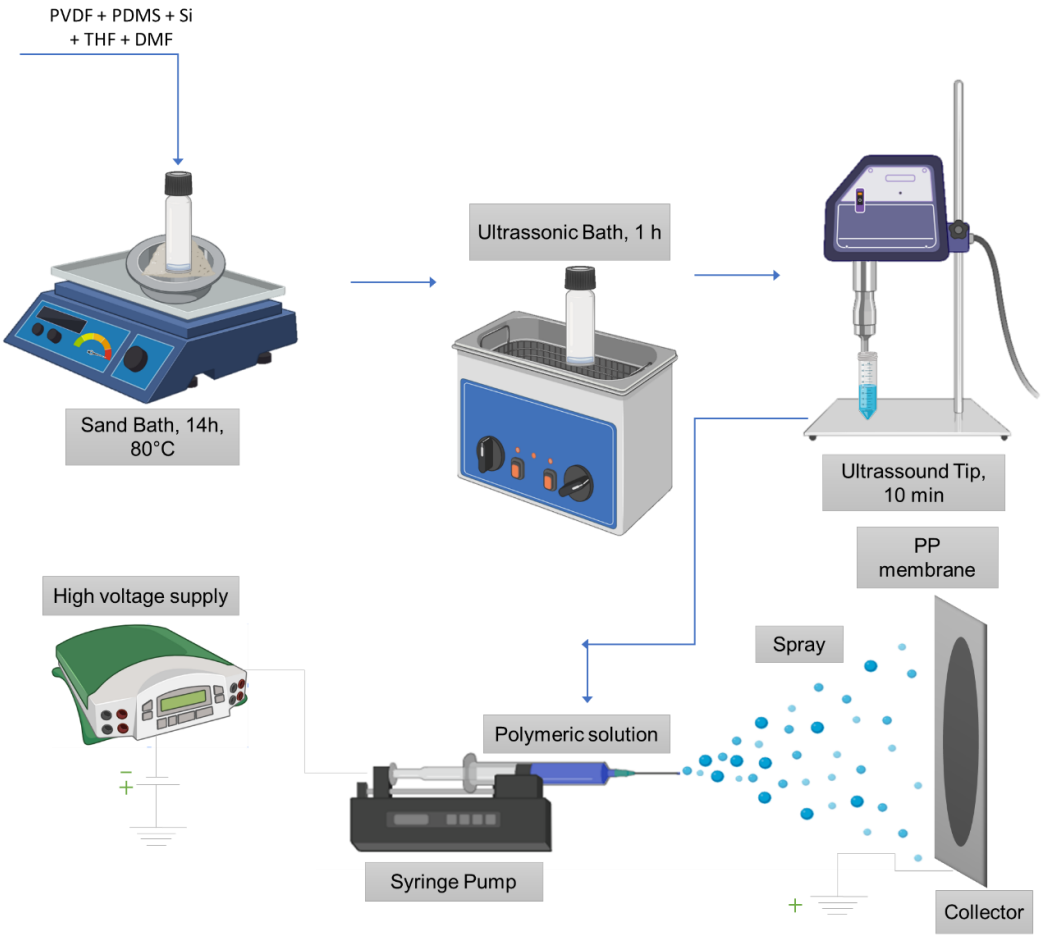

Font: The Author (2021)

3.2.1.2 PA modification using PDMS vinyl terminated, without curing agent

According to the results obtained in section 3.2.1.1, the best modifications were selected by the highest water contact angles. Furthermore, these modifications were reproduced on a PA substrate. The doping solution concentration consisted of 2 wt% PVDF, 10 wt% PDMS vinyl terminated, and 20 wt% of silica nanoparticles (to the total polymer concentration). The same solution was designed only with the polymers, consisting of 2 wt% PVDF, 10 wt% PDMS vinyl terminated, to investigate the silica effects on membrane hydrophobicity. The methodology to design the dope solutions and the electrospraying conditions was the same as proposed to PP modifications, without any pre-treatment.

Before each batch of electrospraying, the solutions were stirring on an ultrasonic tip for 10 min. This modification aimed to test the influence of the membrane substrate in the hydrophobicity after the modification. The time under the spray was fixed in 90 min.

3.2.1.3 PP modification using PDMS with a curing agent (Sylgard 184)

For this proposed modification, the PDMS without curing agent was replaced by Sylgard 184, which consists in two parts: The prepolymer, vinyl terminated poly(dimethylsiloxane) (PDMS); and the curing agent, trimethylsilyl terminated poly(dimethylsiloxane-co-methyl-hydro siloxane), containing Si–H and platinum (Pt) catalyst for the hydrosilylation reaction. The main goal was to investigate the influence of polymer cross-link in membrane hydrophobicity. The methodology to design the polymer solutions changed once a chemical reaction occurred in the solution stirring. This reaction is represented in Figure 17.

Figure 17 – Cure reaction of PDMS vinyl terminated – Sylgard 184

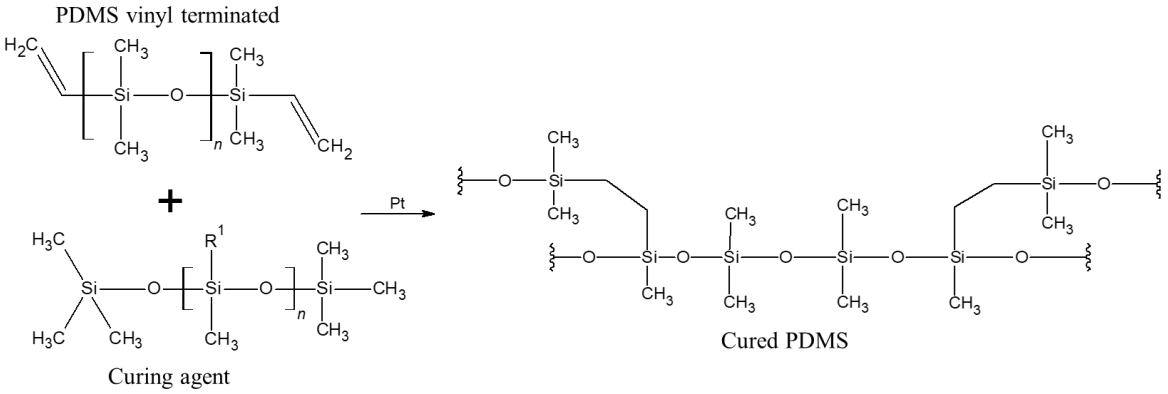

Font: The Author (2021)

First, the prepolymer was added in a THF: DMF (1:1) solution and stirred for 30 min at 80 ºC, aiming at the solution's polymer homogenization. After this step, the curing agent was added to the solution in 10:1 ratio to the prepolymer, and stirred at 80 ºC for 6 h, to complete the hydrosilylation reaction. 2 wt% of PVDF and the different Silica nanoparticle concentrations (0, 10, 20, or 30 wt% to the total polymer concentration) were added to the solution. The solutions were stirred for 4 h at the same temperature to guarantee complete homogenization. Immediately before the electrospraying batches, each solution was sonicated

in a ultrasonic tip for 10 min. This methodology was based on (JIA *et al*., 2019) and can be visualized in Figure 18.

The electrospraying was done following the same parameters of the previous sections. The time under the spray was fixed in 90 min. The variations on membrane modification involved the Sylgard concentration (6 and 10 wt%) and the Silica Nanoparticles concentration (0, 10, 20, and 30 wt%), resulting in 8 different membranes. After the electrospraying, the modified membranes were dried in an oven for 24 h, to evaporate the remaining solvents.

3.2.2 Membrane Characterization

The characterization comprised in this work included analyses of pristine and modified membranes before and after the DCMD operation. The modified membranes were first analyzed in terms of water contact angle and membrane porosity, aiming to select the best membranes to further characterizations. Fourier-Transform Infrared Spectroscopy (FTIR), Differential Scanning Calorimetry (DSC) analysis, Scanning Electron Microscopy (SEM), Energy-Dispersive X-ray Spectroscopy (EDX), Zeta Potential, thickness measurement and the determination of swelling degree were performed in the selected membranes, as it will be explained in the followed sections.

After the DCMD process, each membrane was analyzed again to analyze wetting, fouling, or other phenomena on the membrane surface. The spanned analysis after the DCMD testes consisted of FTIR, water contact angle, membrane thickness, SEM, and Energy-dispersive X-ray spectroscopy (EDX).

Moreover, the dope solutions' rheology was investigated through the viscosity measurements, aiming to link the rheology with the drop’s morphology.

Figure 18 – Schematic diagram of the experimental procedure to membrane modification using Sylgard 184

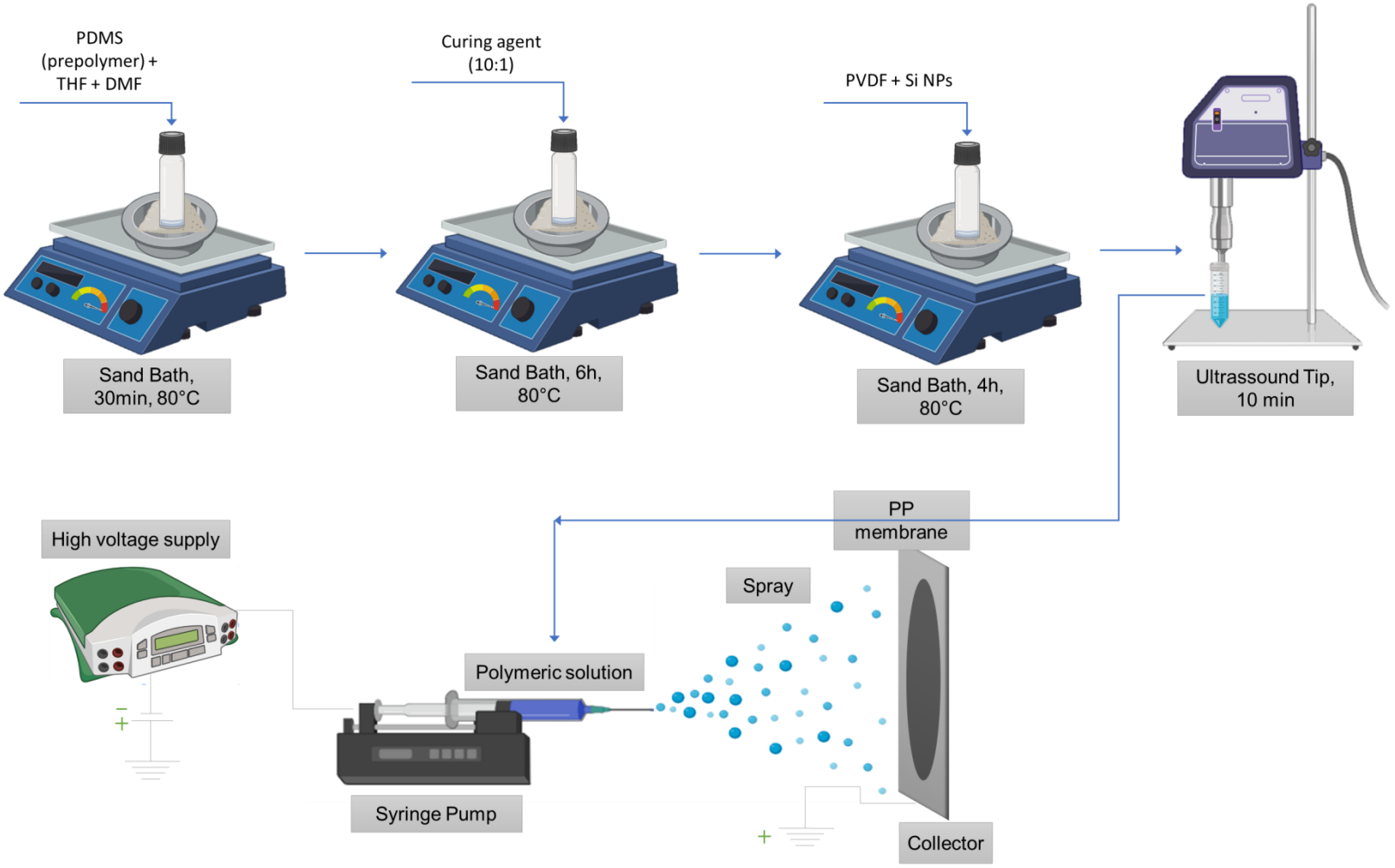

Font: Author (2021)

3.2.2.1 Contact Angle Measurement

The contact angle is a parameter related to membrane hydrophobicity. It can be considered the most important analytical measurement in this work, once the main goal was to improve the hydrophobicity of PP and PA membranes to avoid the wetting phenomena. This measurement was performed with all modified and pristine membranes. The solutions used to contact angle measurement consisted of distilled water, 30 mg L^{-1} of dye (Reactive, Disperse, Acid, and Direct), and 30 mg L^{-1} aqueous surfactant solution.

The equipment consisted of a goniometer (Krüss brand, model DSA25E), equipped with the software DSA4 to process the images. Each measurement's drop size was around 5 µL, and all measurements were done in triplicate to obtaining a medium contact angle and its standard deviation.

All the measurements were performed with a dry membrane sample at Materials Laboratory (LABMAT) of Materials Engineering – UFSC.

3.2.2.2 Membrane porosity

As the contact angle, the porosity consisted of a selection criterium. The porosity of modified and pristine membranes was determined by the gravimetric method (BELLINCANTA *et al*., 2011).

The modified membranes were cut in a sample of 1 cm x 2 cm. (1) They were dry weighted (2), followed by their immersion in ethanol for 24h. (3) The wet membranes were weighted again. The porosity was calculated according to Equation 1.

$$\varepsilon = \frac{\frac{M_w - M_d}{\rho_e}}{\left[\frac{M_w - M_d}{\rho_e}\right] + \frac{M_d}{\rho_m}} \quad (1)$$

where M_w and M_d are the weight of wetted and dry membranes, respectively (kg), and ρ_e and ρ_m are the specific mass of ethanol and membrane, respectively (kg m^{-3}). The specific mass of all modified PP membranes was approximated to the specific mass PP membrane (860 kg m^{-3}). For the PA membranes, the specific mass was considered 1482 kg m^{-3}, according to Ramlow (2018). The specific mass of ethanol was 870 kg m^{-3}.

3.2.2.3 Membrane thickness

The thickness of each selected membrane was measured using an analogical micrometer (MDC-25P Mitutoyo). Ten different measurements were performed for each membrane to obtaining a medium thickness and its standard deviation.

3.2.2.4 Fourier Transform Infrared (FTIR)

To investigate the functional groups before and after the membrane modification and the solid deposition after de DCMD process, the Fourier Transform Infrared, Attenuated Total Reflection (ATR-FTIR) analysis was employed. Through this technique, an evaluation of the polymer structure can be performed using the vibrational level measurement.

The evaluation of the modified membrane using FTIR analysis allows the observation of how the surface modification changed the membrane surface's chemical structure and connected these changes with the improvement – or not - in membrane hydrophobicity. Through this analysis, wetting or fouling phenomena against different feed solutions can also be explained by chemical interactions between the membrane and the solution.

FTIR analyses were also employed in the membranes after DCMD tests to investigate the solute adsorption from feed solution on the membrane surface. The chemical resistance of the proposed modification after the DCMD was also investigated, comparing pristine and contaminated membranes' chemical structures. The Attenuated Total Reflection (ATR) was chosen due to the membrane opacity. This technique employee a high refraction index crystal and low infrared absorption in direct contact with the sample. This method was carried out in the Central Analysis Laboratory at EQA –UFSC.

3.2.2.5 Scanning Electron Microscope (SEM)

The Scanning Electron Microscope analysis allows evaluating pristine membranes' morphology compared with modified ones and the DCMD process's influence in membrane morphology. Through this technique, the spray deposition can be observed, the drop size can be measured, and the changes in membrane pore size can be noted. SEM images also infer the surface roughness.

This analysis is based on the bombardment of a thin beam of electrons of high voltage in the analyzed sample. A series of radiation is emitted due to the interaction between the electron beam and the sample surface, providing information.

This technique was used only in the selected membranes, once it is a high-cost analysis that requires sample coating in gold. Therefore, SEMs were performed on the pristine and selected membranes before and after the DCMD process. The analyses were carried out in Materials Laboratory (LABMAT) of Materials Engineering – UFSC, using a conventional scanning microscope with a tungsten filament, VEGA3 TESCAN. To the coating with gold, an overlay LEICA EM SCD500 was employed.

Besides the SEM images, and Energy-dispersive X-ray spectroscopy (EDX) was employed to perform an in-depth study of chemical elements presented in membrane surfaces.

3.2.2.6 Zeta potential

The rejection mechanism of the membrane in MD operations directly depends on the electrostatic interactions between charged solutes and a porous membrane. The zeta potential measurements consist of a way to quantify these interactions. The superficial charge originates a surface potential, which decreases with increasing distance from the solid surface. It infers about the fouling phenomena, once when equal charges are reached between the membrane surface and the solute, repulsion forces predominate, avoiding fouling (PURKAIT *et al.*, 2018). The zeta potential depends on solid surface functionality and solution composition.

The zeta potential measurements were carried out using a kinetic analyzer (Surpass Anton Paar brand, model GmbH). Samples of each membrane were put on supports and fixed assets in a cell. As the electrolyte, a solution of potassium chloride was selected, and its pH was adjusted using solutions of hydrochloride acid and sodium hydroxide (0.1 M each). The software Attract 1.1 was used to calculate the charge density on membrane surfaces. All these measurements were done in the Central Analysis Laboratory at EQA –UFSC. The zeta potential measurements were made only in the selected membranes before the DCMD operation.

3.2.2.7 Rheologic study of electrospraying solutions

The study of fluid rheology aims to determine and investigate physical properties that influence the transport of a fluid's movement. It studies the deformative behavior of a fluid submitted to tensions under determined thermodynamic conditions in a defined period. The

fluid viscosity is the measurement of the internal resistance when a fluid is submitted to a tension. As more viscous, as harder to drain and the higher is the viscosity coefficient of the fluid. In other words, the viscosity is the drain resistance or deformity resistance (SISSOM; PITTS, 1979).

As mentioned in the previous section, the electrospraying technique depends on the dope solution's rheologic characteristics. All dope solutions made in this work were investigated in terms of apparent viscosity, the influence of the viscosity on drop morphology, and fluid classification according to the viscosity behavior.

The rheologic study was carried on a Haake Mars Rheometer, Thermo Electron (Karlsruhe) GmbH, model 379-0200 (006-0572), with a parallel plate geometry (PP20 Ti, D = 20 mm) at room temperature. The rheogram of the slurry was made at a shear rate of 0.01 to 250 s^{-1}. The analyses were performed at Polymer Design and Process Control Laboratory (LCP – UFSC).

3.2.2.8 Differential scanning calorimetry (DSC)

The DSC consists of a thermal analysis, which enables to follow thermal or chemical phenomena occurring when the samples were submitted to a controlled heat and colling an inert atmosphere. Regarding the Differential Scanning Calorimetry (DSC) analysis comprised in this work, the DSC instrument consisted of a Heat Flow DSC. The measured physical property was the temperature difference between the sample and the reference material. This difference becomes proportional to enthalpy variation, calorific capacity, and total thermal resistance against the heat flow. The DSC analysis allows to determine the crystallinity degree of a polymer, detect the additives polymers and the percentage of mixtures, follow the crystallinity kinetic, the induced oxidation in polymeric materials, polymerization and cross-linking reactions and their kinetics, as well as the cure degree (CANEVAROLO JR, 2003).

Differential scanning calorimetry studies of pristine and modified membranes were carried out using a DSC analyzer (Jade-DSC Perkin Elmer) at a heating and cooling rate of 10ºC/min in an inert atmosphere of nitrogen (50 mL/min). The pans employed in this analysis were made of standard aluminum. The experiments were conducted from -30ºC to 300ºC ºC for all the samples. The glass transition temperatures (T_g) and the melting behavior were observed in DSC data's second heating run. The DSC peaks' alterations were compared among the pristine and modified membranes to determine the influence of the coating layer on the thermal behavior.

According to Canevarolo Jr (2003), the DSC analysis allows calculating the purity percentual of the polymers in the sample through Equation 2.

$$Purity = \frac{\Delta H_{f,peak}}{\Delta H^{\circ}_{f}} \quad (2)$$

3.2.3 DCMD operation

The experiments in Direct Contact Membrane Distillation were carried out using fixed operational conditions to test and validate the modified membranes. All the selected membranes were tested in DCMD operation, and their performances were compared with the pristine ones.

The DCMD unit contains a feed side (hot) and a permeate side (cold), maintained in flux during the operation using two different pumps. The feed side flows counter-current to the permeate side, both opposite the membrane surface. The structural diagram of the DCMD experiment can be visualized in Figure 19.

Figure 19 – DCMD unit operation

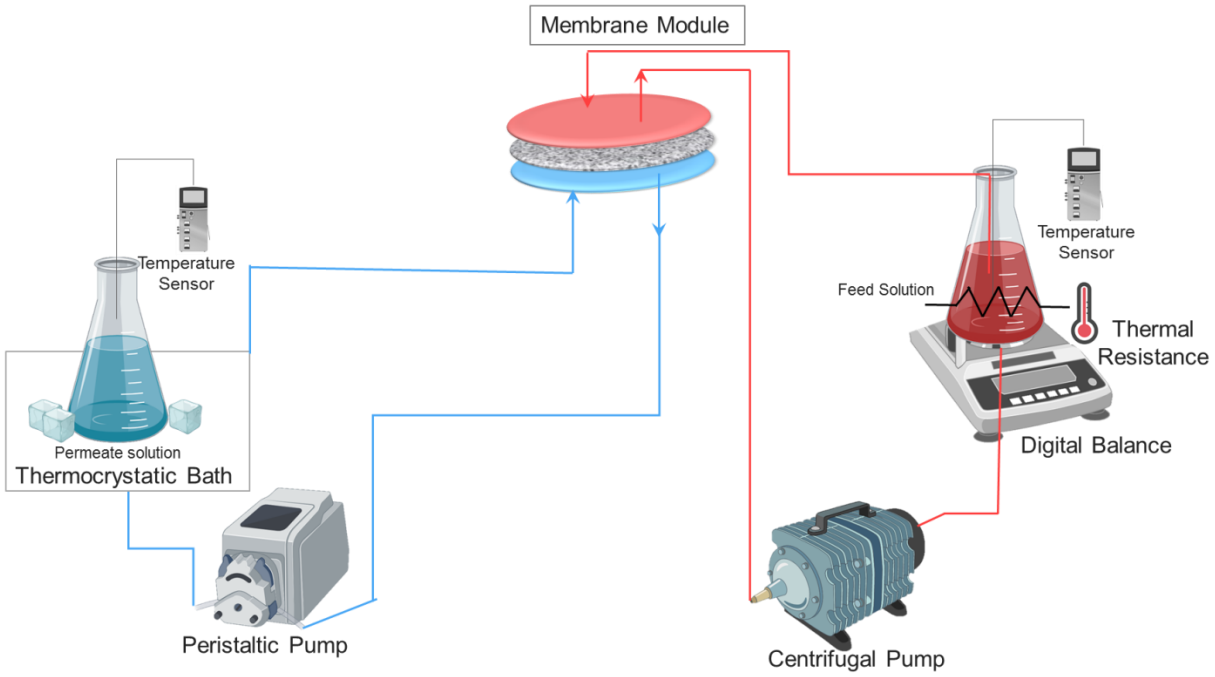

Font: Madalosso *et al*. (2020)

The solutions employed as a feed for each membrane were selected based on the contact angle measurements with all dyes' classes (Direct, Acid, Disperse, and Reactive) and surfactant

(detergent) solutions. All DCMD tests were carried out with modified and pristine membranes to each solution to compare their performances.

The PP pristine and modified membranes were tested with distilled water and four different dyes employed in the textile industry. The feed solutions consisted of aqueous solutions of Reactive, Disperse, Direct, and Acid Blacks dyes in a 30 mg L^{-1} concentration. The established dye concentration was based on our group's previous studies (SOUSA SILVA, 2019; RAMLOW, 2018; TOLENTINO FILHO, 2019). On the other hand, the PA modified membranes were only tested with distilled water, Reactive Black dye solution (30 mg L^{-1}), and aqueous surfactant solution (30 mg L^{-1} of detergent Colorswet), which consisted of the components of a cotton dyeing bath. The surfactant concentration was determined based on the typical concentrations employed to test modified membranes using electrospinning (DEKA *et al*., 2019; HOU *et al*., 2019b; LEE; DEKA; AN, 2019a).

The feed solution presented an initial volume of 1.3 L, while the permeate solution, which consists of distilled water, presented an initial volume of 0.5 L. The temperature was controlled using a thermal resistance on the feed side and a thermocriostatic bath for the permeate side. The experiments were carried out for 4 h, consisting of the time after which there is no harsh change in the permeate flux in DCMD operation, previously determined by Sousa Silva (2019). In terms of experiments economy, the time was fixed in 4h. The feed side temperature was fixed at 60ºC, while the permeate side's temperature was about 20ºC. The feed and permeate flow rates were fixed in 1.5 L h^{-1} and 0.7 L h^{-1}, respectively.

The feed and permeate reservoirs were weighed at the beginning and the end of the DCMD process to determine the permeate mass transferred through the membrane. Samples of both sides of the DCMD unit were collected for the flux analysis and the rejection rate calculation. The permeate flux, J (kg $h^{-1}m^{-2}$) through the membrane were calculated using Equation 3.

$$J = \frac{\Delta M}{A \times \Delta t} \tag{3}$$

where ΔM is the weight of collected permeate (kg), A is the effective membrane area (m^2), and Δt the total time of the MD process (h).

On the other hand, the Rejection Rate (RR%) was determined using Equation 4, where C_F is the dye concentration in the feed side, and C_P is the dye concentration in the permeate side. For the PP membranes, a dilution factor for determining the permeate side's solute

concentration was considered for the rejection rate calculations (Equation 5). For these membranes, the permeate flow is high and involves the dilution of solutes. The same is not valid for the PA membranes since its dense matrix results in lesser vapor passing to the permeate side (up to 10 times smaller), with no solute dilution.

$$RR = \frac{C_A - C_P}{C_A} \times 100 \quad (4)$$

$$C_p = \frac{(C_f \times M_f) - (C_i \times M_i)}{M_f - M_i} \quad (5)$$

M_i and M_f are the initial and final mass of the permeate side, and C_i and C_f are the cold side's initial and final concentrations.

The DCMD process assumed that only the water vapor could pass through the membrane pores from the feed side to the permeate side. In this way, the solute molecules are retained in the feed side, which causes a graduate concentration of this stream. The rejection rate (RR) varies between 0-100%, where 0 represents the whole passage of solute through the membrane pores, and 100% represents their complete rejection.

3.2.3.1 Colorimetric method to the determination of dye concentration

The use of Equations 3 and 4 requires the determination of dye concentration using analytical equipment. In this context, an UV/visible spectrophotometer (AJX-900 Micronal) was employed. This equipment detects the absorbed light in the maximum wavelength, which calculates the dye concentration. The calibration absorption versus dye concentration curve was constructed using synthetic solutions of the dyes in a determined concentration. The measurements were performed at Polymer Design and Process Control Laboratory (LCP-UFSC).

3.2.3.2 Determination of the detergent concentration

To calculate rejection rates in the experiments involving the detergents, its concentration was determined through a calibration curve in a Digital Tensiometer (Sigma 702). The measurements were performed using the Wilhelmy plate method, which consists of reading the force necessary to remove the plate from the liquid surface. The readings were taken in triplicate

for each sample. The plate was washed with ethanol and ammonia and then flamed after each analysis.

3.2.3.3 Determination of the swelling degree

The experimental procedure to calculate the swelling degree was carried out weighing the dry membranes and weighing the membranes after immersion in water or different textile solutions every one hour up to 4h, after 12, 24, and 48h. The measurements were performed in triplicate, presenting an average and a standard deviation. The swelling degree (SD) was calculated according to Equation 6.

$$SD = \frac{M_w - M_d}{M_d} \quad (6)$$

where Mw and Md are the weight of wetted and dry membranes.

4 RESULTS AND DISCUSSION

This section will present and discuss the results of each methodology to modify commercial membranes. The followed sections will be classified and separated according to the proposed modifications. Also, the resulted performances of each selected membrane in the DCMD unit are presented.

4.1 PP MEMBRANE MODIFICATION USING PDMS WITHOUT CURING AGENT

The membrane modification using PDMS without curing agent consisted of the first experimental test of this work. The PVDF was chosen due to its hydrophobic characteristic, and to achieve an ideal solution viscosity and to enable the droplet formation. The PVDF concentration was fixed at 2%, while the PDMS concentration was varied in 6 and 10%. Based on Lee, Deka, An (2019a), the electrospraying parameters were adapted to the electrospinning unit at PROCER. The effect of silica concentrations (0, 10, 20, and 30%) in membrane hydrophobicity and membrane porosity was studied. The silica was employed to obtain micro/nano hierarchical structures with high roughness, increasing the membrane wetting resistance (HOU *et al*., 2019b).

The time of electrospraying under the membrane was evaluated. There are no reports in the database about the influence of the time under the spray in desirable features of modified membranes. All modified membranes were evaluated in terms of hydrophobicity and porosity. Other analytical evaluations only were performed in the membranes that showed the highest values of these properties.

4.1.1 Water-repellent properties

The average water contact angle and its standard deviation were determined for the 24 membranes. Figures 20 and 21 show the results for 6% and 10% of PDMS.

Figure 20 – Contact angle measurements for 6% PDMS membranes

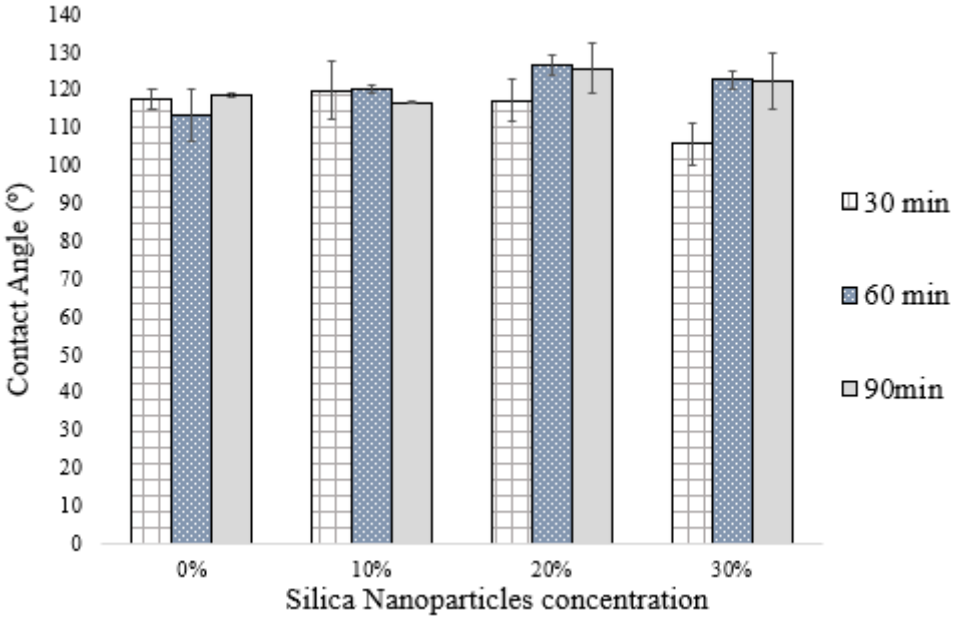

Font: The Author (2021)

Figure 21 – Contact angle measurements for 10% PDMS membranes

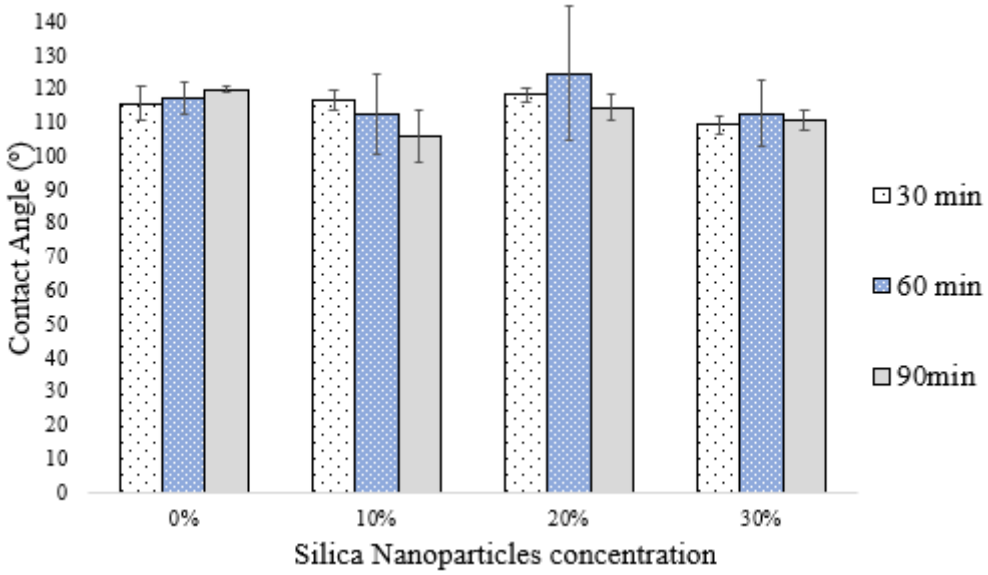

Font: The Author (2021)

The Water Contact Angle (WCA) of the pristine PP membrane is 118.92º +/- 3.081. The analysis of Figures 20 and 21 allowed to verify a maximum increment in WCA of 6.5% for modified membrane using 20% of Si NPs and 10% PDMS (126.7º) in 60 min under the spray. The second major WCA was obtained in the same spray time, with the modified membrane using 6% of PDMS and 20% of Silica, corresponding to an increment of 4.5 % (124.6º).

4.1.1.1 Statistic analysis of the water contact angle of PP modified membranes using PDMS

Aiming to verify the significance ($p < 0.05$) of the increase in contact angle proposed by these modifications, the Analysis of Variance (ANOVA) and the Tuckey test were performed (Appendix Q). It was observed that there was no significant difference among the results ($p > 0.05$) for comparison of contact angle of pristine and modified PP membranes through the Tuckey test. In other words, the proposed modifications involving PDMS vinyl terminated, Si NPs, and different times under the spray did not significantly increase the hydrophobicity of the pristine PP ($p > 0.05$).

However, a significant difference ($p < 0.05$) was observed for the silica concentration when comparing the modified membranes with 2% PVDF, 6% PDMS, and 0 or 10% Si NPs, at 90 min under the spray. For these membranes, the silica concentration significantly reduced the water contact angle. For all modified membranes using 6% PDMS, the time under the spray did not show a significant influence on membrane hydrophobicity.

On the other hand, the modified membranes using 2% PVDF, 10% PDMS, and 30% Si NPs at 30, 60, and 90 min presented a significant increase in the membrane hydrophobicity with the increase of the time under the spray. Increasing Si NPs in the membranes 2% PVDF, 10% PDMS, and 10 or 30% Si NPs, at 30 min under the spray, led to a significant decrease in the membrane hydrophobicity.

Finally, there was no significant difference among the polymer concentration (6 and 10%) for all the modified membranes.

Those results evidence a non-improvement of membrane hydrophobicity through the proposed modifications using PDMS without curing agent than the pristine PP membrane. This fact was may related to the chemical nature of the PDMS vinyl terminated. A significant increase in membrane hydrophobicity would be obtained using a curing agent to PDMS polymer to obtain a more reticulated chain. The polymer cross-link may improve the water repellence due to an elongation of non-polar chains.

In the face of these results, the membrane 2% PVDF, 10% PDMS, 20% Si NPs at 90 min was chosen to evaluate further the modified membranes presented in this section. By comparing the time under spray of modified membranes with 10% PDMS and 30% Si, the electrospray time for further modifications was fixed at 90 min. Also, an intermediate concentration of silica nanoparticles was chosen to determine their influence on the membrane surface.

4.1.2 Membrane porosity

The membrane porosity was measured for all modified membranes. The pristine PP membrane shows a porosity of 82.74 +/- 0.84. The results are shown in Figures 22 and 23.

Figure 22 – Membrane porosity for 6% PDMS membranes

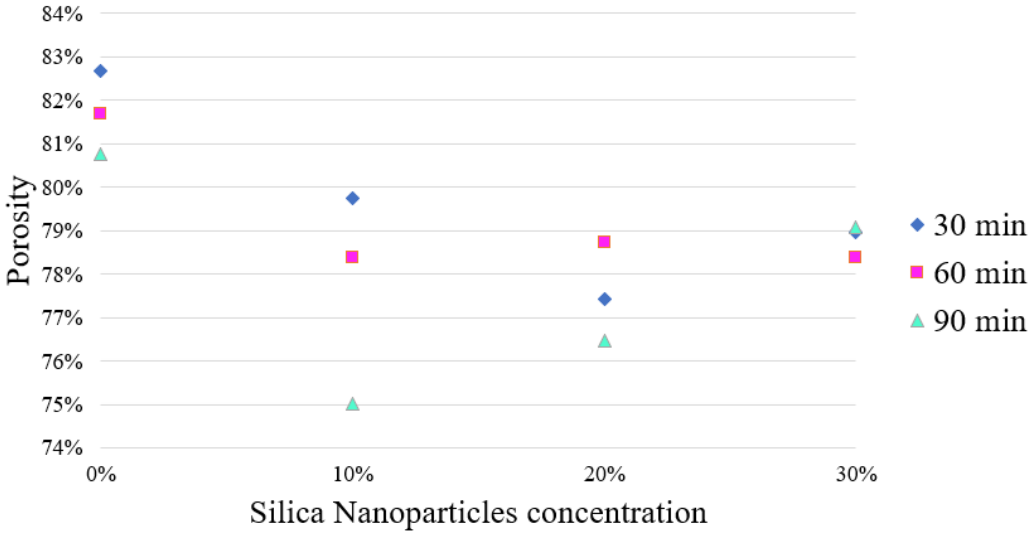

Font: The Author (2021)

Figure 23 – Membrane porosity for 10% PDMS membranes

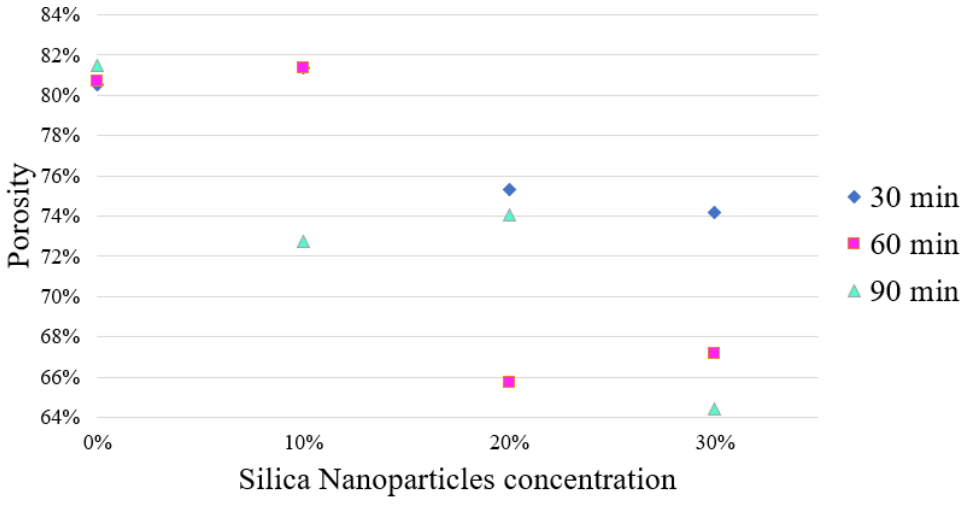

Font: The Author (2021)

The membranes to MD operation should have high porosity, leading to MD operations with high permeate fluxes. In this context, the membrane modifications aimed to increase membrane hydrophobicity without significant porosity losses. The analysis of Figure 22 shows that the increase in exposure time decreased the membrane porosity in most Si NPs

concentrations. Also, the increment of Si NPs decreased the membrane porosity. This behavior can be explained by the deposition of nanoparticles in the membrane surface, which increases with the nanoparticle concentration, and increasing the membrane density. The lowest porosity is obtained in 90 min, to 10% of silica (75%). Although there were losses in membrane porosity in all cases, they are low (up to 7.74%), which probably would not affect the MD operation.

Similarly, Figure 23 infers a decrease in membrane porosity with increased exposure time in most cases. Also, the increment in Si NPs concentration decreased the membrane porosity. Compared to Figure 22, it was noted that increasing the concentration of PDMS decreases membrane porosity once the membrane density increases, leading to partial pore closure. In this case, there was a more significant loss in membrane porosity, up to 18.7% in 30% of Si, 90 min, compared to the pristine PP membrane.

The presented modifications did not affect the membrane hydrophobicity but influence the membrane porosity. The increase in Si NPs concentration decreased the membrane porosity. The polymer concentration did not affect the membrane hydrophobicity, but its increment decreased the membrane porosity.

4.1.3 Analysis of chemical and morphological structures of the modified PP membranes

Based on the criteria explained in the previous section, the membrane with 2% PVDF, 10% PDMS, and 20% Silica nanoparticles concentration was selected. In this concentration, it was not observed high losses in membrane porosity. An FTIR analysis was carried out with this membrane and with the membrane containing only polymers at the same concentration (Figure 24)0 to investigate silica nanoparticles' influence on the membrane chemical surface. The results were compared with the chemical analysis of the pristine PP membrane.

Figure 24 (a) analysis led to note an sp^3 carbon (C-H) between the wavenumbers of 2950 and 2840 cm^{-1}, which is characteristic of the PP molecule. The peaks in the wavenumbers of approximately 1460 and 1378 cm^{-1} corresponded to the carbon that bonds two and three hydrogens, respectively. The modification proposed in Figure 24 (b) seems to did not alter the chemical structure of the PP membrane once the same peaks were observed. Even using a fluoride polymer combined with a polymer with silicon chains, the proposed modification concentration seemed not to alter the chemical structure of the membrane. Peaks expected in this FTIR spectra corresponding to C-F bonding among 1400-730 cm^{-1}, and the presence of an sp^2 carbon among 3100 – 3000 corresponding to the vinyl terminated PDMS. Thus, it can be concluded that the proposed surface modification was not carried out homogeneously on the

entire surface of the analyzed sample (Figure 24 (b)), or the concentration of polymers used in the modification was not high enough to cause a superficial modification. The peaks presented in Figure 24 (c) distinguish themselves visibly from the pristine membrane, inferring a chemical surface modification of the analyzed sample. The fingerprint region suggested Si-O-Si stretching among the wavenumbers of 1100 and 1000 cm^{-1}, characteristic of the silica nanoparticles. Besides, a peak of 791 cm^{-1} assigned to the $Si\text{-}CH_3$ bonding confirmed the PDMS presence, as observed by Lee, Deka, An (2019). A peak in the fingerprint region corresponding to 1258 cm^{-1} suggested C-F bonds' presence, characteristic of the PVDF inserted in the proposed modification blend. Finally, the peak corresponding to 3417 cm^{-1} corresponded to an O-H termination of the hydrophilic silica.

Figure 24 – ATR-FTIR analysis of pristine PP (a) and modified PP membranes with 2% PVDF, 10% PDMS (b), and with 2% PVDF, 10% PDMS, 20% Silica Nanoparticles (c).

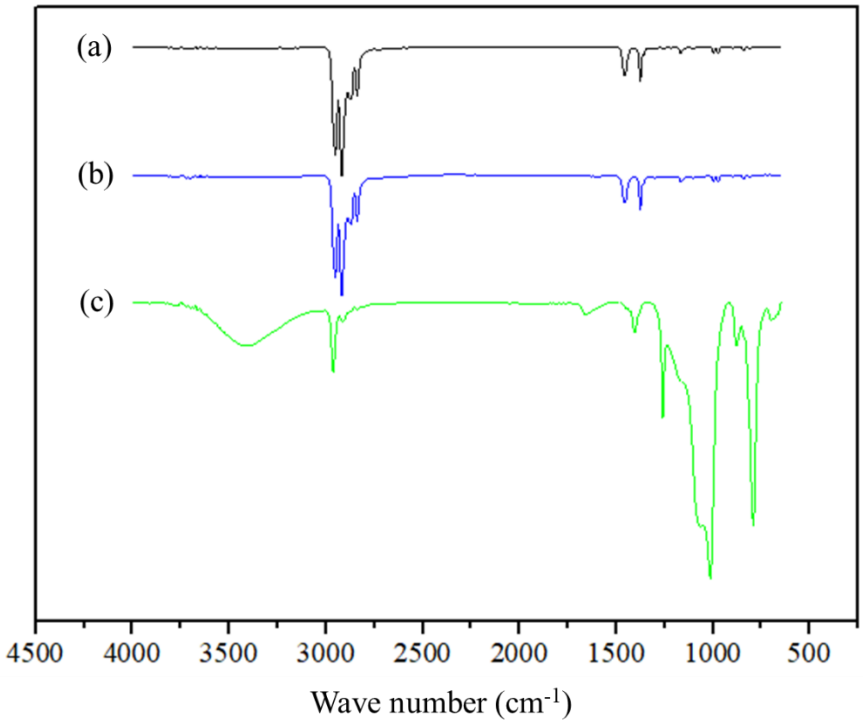

Font: The Author (2021)

Compared to the PP membrane, the maintenance of the water contact angle for modified membranes using the blend of PDMS without curing agent and PVDF was corroborated by the chemical surface analysis. The hypothesis of a non-homogeneous cover of the analyzed sample could confirm the weak increase in the modified membranes' contact angle. Thus, comparing

the chemical structure, contact angle, and porosity of the modified membranes with and without silica led to discarding further investigations in the PP modified membrane with the blend of PDMS + PVDF polymers.

A study of the chemical elements presented in the membrane surface before and after membrane modification was also carried out using the EDX analysis (Appendix A) and the study of surface morphology (Figure 25) to further investigations in the modified membrane using silica. The fluor, oxygen, silicon, and carbon elements in the modified membrane were detected in concentrations of 6.5, 20.9, 27.3, and 45.4 wt %, respectively. It also confirmed the presence of PDMS, Silica nanoparticles, and PVDF in the modified membrane's surface, corroborating the membrane chemical surface changes.

The Scanning Electron Microscope (SEM) allows the visualization of superficial morphological changes in the PP membrane after the proposed modification. Figure 25 shows the SEM images of pristine and modified PP membrane with 2% PVDF, 10% PDMS, and 20% Si NPs, expanded from 1000 to 10000 times.

The pristine PP membrane shows a regular and porous structure, which conceives to this membrane high homogeneity. The proposed modification (Figure 25, b) using the electrospraying generated regular drops on the membrane surface. The software of image processing *ImageJ* was employed to magnified the drop size for this modification. The measurements were performed in the amplified images of 10,000 times in order to increase the measurement precision. For each image, 50 drops were measured. The average drop size was calculated according to the equipment's scale, and this value was equal to 1.254 ± 0.244 μm. Through the analysis of SEM images, it became possible to observe that the modification increases the surface roughness due to the drop deposition on the membrane surface. Besides, the drops' overlapping gave rise to a reentrant hierarchical surface, evidenced by the contrast difference observed in the images. The non-visualization of the PP membrane's original pores could suggest a pore blockage, which was not confirmed by the porosity measurements. The overall volumetric porosity of the pristine PP membrane was maintained after the modification.

Figure 25 –SEM images of pristine PP (a) and modified PP membranes with 2% PVDF, 10% PDMS, 20% Silica Nanoparticles (b), approximated in 1000, 3000, 5000 and 10000 times.

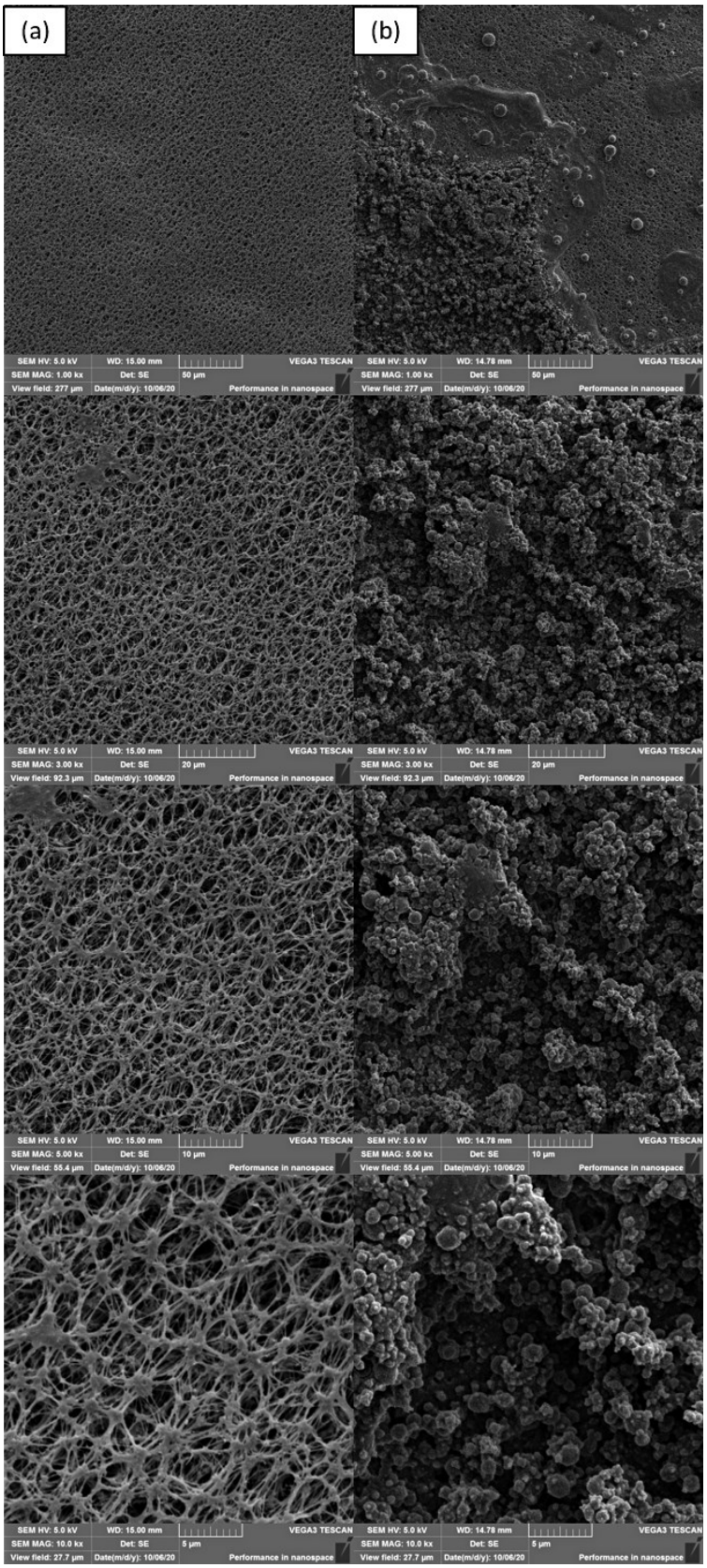

Font: The author (2021)

Incorporating nanoparticles in the dope solutions to achieve desirable membrane properties was also reported by Attia *et al.* (2018a). In this work, a regular drop structure on a polymeric membrane surface was obtained through the electrospinning and electrospraying of alumina nanoparticles, which achieved high surface roughness without significant losses on membrane porosity. (LEE; DEKA; AN, 2019a) related the nanoparticles' concentration with drop size on the membrane surface, where a decrease in drop size was observed with the increase of silica aerogel. The influence of silica nanoparticles will be further investigated in modifications on PA membrane.

4.1.4 Thermal analysis of modified membranes

The thermal analysis of membranes to DCMD applications becomes fundamental to investigate how the proposed modification affects the melting point and the temperature range of the modified membranes' applications. The DSC analysis also allows inferring the percentage of modifier agents in the sample's total composition and the purity of the pristine membrane. Figure 26 display the thermal analysis of pristine PP membrane compared to PP modified with 10% PDMS, 2% PDMS, and 20% Si NPs. The analysis was carried out from -30 to 300º, at $10^{o}C.min^{-1}$. The samples weighed 1.608 mg to pristine PP and 2.355 mg to modified PP membrane.

The analysis of Figure 26 leads to observe two thermal events: one transition of the first order and one of the second. The second-order transition was not well visualized once the range of investigates temperatures began at -30ºC. Even though it is possible to note an increase in calorific capacity, remarkable by the change on the baseline, corresponding to -17.44 ºC to pristine PP and -16.40 ºC to modified PP membrane. These temperatures were equivalent to the glass transition temperature. The pattern glass transition temperature of the polymer PP is around -20 ºC (CANEVAROLO JR, 2003). In this sense, it was the first indication that the PP membrane was not compounded of 100% of PP. The proposed modification slightly changed the pristine membrane's glass transition temperature once some functional groups were added to the membrane surface.

The first-order transition evidenced in both curves consists of an endothermic event corresponding to the melting. The melting point for both curves was equivalent to approximately 163.5 ºC, which revealed that the modification did not alter the pristine membrane's melting point. It consists of a good indication for DCMD operation since the modification does not limit the temperature range of membrane applications.

Figure 26 – DSC analysis of Pristine and modified PP membrane using 2% PVDF, 10% PDMS, and 20% Si NPs

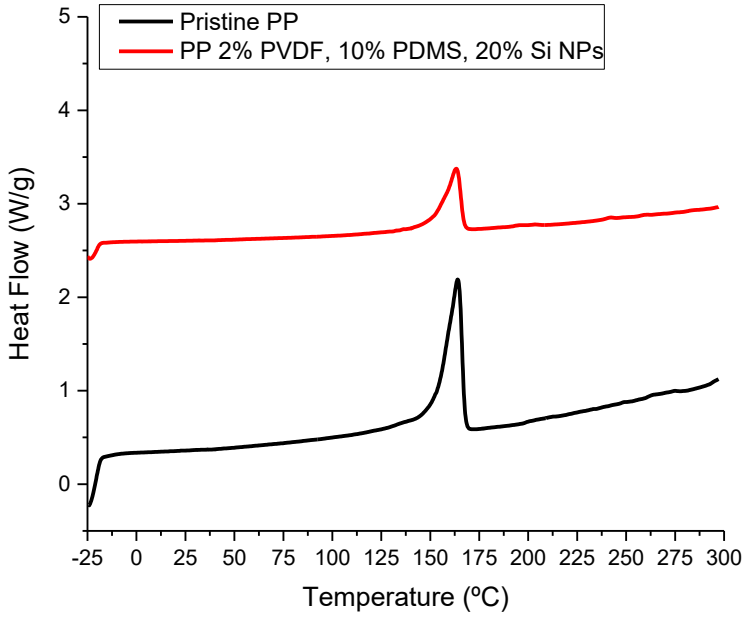

Font: The Author (2021)

The peaks' area corresponds to the melting heat (ΔH_f) ($J.g^{-1}$), which is equivalent to the integral of the peaks. For the pristine PP membrane, this value was equivalent to 17.05 J g^{-1}.

It is important to emphasize that the proposed modification decrease the melting heat of the membrane by 59.17%. Despite this reduction, the modified membrane did not have its melting point altered. Then, the proposed modification did not reduce the temperature range of applications in DCMD operation, which would not alter the modified membrane's thermal behavior against the operational conditions.

4.2 PA MEMBRANE MODIFICATION USING PDMS WITHOUT CURING AGENT

As previously mentioned, the PA membrane was modified with the dope solution that resulted in the selected membrane for PP membranes (2% PVDF, 10% PDMS, and 20% Silica nanoparticles). It was modified with the dope solution containing only polymers to study silica nanoparticles' influence on the hydrophilic membrane surface. The time under the spray was fixed in 90 min, according to the establishment of previous results.

4.2.1 Water contact angle of PA membranes

The water contact angle analysis of PA modified membranes (Figure 27) revealed a hydrophilic behavior of pristine PA membrane (75.73 ± 3.86º) completely changed when the membrane was submitted to the modification treatment. The highest water contact angle was obtained through the modification with Si NPs and consisted of 167.13 ± 22.29º. The modified membrane's hydrophobicity was even higher than the pristine PP membrane, which becomes a promising candidate for the MD application. The silica nanoparticles affected the membrane roughness, creating a re-entrant hierarchical structure. The thin and quickly designed cover seems to increase the membrane hydrophobicity positively to the required operation.

Figure 27 – Water contact angle of pristine and modified PA

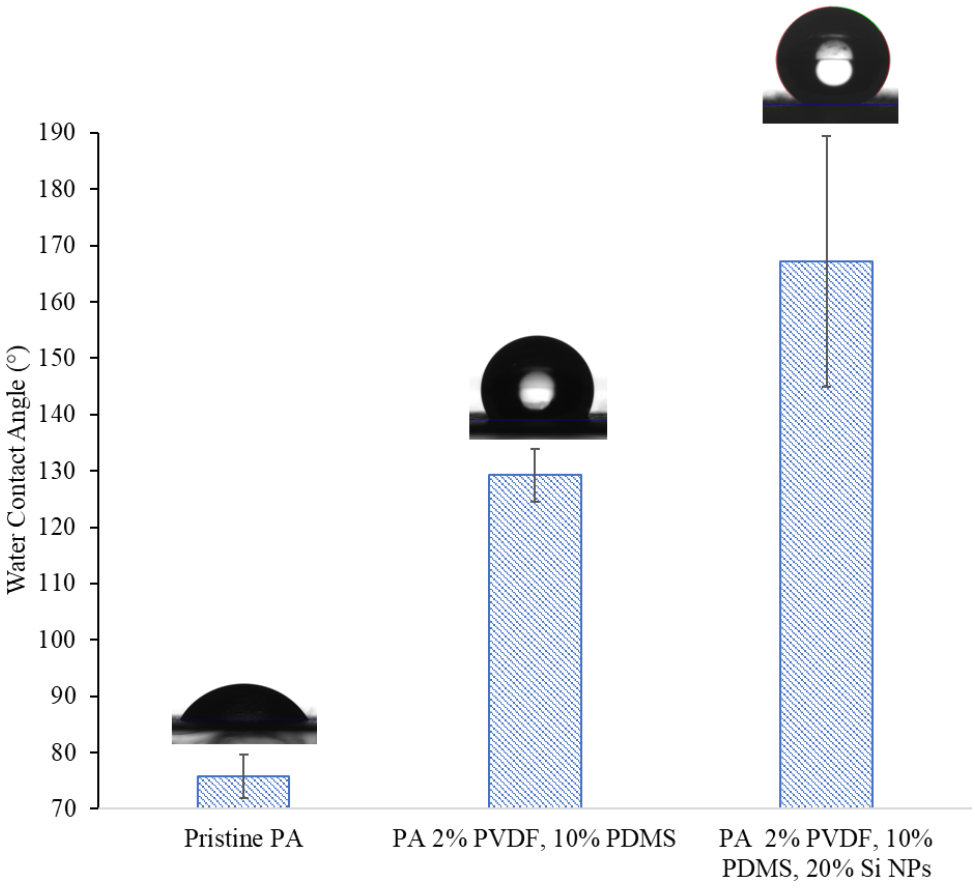

Font: The Author (2021)

Comparing to the modifications using the same dope solution in the PP membrane matrix, it was possible to note a different behavior with the proposed modification. The increase in Si NPs increased the membrane hydrophobicity. The high increase in water contact angle occasioned in the PA membrane was related to this membrane's distinct water behavior and

pore structure. The dense matrix suffered a harsher effect of drop deposition on its surface, which increased the membrane surface roughness. The increment in water contact angle, for this case, was not only related to the chemical nature of the polymers (that presents lower surface energy comparing to the polymer of the membrane matrix) but also with the harsh change in the membrane roughness. Also, the lower amount of pores in this membrane matrix contributed to the water contact angle increment.

4.2.2 Porosity and membrane thickness of PA membranes

The silica influence on the membrane modification also showed a high effect on the membrane thickness, which increased up to 40 μm, as shown in Table 11. The increment in membrane thickness can difficult the mass transfer during the MD operation. A high membrane thickness combined with the PA membrane's dense matrix led to expecting low flux values for these membranes due to increased mass transfer resistance. Although the higher thickness was obtained for the modification using silica, this membrane's porosity value was maintained compared to the pristine PA membrane.

The PA membrane employed as a substrate consisted of a dense membrane, showing a smaller porosity than the MD process's typical membranes, such as the PP, PVDF, and PTFE. The proposed modifications did not affect the pristine membrane's porosity after 90 min under the spray. The modified membrane using only polymers resulted in a thinner coating under the membrane than the membrane cointaining Si NPs. The Si NPs harsh increased the membrane thickness, due to the particle deposition, leading to expect lower permeate fluxes for this membrane.

Table 11 – Porosity and membrane thickness of pristine and modified PA membranes

	Pristine PA	**PA (2% PVDF, 10% PDMS, 20% Si)**	**PA (2% PVDF, 10% PDMS)**
Porosity (%)	50.59 ± 3.34	48.10 ± 3.18	49.26 ± 3.34
Thickness (μm)	147.3 ± 3.13	183.4 ± 8.01	154.5 ± 6.76

Font: The Author (2021)

4.2.3 Analysis of chemical and morphological structures of PA modified membranes

An ATR-FTIR analysis was carried out in the PA samples (Figure 28) to observe the proposed modifications' influence on the membrane's chemical surface. Through this analysis,

the silica influence on the membrane surface could be investigated more deeply. The technique also allows the understanding of chemical changes caused by the polymers employed in the membrane modification.

Figure 28 – ATR-FTIR analysis of pristine PA (a) and modified PA membranes with 2% PVDF, 10% PDMS (b), and with 2% PVDF, 10% PDMS, 20% Silica Nanoparticles (c)

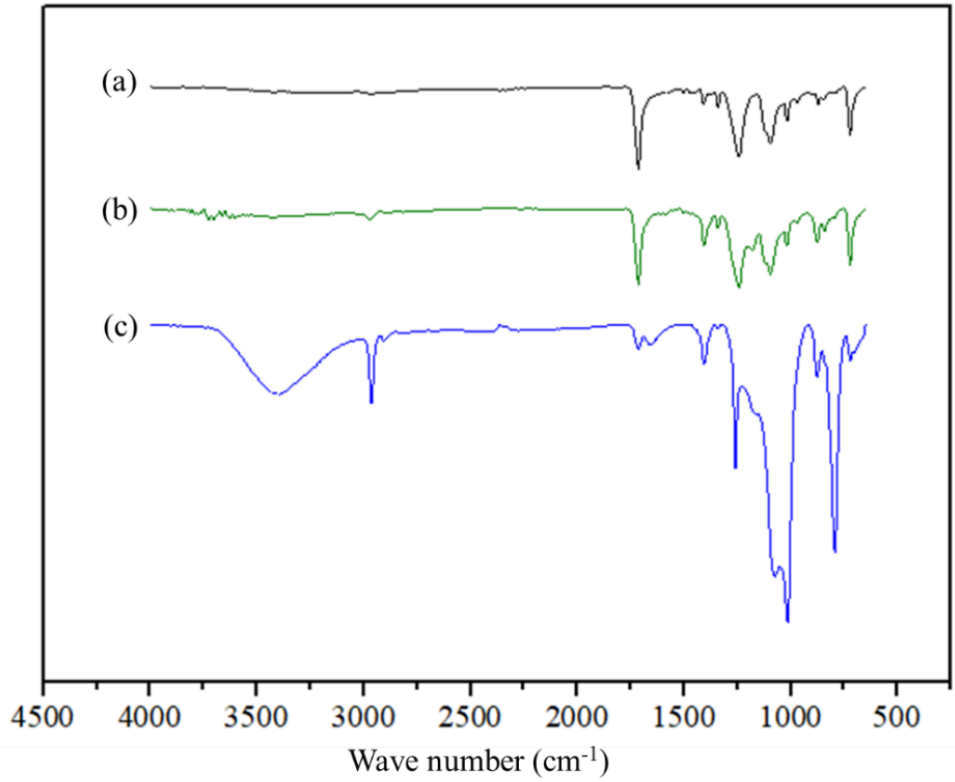

Font: The Author (2021)

The pristine PA membrane (Figure 28 (a)) was characterized by the peaks located in 1716 cm^{-1}, corresponding to C double bonds with O, characteristic of amides. The peak in 719 cm^{-1} confirmed the N-H bonds of this functional group, and the C-N bonds were located in the fingerprint region, corresponding to 1241 cm^{-1}. Some alterations in the chemical structure were observed in the modification with the blend of PDMS and PVDF (Figure 28 (b)). There was a maintenance of the characteristic peaks of amide, and peaks corresponding to C-F bonds (1407 cm^{-1}) and Si-CH_3 bonds (879 cm^{-1}) appeared, confirming the blend presence of PVDF and PDMS, respectively. Moreover, a slight peak in 2964 cm^{-1} suggested the presence of an sp^3 carbon, characteristic of alkanes. The EDX analysis presented in Appendix B (b) confirmed the elements in the sample surface, corroborating the ATR results. Through this technique, it becomes possible to infer that the surface of the modified membrane with the blend

PDMS+PVDF was constituted mainly by carbon (46.7 wt%), followed by fluor (35.7 wt%), oxygen (13.3 wt%), and silicon (4.3 wt%).

On the other hand, the presence of silica nanoparticles in the polymer blend significantly changed the pristine PA's chemical structure, as observed in Figure 28 (c). An intense peak located between 1,100 and 1,000 cm^{-1} evidenced Si-O-Si bonds' presence, characteristic of silica nanoparticles. The presence of sp^3 carbon was confirmed by the peak located in 2,964 cm^{-1}, similarly in the blend without silica. The wavelength of 1,258 cm^{-1} identified the C-F bonds of PVDF, and the peak of 791 cm^{-1} confirmed the $Si-CH_3$, characteristic of the PDMS. A peak corresponded to 3,412 cm^{-1} in the spectra functional group region appeared, suggesting O-H bonds of hydrophilic silica employed in the blend. The EDX analysis presented in Appendix B (c) contributed to completing the modified PA membranes' chemical surface analysis. The presence of the elements such as silicon, carbon, oxygen, and fluor, in the concentrations of 35.7, 32.1, 22.9, and 9.2 wt%, respectively, confirmed the ATR results of the chemical surface modification achieved through the proposed modification.

Aiming to investigate the morphological changes on modified PA membranes' superior surface, SEM images were performed, amplifying the membrane images from 500 to 10,000 times. Figure 29 show the obtained SEM images.

Similar to the PP modified membranes, the software *ImageJ* was employed to measure the drop size and the fiber size for pristine PA membrane. Fifty measurements were performed with each image, in amplification of 3,000 times to pristine PA membrane and 10,000 times to modified PA membranes, using the equipment's scale. The pristine PA membrane showed an average fiber diameter of 16.2 μm, with high homogeneity and a small number of pores, evidencing its dense structure. The high homogeneity of the fibers, combined with the Polyamide's hydrophilic nature, conceives to this membrane a low roughness and high water affinity. The first proposed modification (Figure 29 (b)) with a polymer blend containing 2% PVDF + 10% PDMS covered the surface with small drops, with an average distribution of 1.308 ± 0.252 μm. The PA surface was regularly covered by the proposed modification, which increases its roughness, proved by the increase in water contact angle.

Figure 29 – SEM images of pristine PA (a) and modified PA membranes with 2% PVDF, 10% PDMS (b), and with 2% PVDF, 10% PDMS, 20% Silica Nanoparticles (c), approximated in 500, 1000, 3000, 5000 and 10000 times.

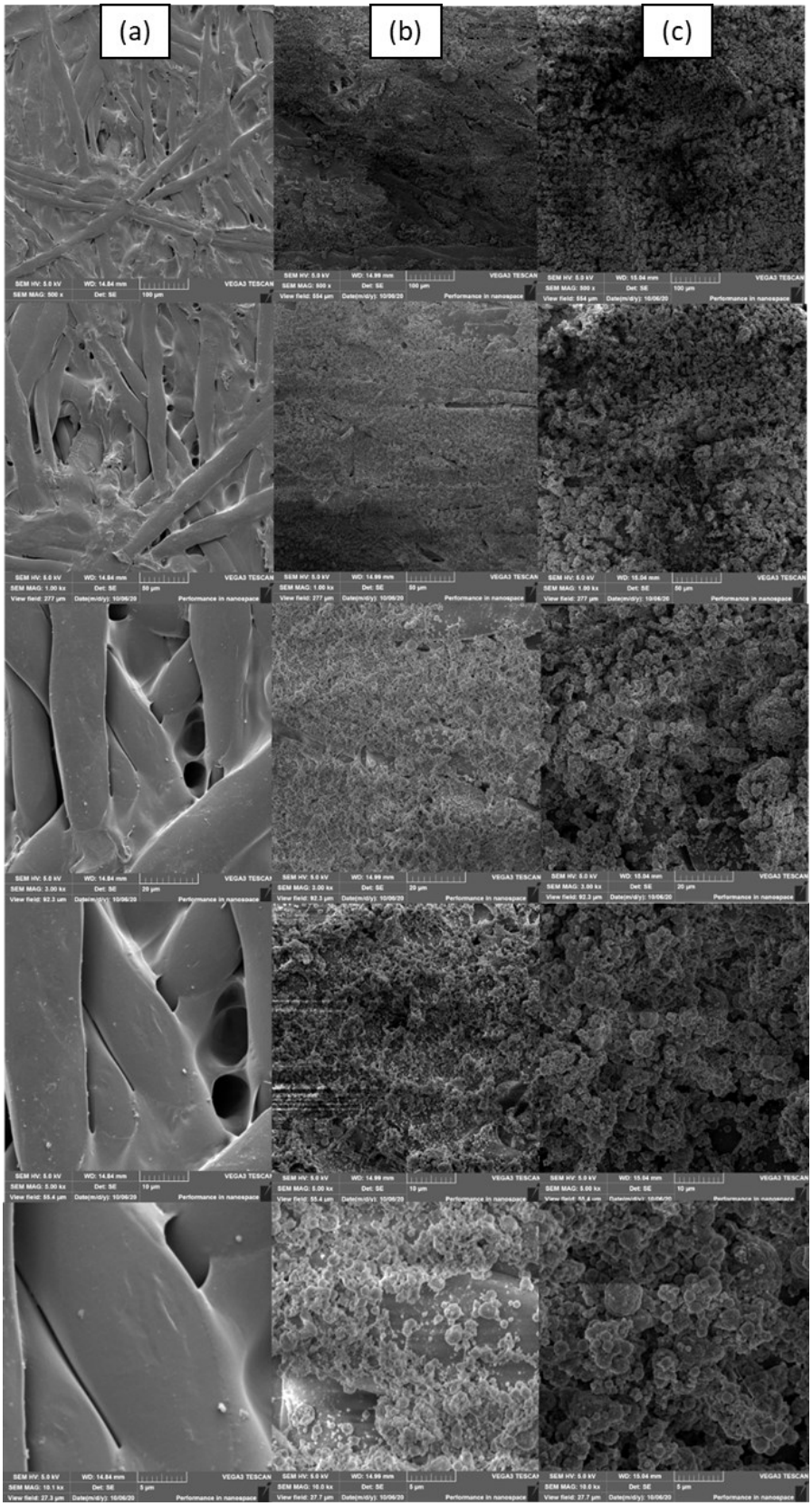

Font: The Author (2021)

The incorporation of silica nanoparticles on polymer blend seems to cause a slight decrease in drop size, resulting in an average of 1.244 ± 0.36 μm (Figure 29 (c)). The same trend was observed by Lee, Deka, An (2019a), where the increase in silica aerogel concentration on the dope solution decreased the drop size on the membrane surface. For this reason, the modified PA membrane using the polymer blend combined with 20% of SiNPs showed high roughness and higher water contact angle. Despite the same time under the spray, the silica nanoparticles seem to propitiate a more covered surface than the modification using only polymers. The droplets' overlapping originated a hierarchically re-entrant structure, remarkable by the drops contrast on the SEM image. The SEM results corroborating the high contact angles obtained to this modification with water and low surface tension solutions.

A similar drop size was obtained to the same modification (2% PVDF, 10% PDMS, and 20% SiNPs) in different water-behavior membranes (PP and PA). This result indicated that the substrate did not affect the drop size formed in the electrospray technique. The drop size is mainly affected by the dope solution's viscosity and composition, the syringe's diameter, and the coating flow rate. The same pattern of droplet formation was found for different substrates (PA and PP). The extreme variation in contact angles obtained for each modification was due to the membrane's pore structure. Greater contact angles are obtained to modify the PA membrane with the blend of polymers and silica nanoparticles, mainly because it consists of a dense membrane. Also, its polar structure can increase the affinity between the modification and the substrate, increasing the homogeneity of the modification.

4.2.4 Thermal analysis of pristine and modified PA membranes

The main goal of the Differential Scanning Calorimetry analysis for membranes to DCMD application was to determine if the proposed modification affects the temperature range of applications of these membranes, concerning the operational conditions. Figure 30 shows the DSC curves comparing the pristine and modified PA membranes' thermal behavior. The analysis was carried out from -30 to 300ºC, at 10ºC.min^{-1}, under an inert atmosphere.

The transition of first order observed in the three curves corresponded to the melting, which consists of an endothermic event. By analyzing the melting phenomenon, it becomes possible to determine the melting heat (melting enthalpy), detect the presence of plasticizer additives, and determine the percentage of mixtures of each sample.

Figure 30 – DSC analysis of Pristine and modified PA membranes with 2% PVDF, 10% PDMS, 0% or 20 % Si

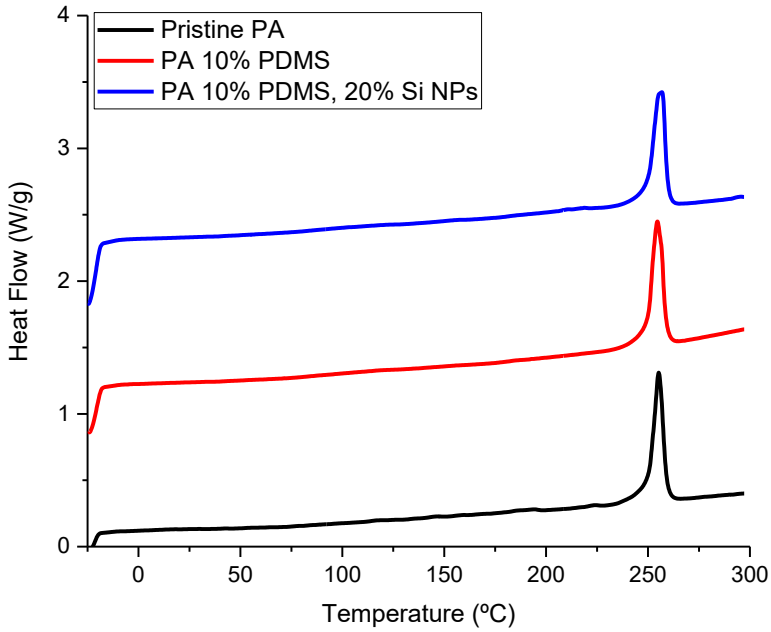

Font: The Author (2021)

The melting point of the pristine PA membrane is equivalent to 255.25 ºC. It was known that the PA membrane (commercial name NF90) is composed of the polyamide 6 supported in a PET substrate. The theoretic melting heat of Polyamide 100% pure is 53.55 J g^{-1} (GOMES DE ARAÚJO, 2002). The melting heat of the analyzed pristine PA was determined using the Origin Software to calculate the peaks' integral. This value was equivalent to 6.93 J g^{-1}.

The proposed modifications induced a slight reduction in the pristine membrane's melting heat, which was equivalent to 6.88 % for the modified PA using 2% PVDF and 10% PDMS, and 5.125 % modified PA membrane with 2% PVDF, 10% PDMS, and 20% Si NPs. The pristine membrane melting point (255.25ºC) was not harshly affected by the proposed modifications, reaching 254.63ºC for the polymer modification and 256.59 ºC for the modified membrane using silica nanoparticles. The melting point has a small increase for this modification, which adds good characteristics to this membrane. For this reason, the range of temperatures where these membranes can be applied and the thermal resistance were maintained. The modified membranes enabled the DCMD processes using the same operational conditions.

4.2.5 Zeta potential of PA modified membranes

The Zeta Potential of each pristine and modified membrane was measured to determine the membranes' superficial charge. It enables understanding the physicochemical interactions among the membranes and the dyes, used to explain some results in DCMD applications. The measurements were carried out in the pH range of 3-11. To better understand the relation between the membranes' zeta potential and the different dyes applied in this work, the dye solutions' pH was measured and shown in Table 12. Figure 31 shows the zeta potential of pristine and modified PA membranes.

Table 12 – pH of dye solutions

Dye solution (30 mg L^{-1})	pH
Reactive Black	7.83
Disperse Black	5.92
Direct Black	7.19
Acid Black	6.94

Font: The Author (2021)

Figure 31 - Zeta Potential as a function of pH of pristine and modified PA membranes

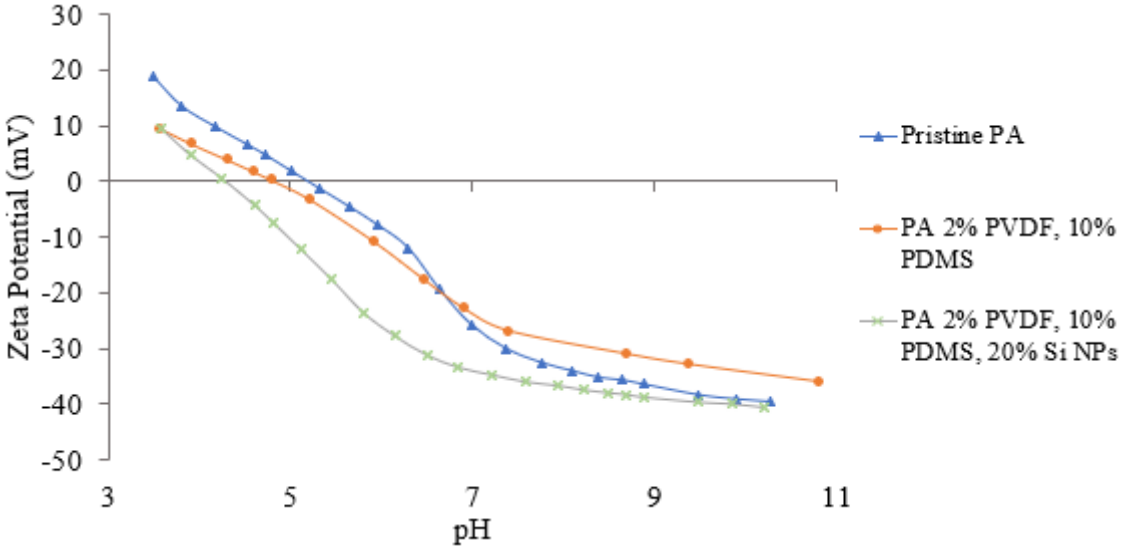

Font: The Author (2021)

The PA membranes showed negative results of the zeta potential in the pH range of tested dye solutions (6.0 – 8.0). The isoelectric point is defined as the pH where the zeta potential is equal to 0 mV. This value was equivalent to 5.32, 4.78, and 4.24 for pristine PA membrane, membrane modified only with polymers, and membrane modified with Si NPS,

respectively. The isoelectric point of modified membranes can suggest an amplification of pH range where the membrane can be employed in a DCMD process. This range is singularly amplified as more materials are incorporated on the membrane surface, being larger for membrane modified with PDMS and Si NPs. In this case, even at lower pH, the membrane would develop negative charges on its surface, enabling repulsion forces between the membrane and an acid solution. These repulsive forces would increase the separation potential of this membrane, contributing to developed antifouling properties.

The zeta potential results of PA modified membrane will support the discussion of the permeate fluxes and rejection rates in the section of DCMD tests.

4.3 PP MEMBRANE MODIFICATION USING PDMS WITH CURING AGENT (SYLGARD 184)

The first modification proposed to the PP membrane did not significantly change the membrane water contact angle. The PDMS vinyl terminated in these modifications encouraged the polymer reticulation with a curing agent, which led to the PDMS substitution by the kit Sylgard 184. It consists of the PDMS vinyl terminated and its curing agent. The methodology to design the dope solution was changed, but the concentration of polymers and silica was maintained, as well as the electrospraying conditions.

4.3.1 Water contact angle of PP modified membranes with Sylgard 184

The polymer reticulation seemed to significantly increase the water contact angle of all modified PP membranes (Figure 32), at most 24º and at least 17º. The tested solutions containing Sylgard had their concentrations varied in 6 and 10%. The highest water contact angle was obtained in the modification using 2% PVDF and 6% Sylgard and consisted of 142.07 ± 1.67º. The water contact angle reduced with the increase of silica nanoparticles for the modifications using 6% of Sylgard but increased when 10% of Sylgard was employed.

Similar water contact angles were obtained by Khan *et al*. (2019b), where the kit Sylgard 184 combining with SiNPs and 1H,1H,2H,2H perfluorodecyl triethoxysilane (FAS) was applied to modify a Polyethersulfone (PES) membrane via dip-coating. The resultant membrane reached 131º of water contact angle, that is lower than the contact angle of all modified membrane using Sylgard 184 comprised in this work. Siyal *et al*. (2018) also combined a cured PDMS was with fluorographite to modify a glass fiber membrane using the same technique.

This work achieved a water contact angle of 143º for the modified membrane, corroborating the cured PDMS's low surface energy, which enables high hydrophobicity to cover surfaces.

Figure 32 – Water contact angle of PP modified membranes using Sylgard 184

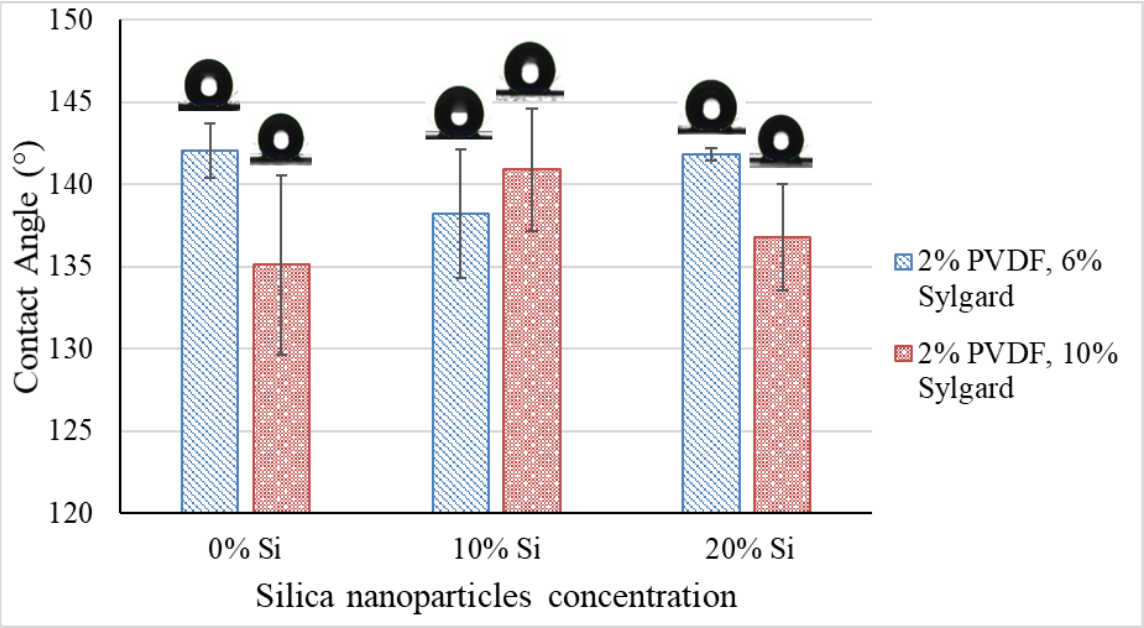

Font: The Author (2021)

The polymer cure replaced the PDMS vinyl terminated bonds to rise cross-linked chains containing C-Si-C bonds. The most non-polar chemical structure of the cured PDMS contributed to the high hydrophobicity achieved through the modifications.

The Si NPs incorporation did not positively affect the membrane hydrophobicity once the water contact angles obtained for these modifications showed lower values. It may be possible that the hydrophilic behavior of silica nanoparticles employed in this work contributed to decrease the water contact angle, despite the high surface roughness created by them. The Si NPs presented an opposite behavior when dealing with the PA membranes, and it could be explained by the difference among the membrane matrix. The PP membrane consists of a porous membrane that was not so deeply affected by the particle deposition in the increment of roughness as it was the PA dense membrane. For this reason, the porous PP membrane had its water contact angle harsher affected by the polymer's surface energy and SiNPs water behavior than by the roughness created by the nanoparticle's deposition.

The contact angle was a criterium to select the best membranes for further analytical investigations. For this reason, the membrane containing 2% PVDF and 6% Sylgard was selected for further analysis and consisted of a promisor candidate for the MD operation.

4.3.2 Porosity and membrane thickness of PP modified membranes with Sylgard 184

In addition to the increase of membrane hydrophobicity, the proposed modification using 6% of Sylgard did not affect the membrane porosity, showing a reduction of only 2%. It consisted of a thin coat under the membrane surface with approximately 3 μm (Table 13). The maintenance of membrane porosity agreed with membrane distillation requirements, and the thin coating contributed to may not increase the mass transfer resistance in this operation.

Table 13 – Porosity and membrane thickness of pristine and modified PP membranes

	Pristine PP	**PP (2% PVDF, 6% Sylgard)**
Porosity (%)	82.74 ± 0.84	80.35 ± 1.03
Thickness (μm)	120.3 ± 0.64	123.6 ± 6.76

Font: The Author (2021)

The absence of silica nanoparticles resulted in a thinner membrane, compared to the modified PA membrane. The proposed modification did not harshly affect the membrane thickness, which consist of an important feature to guarantee the mass transfer in DCMD operation.

4.3.3 Chemical and morphological analysis of PP modified membranes using Sylgard 184

The ATR-FTIR analysis was carried out in the modified PP membrane, aiming to study the influence of the cross-link reaction between the PDMS and its curing agent in the PP membrane's chemical structure. In this modification, silica nanoparticles were not employed in the polymers blend. The ATR spectra for modified and pristine PP membranes are shown in Figure 33.

Comparing the IR spectra of modified and pristine membranes, it was noted the maintenance of the peaks corresponding to sp^3 carbon (C-H) between the wavenumbers of 2,950 and 2,840 cm^{-1}, indicating the alkane nature of the PP molecule. Besides, peaks located in 1,454 and 1,374 cm^{-1} wavenumbers corresponded to carbon bonded with two and three hydrogens in both spectra. The chemical modification in the sample surface (Figure 32 (b)) was confirmed by analyzing the fingerprint region, where the peak among 1,100 and 1,000 cm^{-1} corresponding to Si-O-Si bonds arose, characteristic of the PDMS (a silica-based material). The PDMS presence was also corroborated by the peaks of 840 cm^{-1} corresponding to Si-CH_3 bonds

and 1257 cm^{-1} of Si-C bonds. The PVDF presented in the blend of polymers at a low concentration is evidenced by the peak of 1,170 cm^{-1}. Corroborating the IR discussion, an EDX analysis was carried out in the modified membrane (Appendix A). The majority of carbon on the membrane composition was evidenced (79.6 wt%), mainly corresponding to the carbon of the membrane matrix. Oxygen was found in 9.9% of the surface composition, related to the oxygen from Sylgard 184 molecules. Fluor (7.4 wt%) and silicon (3.2 wt%) were revealed in the membrane surface, related to the PVDF and Sylgard 184 molecules, respectively.

Figure 33 – ATR-FTIR analysis of pristine PP (a) and modified PP membrane with 2% PVDF, 6% Sylgard 184 (b)

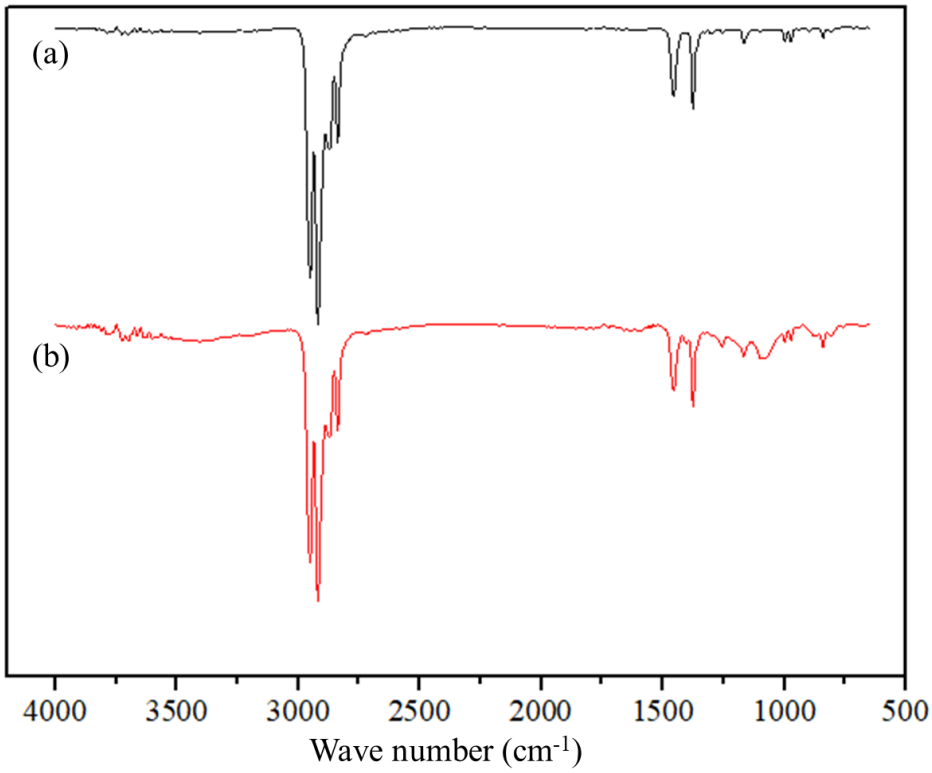

Font: The Author (2021)

By analyzing the microphotographs of the superior surface obtained by SEM analysis, superficial morphological changes on the PP membrane after the proposed modification were evidenced. Figure 34 shows the SEM images of pristine and modified PP membrane with 2% PVDF, 6% Sylgard 184, expanded from 1000 to 10000 times.

Figure 34 – SEM images of pristine PP (a) and modified PP membranes with 2% PVDF, 6% Sylgard (b), approximated in 1000, 3000, 5000, and 10000 times.

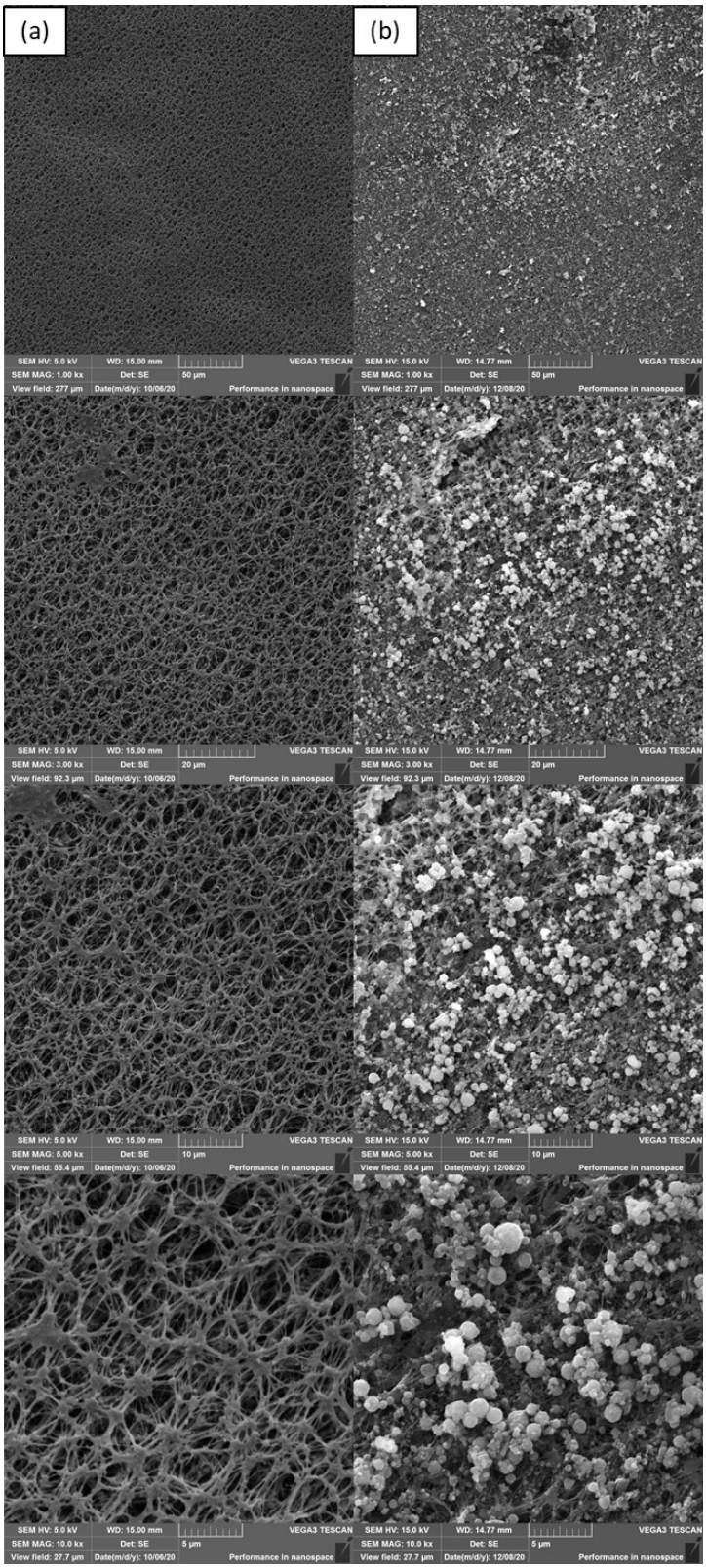

Font: The author (2021)

The covered PP surfaces showed high homogeneity with different drop sizes, conceiving high surface roughness without losses in volumetric porosity. The same method to measure the drops using *ImageJ,* proposed in the previous sections, was employed. Fifty measurements were carried out with each image amplified 10,000 times to guarantee higher measurement precision. The average drop size was calculated according to the equipment's scale, and this value was 1.373 ± 0.29 µm. It was possible to observe that the range of drop size to the modification using Sylgard 184 was higher than the modified membranes with only PDMS, and the average value of the drop size is also higher. This higher range of drop size, occasioned by the high difference in the drop size deposited on the membrane surface, combined with the cure of PDMS, revealed a high increase in the membrane hydrophobicity, even with different dyes classes. This behavior is related to the solution viscosity, discussed in the following sections. It supplied high roughness to the membrane surface because of the drops' overlapping, forming a more evidenced reentrant hierarchical surface.

4.3.4 Thermal analysis of PP modified membranes using Sylgard 184

The DSC analysis had the primary goal of investigating the effect of the proposed modification in the temperature range of applications concerning the MD operational conditions. The DSC curves of pristine and modified PP membranes using PVDF and Sylgard are shown in Figure 35. The pristine PP sample weighed 1.608 mg, and the modified PP sample weighed 1.792 mg.

Thermal events corresponding to second-order transitions were not well visualized due to the temperature range limitation in these analyses (-30º). Nonetheless, the increase in the calorific capacity, evidenced by the baseline change, corresponded to both samples' glass transition temperatures.

The first-order transitions corresponded to an endothermic event in both curves, equivalent to the samples' melting. The pristine PP membrane's melting point was 163.5ºC, while this point for the modified membrane was 164.5ºC. In this sense, it can be concluded that the proposed modification caused a slight increase in the thermal resistance to the membrane, adding an outstanding characteristic to the DCMD operation.

The area of the melting peaks corresponds to the melting heat (ΔH_f) ($J.g^{-1}$). The software Origin was used to calculate the peaks' integral, resulting in melting heat values of 17.05 J. g^{-1} for pristine PP membrane and 16.51 J. g^{-1} for the modified PP membrane.

Figure 35 – DSC analysis of Pristine and modified PP membranes with 2% PVDF and 6% Sylgard

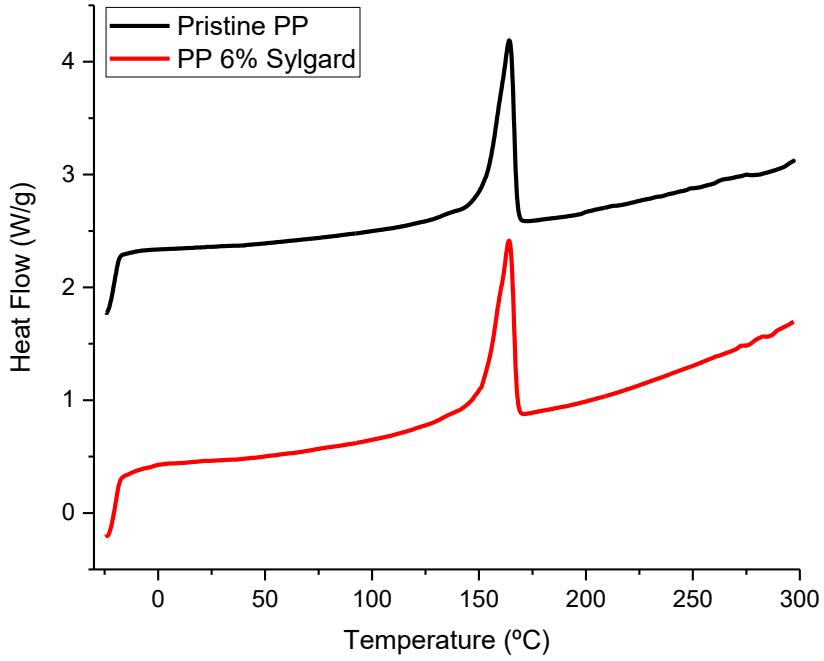

Font: The Author (2021)

The proposed modification did decrease the membrane's melting point. The small reduction in the modified membrane's melting heat did not affect the range of temperatures where this membrane can be applied since the melting point suffered a small increase. Then, the pristine membrane's thermal resistance was slightly increased after the proposed modification. The modified membrane could use the same operational conditions for the DCMD processes as the pristine one.

4.3.5 Zeta potential of PP modified membranes

The Zeta Potential of PP membranes are shown in Figure 36. The PP membranes showed negative results to the zeta potential in the pH range of tested dye solutions (6.0 – 8.0). The isoelectric point of pristine PP membrane was 5.77, while for the modified membrane using PVDF and Sylgard was 4.036. As observed for the modified PA membranes, the proposed modification also amplified the pH range where this membrane can be employed in the DCMD

process. The modified membrane would assume negative charges at lower pH than the pristine PP.

Figure 36 - Zeta Potential as a function of pH of pristine and modified PP membranes

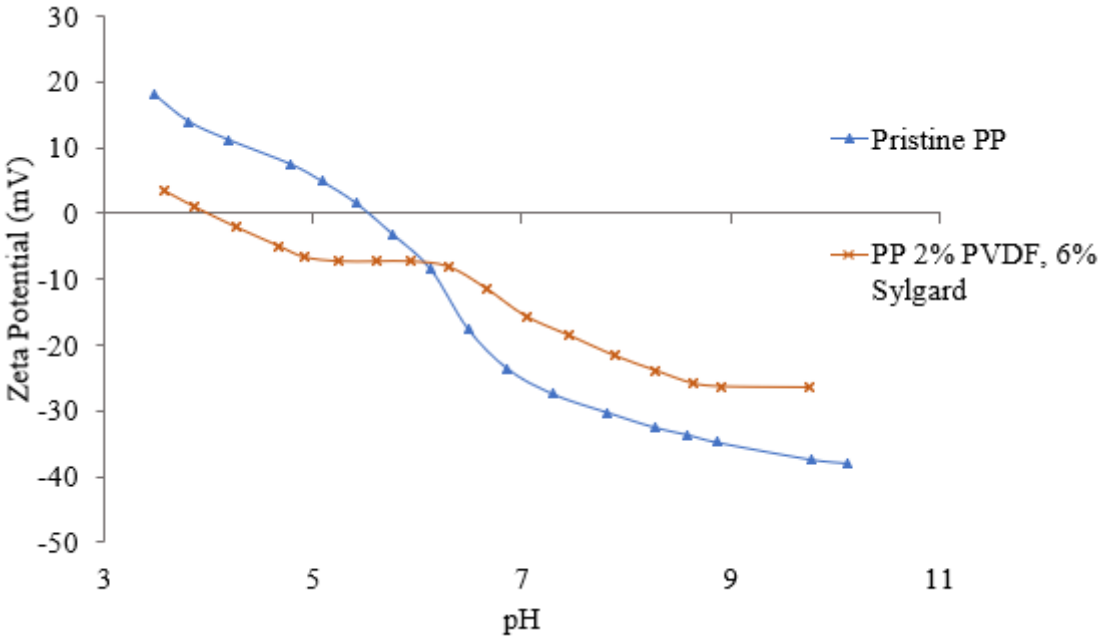

Font: The Author (2021)

The charging behavior at the solid-liquid interface, defined by the zeta potential, is explained using the electrical or electrochemical double layer (EDL). In this model, the zeta potential is described as a shear plane that separates a stationary layer and a mobile layer of charges. This property is dependent on ionic strength, additive concentration, temperature, material swelling, size, porosity, electronic conductance, surface roughness, and pH value. The pH value is the most important parameter of the liquid phase that affects the zeta potential. It may also reveal information about the solid surface hydrophilicity, material swelling, and buffer capacities of bases and acids (LUXBACHER, 2014). In this work, besides the points about the pH range of membrane applications, the zeta potential will explain the permeate fluxes and rejection rates obtained in the DCMD experiments, as discussed in the following sections.

4.3.6 Rheologic study of electrospraying solutions

Rheograms of each dope solution applied to design the modified membranes using electrospraying were built to investigate how the apparent viscosity affects the drop size on

membrane modification. The results are shown in Figure 37. It is important to emphasize that these solutions consist of mixtures of polymers (PVDF and PDMS vinyl terminated or cured), containing 0 or 20% of Si NPs, solubilized in a ratio 1:1 of THF: DMF. All measurements were carried out in triplicate.

Figure 37 – Rheogram of the fluids employed as dope solutions on electrospraying modifications

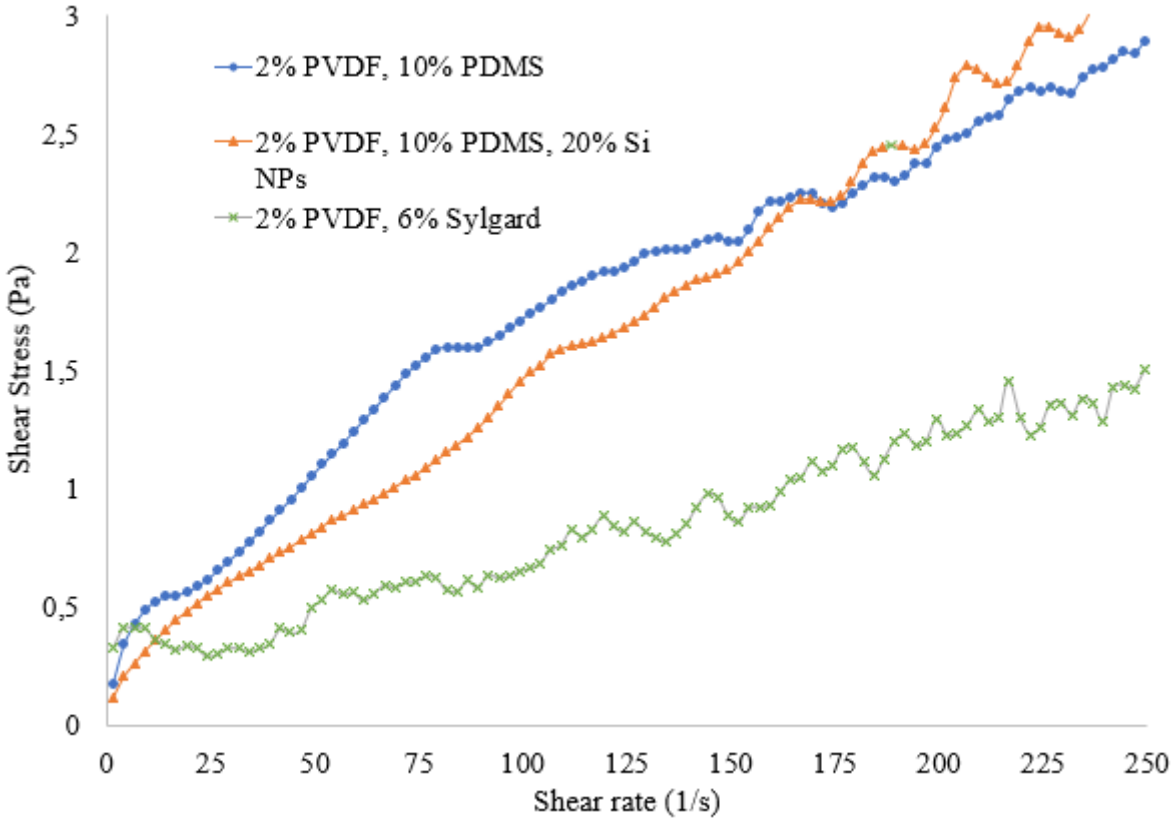

Font: The Author (2021)

All the fluids investigated in this work did not show a linear proportion between the shear stress and the shear rate, concluding that they cannot be classified as Newtonian Fluids. The analysis of Figure 37 allows inferring that the solutions containing PVDF and PDMS vinyl terminated with or without silica nanoparticles consist of pseudoplastic fluids once their viscosity seems to decrease with the shear stress. In this case, the molecules were guided according to the stress direction. The solution containing the cured PDMS (Sylgard 184) required an initial shear stress to drain. For this reason, this solution can be classified in a Herschel-Bulkley Fluid.

The apparent viscosity hardly affects the modification morphology since it consists of a determinant parameter of the electrospraying technique. Figure 38 shows the relation between the viscosity and the spray drop size. The viscosity presented in Figure 38 was calculated based on the average apparent viscosity of each solution when it achieves a constant behavior.

Figure 38 – Relation between the apparent viscosity and the spray drop size of each dope solution

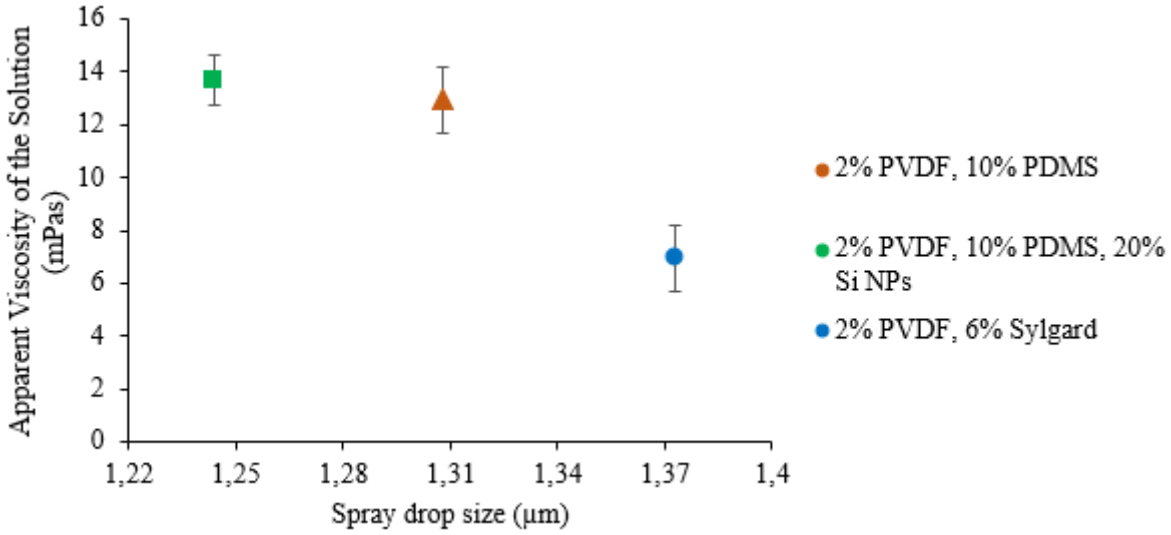

Font: The Author (2021)

The polymer concentration strongly influences the solution viscosity, which increases with the increase in polymer concentration. In this case, it is possible to observe that the cure of PDMS vinyl terminated, illustrated by the solution "2% PVDF, 6% Sylgard", harshly reduces the solution viscosity when comparing with "2% PVDF, 10% PDMS" (almost 100% of decrease). The viscosity using Sylgard was also lower because of the lower polymer concentration. The chemical reaction involved in the cure process changed the molecular weight of the PDMS polymer. The addition of silica nanoparticles increased the average apparent viscosity of the solution by almost 1 mPa s. An increase in the dope solution viscosity by incorporating nanoparticles was also reported by Attia *et al*. (2018a), where the electrospinning dope solution had its viscosity increased by the addition of alumina nanoparticles.

In the electrospraying process, droplets formed a Taylor cone shape on the syringe tip. The droplets are captured by a collector when the liquid's superficial tension was overcome by electrostatic repulsion in a high voltage electric field. The viscosity affects this drop formation and also the structure formed in an electrospraying system. When dealing with dilute polymers

at very low concentrations, drops are not formed due to the poorly superficial tension and low solution viscosity. On the other hand, at high polymer concentrations, the particle formation is changed by fiber formation (electrospinning). For this reason, the viscosity also acts as a limiting parameter to the droplet formation. The viscosity is linked to the polymer's entanglement in solution, being high at high polymer concentration, creating dense particles (NIU *et al*., 2020).

Figure 38 reveals the influence of the solution viscosity on the drop size formed by electrospraying. Higher viscosities resulted in a smaller drop size of the formed particles, as was illustrated by the solution containing silica nanoparticles. Similar results were also reported by Attia *et al*. (2018a), where a solution containing 6% of PVDF had its viscosity increased by 25.2% with 30% of alumina nanoparticles. This addition reduces the drop diameter from 1.8 to 1.4 μm. Liu *et al*. (2007) demonstrated that increased polymer viscosity leads to reduced drop size. The correlation between the viscosity and the drop size is explained by the dope solution's constituted materials' entanglement. Low entanglement of polymers into a solution, occasioned by low polymer concentration and low solution viscosity, turns the solution more prone to the repulsive forces between the polymer molecules, creating more larger drops (LEE *et al*., 2017). Moreover, the smaller drop size propitiates more roughness to the membrane surface due to the microsphere’s formation.

4.4 DCMD TESTS

4.4.1 Repellence properties of modified membranes against different textile solutes

Contact angle measurements and an evaluation of the best-selected membranes' swelling degree were carried out to predict how the modified membranes will work against different textile solutions. Through these analyses, the DCMD tests were guided, based on the higher contact angles obtained to each solution, to guarantee enhanced performances.

The solutions involved in these measurements consisted of four different dyes (reactive, disperse, acid, and direct black dyes) at 30 mg L^{-1} and a surfactant solution (Colorswet 30 mg L^{-1}).

The contact angle measurements of all selected membranes with dye classes and surfactant solutions are found in Appendix C. These analyses played a key role in selecting the membranes according to their potential for each solution, reducing the number of DCMD tests.

As mentioned in the previous sections, pristine and modified PA membranes are dense membranes and show smaller pores than PP membranes. The pristine PA membrane showed a hydrophilic character against all tested solutions, with the lowest contact angle of 61.13º with the surfactant solution. Direct and reactive dyes are employed to dye cellulosic substrates, such as cotton, paper and flax, consisting of a hydrophilic matrix. The hydrophilic nature of PA membranes led to high interactions with these dye classes, resulting in lower repellences, evidenced by lower contact angles. The modification of PA membranes using only PVDF and PDMS seems to increase the membrane's repellence against water, achieving 129.3º of water contact angle, attributed to the hydrophobic nature of the PDMS and PVDF employed in the dope solution. However, the hydrophobic groups could not decrease the interactions with the reactive black dye's hydrophilic structure, showing a hydrophilic character against this dye and low surface tension solution (surfactant). Slightly hydrophobic angles (~90º) were obtained to this membrane for disperse, direct, and acid dyes, probably due to dye-membrane's low physico-chemical interactions.

When silica nanoparticles were employed in the polymer blend, the water and surfactant contact angles were highly increased, mainly because of the high roughness created by the Si NPs incorporation combined with the dense substrate of PA membrane, as reported in the morphological evaluation. The use of Si NPs in doping solution of electrospinning modifications promises to achieve oleophobic characters, as reported by Hou *et al*. (2018). In this work, silica nanoparticles were combined with poly (vinyl alcohol) (PVA) to modify a PTFE membrane, achieving 156.5º of oil-contact angle. Also, Si NPs achieved omniphobic behaviors when combined with cellulose acetate in an electrospinning modification of Polyester membrane, revealing anti-wetting properties against surfactant solutions (0.1-0.5 mM of SDS), as studied by (HOU *et al*., 2019a). These works corroborate the results of the use of silica nanoparticles in a dense matrix. Even with the hydrophilic character of Si NPs employed in this work, the highest water and surfactant contact angles of all modified membranes were respective to the PA 2% PVDF, 10% PDMS, and 20% Si NPs.

The pristine PP membrane showed a hydrophobic character against all tested solutions, achieving higher contact angles with dye solutions than water. The proposed modification with 2% PVDF and 6% Sylgard highly increased the water contact angle up to 142.07º and the contact angles with direct dye, acid dye, and surfactant solutions. The acid dyes are anionic, commonly employed to dye polyamides and proteins, forming ionic bonds with the fibers. The modified PP membrane showed its highest repellence against this dye class, related to the weak physicochemical interactions. However, the polymer blend of Sylgard and PVDF proposed in

this modification could not significantly increase the contact angles against reactive and disperse dyes.

Table 14 summarized the highest contact angle obtained to each solution and its respective membrane. All solutions were at 30 mg L^{-1} of concentration.

Table 14 – Membranes with the highest contact angles for each tested solution

Solution	Membrane	Contact Angle (º)
Reactive Black Dye	PP 2% PVDF, 6% Sylgard	132.87 ± 0.51
Disperse Black Dye	PP 2% PVDF, 6% Sylgard	133.33 ± 0.91
Direct Black Dye	PP 2% PVDF, 6% Sylgard	148.38 ± 12.36
Acid Black Dye	PP 2% PVDF, 6% Sylgard	151.50 ± 6.18
Colorswet	PA 2% PVDF, 10% PDMS, 20% Si	160.5 ± 2.6

Font: The Author (2021)

The evaluation of swelling degrees was performed to enhance the understanding of modified membranes' repellence properties against the solutions (Table 14). This analysis infers about the long-term operations and the capacity of the membrane to maintain its hydrophobicity. The liquid absorption occurs because of the penetration of feed solution into the polymeric matrix volume, related to the capillarity phenomenon. Also, through the evaluation of swelling degree, it becomes possible to compare the influence of the modification in the solution absorption over time with the pristine membrane. Figure 39 shows the swelling degree results of pristine and modified PP membranes.

The swelling degree determination is susceptible to high standard deviations. The standard deviation was higher for PP than PA membranes once the weight of PP membranes is almost ten times lower than PA, increasing the measurement's imprecision. Also, the PP membrane's hydrophobic matrix leads to a lower solution absorption, affecting the standard deviation.

Figure 39 – Swelling degree of pristine and modified PP membranes with dyes solutions (30 mg/L)

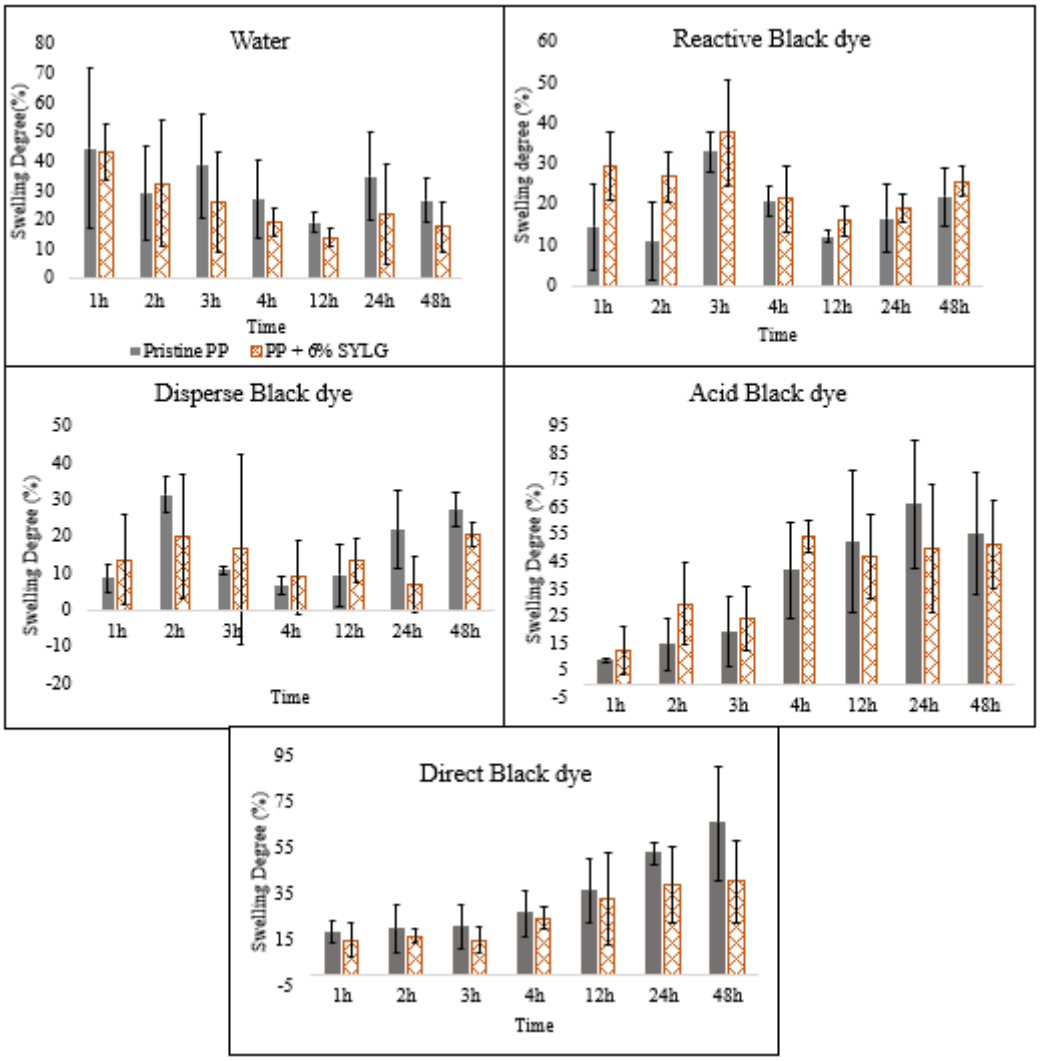

Font: The author (2021)

The pristine PP membrane seems to present the highest swelling degrees than modified PP membranes with all tested solutions, except reactive black dye. The swelling degree is intrinsically related to the membrane hydrophobicity. The lowest swelling degrees of modified PP membranes were linked with their higher contact angles. The higher hydrophobicity avoids the liquid penetration into membrane pores due to the physicochemical repellences between the membrane and the feed solution. For distilled water, reactive and disperse dyes solutions, the swelling degrees of both membranes (pristine and modified) did not increase over the analyzed 48 h. For these solutions, the average swelling degree of pristine PP membrane was 31.5%, 18.65%, and 16.74% for water, reactive black dye, and disperse black dye, respectively. The modified PP membrane showed swelling degrees of 25.1%, 25.3%, and 14.4% for these solutions. The water absorption showed the highest reduction comparing the pristine and

modified PP membrane (6%). The modification seems to increase the interaction among the chromogenic group and the membrane surface for the reactive black dye once the solution's penetration into the membrane matrix increases. The modification did not significantly alter the swelling degree of disperse black dye. These results corroborated the contact angles obtained to these membranes. The proposed modification could not improve the repellence between the membrane and the reactive and disperse chromogenic groups.

On the other hand, the acid and direct black dyes were absorbed into the membrane matrix in a crescent way over time. In these cases, although the increase in swelling degree over time, the absorption differences among the pristine and modified PP membranes were evidenced over 12 h. Starting this time, the reduction of the modified PP swelling degree with the direct black dye evolved from 5% in 12 h to almost 10% in 24 h and 25% in 48 h, comparing to pristine PP. This result evidenced the potential of modified PP membrane to work with these chromogenic groups, maintaining a satisfactory repellence over time. These results agreed with the high contact angles obtained for direct black solutions, where 148º was achieving for the modified membrane. For the acid black dye, the decrease in the swelling degree is not as harsh, but it behaves the same way over time.

In conclusion, the chromogenic groups affected the swelling degree of PP membranes and the liquid absorption behavior over time. The proposed modification in the PP membrane decreased the swelling degree for all tested solutions comparing to the pristine one, except for the reactive black dye. It was also the only solution where the contact angle improvement was not achieved with the membrane modification, corroborating with swelling degree results.

The swelling degree analysis was also performed with PA modified membranes for water, reactive black, and detergent solutions (all of them in 30 mg L^{-1}), which comprises the compounds of cotton dyeing bath. The results are presented in Figure 40.

Figure 40 – Swelling degree of pristine and modified PA membranes with different solutions

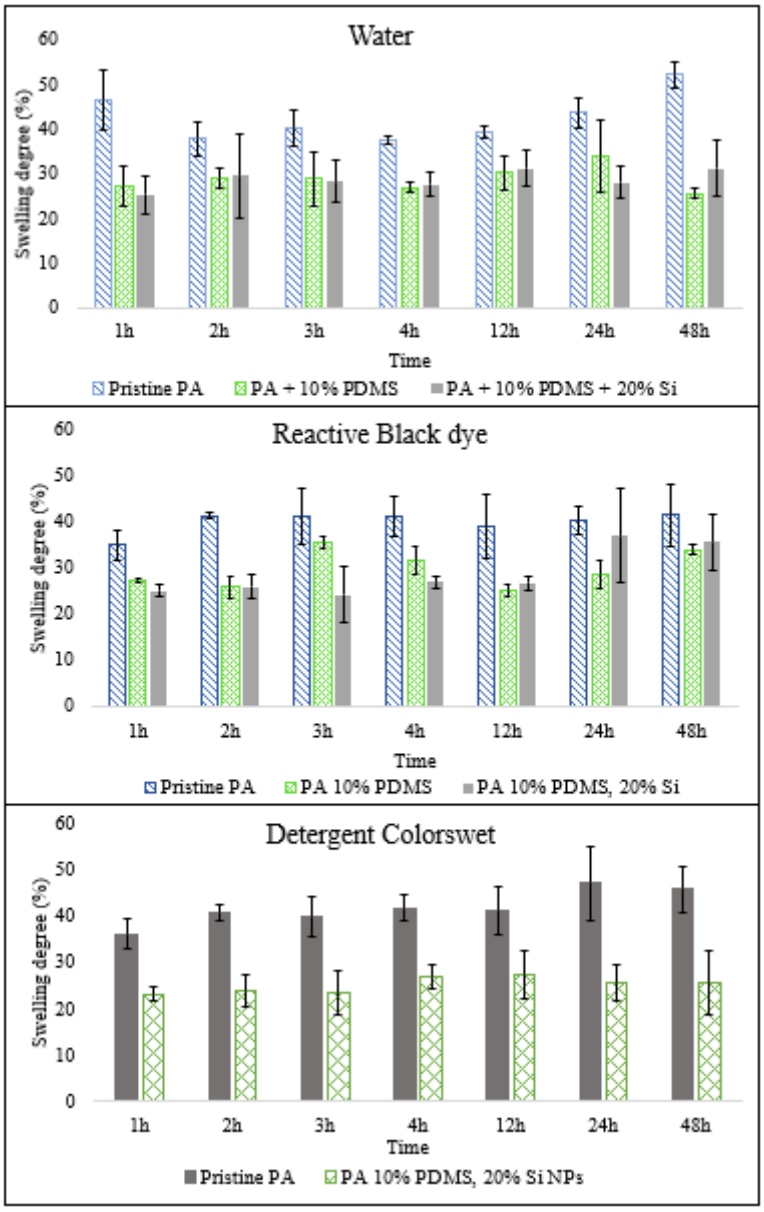

Font: The author (2021)

The pristine PA membrane showed a hydrophilic character, evidenced by the contact angle measurements and by the high swelling degrees obtained for water (average 42.53%), reactive black solution (average 39.81%), and detergent (average 41.7%). The swelling degree for modified and pristine PA membranes for all tested solutions did not increase over time, and the standard deviation is lower than the PP membranes. The absorption mechanism that occurs with hydrophilic membranes is similar to the wetting degrees presented in Figure 9. The water penetration blocks the membrane pores due to the absence of hydrophobicity on the membrane

surface. For this reason, hydrophilic membranes have higher swelling degrees than hydrophobic ones.

For water and reactive black solution, the proposed modifications showed similar behaviors in the swelling degrees. For water, it was achieved averages of 28.78% and 28.73% for modified membranes with PVDF + PDMS and PVDF + PDMS + Si NPs, respectively, and for reactive black dye 29.64% and 28.7%. A 10% reduction of the swelling degree was obtained for both membranes, with both solutions, compared to the pristine PA.

Regarding the detergent, which consists of a low surface tension solution (anionic surfactant), there was a drastic reduction (almost 25%) in the modified membrane's swelling degree, occasioned by the combination of Si NPs, PVDF, and PDMS in the dope solution, which changes the water behavior of the membrane. Its lower swelling degree, combined with the PA membrane's dense matrix, resulted in the highest water contact angle with detergent solutions. This result becomes the PA modified membrane a great candidate for MD operations with low surface tension solutions, justifying the next chooses.

The membranes' selection to operate in the DCMD with each solution was based on the highest contact angle obtained in the previous tests. Table 15 summarizes the DCMD tests carried out in this work.

Table 15 – DCMD tests performed with each selected membrane

(to be continued)

Membrane	Solution	Concentration
Pristine PP	Distilled Water	-
	Reactive Black Dye	30 mg L^{-1}
	Disperse Black Dye	30 mg L^{-1}
	Direct Black Dye	30 mg L^{-1}
	Acid Black Dye	30 mg L^{-1}
PP 6% Sylgard	Distilled Water	-
	Reactive Black Dye	30 mg L^{-1}
	Disperse Black Dye	30 mg L^{-1}
	Direct Black Dye	30 mg L^{-1}
	Acid Black Dye	30 mg L^{-1}
Pristine PA	Distilled Water	-
	Reactive Black Dye	30 mg L^{-1}
	Colorswet	30 mg L^{-1}
PA 10% PDMS	Distilled Water	-
	Reactive Black Dye	30 mg L^{-1}

Table 15 – DCMD tests performed with each selected membrane

(conclusion)

Membrane	Solution	Concentration
PA 10% PDMS, 20 % Si NPs	Distilled Water	-
	Reactive Black Dye	30 mg L^{-1}
	Colorswet	30 mg L^{-1}

Font: The Author (2021)

4.4.2 DCMD tests of modified PP membrane (PP 2% PVDF, 6% SYLGARD)

According to Table 14, the modified PP membrane using the cured PDMS was tested with the four different classes of dyes explored in this work. All DCMD tests were also carried out with the pristine PP membrane to compare the membranes' performance. For a better understanding, this section will be divided into subsections, which will present: the permeate flux obtained to each dye; the rejection rate; and the analytical tests carried out in the contaminated membranes after the DCMD operation, that consists in the morphological and chemical analysis, and measurements of membrane thickness and water contact angle.

4.4.2.1 Permeate flux of pristine and modified PP membranes

In the DCMD process, the feed solution's mass decreases, while the dye concentration is generally increasing during the operation. The permeate flux consists of the quotient between the total mass that crosses the membrane, the total membrane useful area, and the experiment's total time. It is important to emphasize that these experiments' main goal was to validate the separation of the modified membranes compared with the pristine ones, to the detriment of study the MD operational conditions. For this reason, the permeate flux was not analyzed hour by hour, only at the end of the experiment. Figure 41 shows the permeate flux for the pristine and modified PP membranes with distilled water and dye solutions.

The PP membrane has a hydrophobic nature. For this reason, the color rejection mechanism is related to the vapor pressure difference between the two sides of the membrane. The hydrophobic membrane repels water and only allows the passage of the water vapor across the membrane. Theoretically, the dye molecules stay in the liquid solution while the vapor across the membrane pores.

Analyzing Figure 41, a different permeate flux behavior according to the dye class was noted. As observed by Ramlow *et al*. (2019b), the permeate flux is strongly related to the dye

classes' chemical properties and their interaction with the membrane, to the detriment of the exclusion by size, as occurs in other membrane separation processes.

Figure 41 – Permeate flux of pristine and modified PP membranes

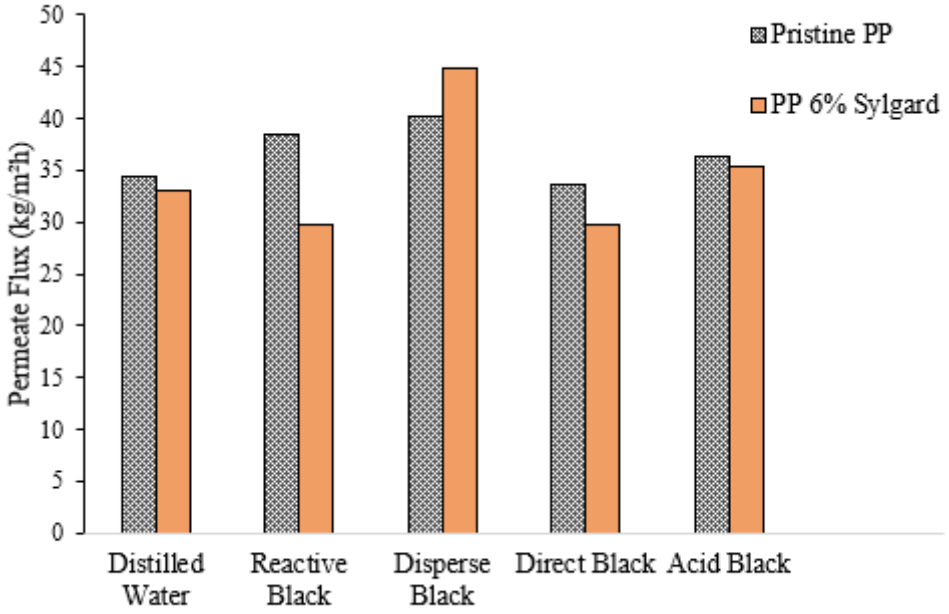

Font: The Author (2021)

Concerning the permeate fluxes of pristine PP membrane, it is possible to observe a higher permeate flux to the disperse black dye solution, comparing with the other tested solutions. In this case, the permeate flux reached 40.19 kg m^{-2} h^{-1}. The disperse dye did not present a superficial charge in the solution once it forms dispersion rather than a solution in the water presence. In the pH value of this dye (5.92), the zeta potential of the PP membrane is slightly negative (between -4 and -5 mV) (Figure 34). The absence of charge in the solution for this dye, combined with the small negative value of the zeta potential of the PP membrane in this pH range, did not cause a harsh repulsion among the dye and the membrane, as occur with the other solutions. The less repulsion can increase the vapor passage across the membrane, resulting in higher permeate fluxes.

Using the same operational conditions, Ramlow *et al*. (2019a) obtained a lower permeate flux using a PP membrane with disperse black dye solution, reaching 17.7 kg m^{-2} h^{-1}, which corresponds to a permeate flux almost 50% lower than the flux obtained in the present work. This fact may be related to the fluid velocity in the experimental DCMD setup, which was higher in the present work due to the smaller DCMD unity (ϕ=4.1 cm). The same behavior

was observed for this author's experiments using reactive black dye and pristine PP membrane, where a permeate flux of 18.8 7 kg m^{-2} h^{-1} was reached.

It can be noted that the permeate flux for modified PP membrane is only higher to disperse dye solution, reaching 44.85 kg m^{-2} h^{-1}, which corresponds to an increase of 11.6%. This high permeate flux is related to the more negative zeta potential obtained to this membrane in the range of pH of disperse dye solution (-7 to -8 mV). As the disperse dye did not acquire charges in solutions, the permeate flux increment suggests that as more negative the zeta potential, the more likely the vapor is to pass through the membrane pores due to the absence of repulsive forces.

For the anionic dyes tested in this work (reactive black dye and acid black dye), the permeate fluxes obtained to the pristine PP were almost the same (38.38 and 36.41 kg m^{-2} h^{-1}, respectively). The anionic character of these classes of dyes, combined with a negative membrane zeta potential, resulted in repulsion forces among the membrane and the feed solutions. This fact is attributed to the interactions among negative charges of the membrane surface and the dyes in solution. For the modified PP membrane, there was a decrease in permeate flux for both classes of dyes. However, this decrease was lower for the acid black dye (2.74%), mainly due to the lesser negative zeta potential of the modified PP membrane achieved in the pH range of this dye (-14 and -15 mV). As the membrane shows a lesser negative potential than the modified membrane in this pH range, the lesser was the repulsion force between the membrane and the solution. Then, more prone was the vapor to pass through the membrane pores, resulting in a higher permeate flux.

The direct black dye shows diazo chromogenic groups that develop negative charges in water. This dye class's pH value was similar to the distilled water and reactive black solution's pH, explaining the similarity of permeate fluxes obtained, mainly for the modified PP membrane.

The charge developed in the membrane surface affects the permeate flux and the molar mass of the dye molecules, feed concentration, operational conditions such as temperature and circulation rate, and the fouling phenomena. As the higher is the attraction of the membrane with the feed solution, the more prone is the dye adsorption in membrane pores, resulting in fouling. The fouling is occasioned by the pore blockage, reducing the permeate flux across the membrane. It can also affect the rejection rate since the dye deposition can originate hydrophilic channels on the membrane surface, leading to wetting. The fouling phenomena will investigate in the morphological and chemical analysis in the following sections.

In conclusion, the modified membrane was able to operate with the tested dye solutions with great permeate fluxes, mostly dealing with the disperse dye, where the permeate flux increased compared to the pristine membrane. The higher reduction in permeate flux occurred with the reactive black dye, where also the lowest contact angle of the modified membrane was achieved. The decrease in permeate flux may also be related to the increase in mass transfer resistance, originated by the increase in membrane thickness, related to the proposed modification. The modified membrane could operate with these classes of dyes, with a decrease in the permeate flux of at most 11.6%.

4.4.2.2 Rejection rate of modified PP membrane using 2% PVDF and 6% Sylgard

The rejection rate expresses how much the membrane is capable of separating water from the contaminant solution. Figure 42 shows the rejection rate of DCMD experiments using PP modified and pristine membranes.

Figure 42 – Rejection rate of pristine and modified PP membranes with dye solutions

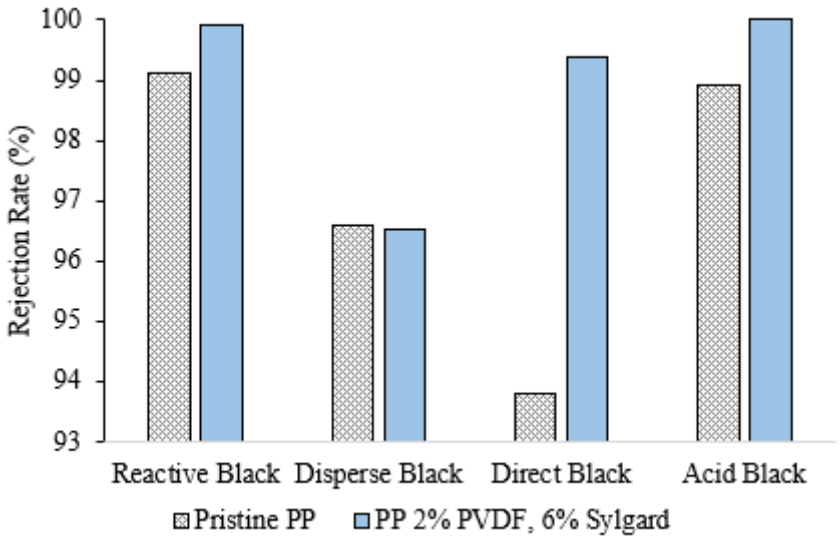

Font: The Author (2021)

The rejection rates of both PP membranes were higher than 93% for all tested solutions, evidencing an excellent performance to remove pure water from a dye solution. Results clearly reveal a relation of the rejection rate with the chromogenic group. The modified membrane showed higher or the same rejection rates for all tested solutions than the pristine one. This result corroborates the higher contact angles obtained to this membrane.

The obtained rejection rate for disperse dye solution was about 96% to both modified and pristine PP membrane. It is important to emphasize that the rejection rate measurements are based on a spectrophotometer calibration curve, which remains high imprecision, especially for the disperse dye solution. It was attributed to the lower maximum wavelength than other dyes (282 nm). Different results using the pristine PP membrane were obtained by Ramlow *et al*. (2019a), where a rejection rate of 100% was achieved using the same operational conditions. Then, this dye's rejection rate results may be linked to an experimental error resulting from the equipment.

The higher hydrophobicity of PP modified membrane using Sylgard was achieved against the acid black dye solution (151.5º). It was related to the highest rejection rate obtained from all DCMD experiments, where 100% of color rejection was achieved, corresponding to an increase of 1.1%. The second-high hydrophobicity was achieved to the direct black dye solution (148.38º), where a rejection of 99.38% was reached, corresponding to an increase of 6% comparing to the pristine PP membrane. For the reactive black dye, both rejections (of pristine and modified PP membrane) were higher than 99%, and the increase in the rejection rate obtained with the modified membrane was 0.78%.

The zeta potential curves for the pristine and modified PP membranes (Figure 34) suggest a higher negative charge to the modified membrane at lower pH ranges (lesser than 6) than the pristine one. This result indicated that this membrane is more susceptible to operating with acid solutions than the pristine. It was attributed to its more negative charged surface, which led to an increase in the repulsion force among the solution and the membrane, guaranteeing a higher rejection rate.

The rejection rate and permeate fluxes' results allowed to conclude that the modified PP membrane using PVDF and Sylgard achieved more robust separations concerning dyes solutions, evidenced by the higher rejection rates. Despite the low reduction (at most 11.6%) in the permeate fluxes for acid, reactive and direct dyes, the rejection rates for these classes of dyes potentially increase (up to 6% for direct black dye), adding significant value to the separation potential for these membranes. The modified membrane was better for the disperse dye solution in terms of permeate flux and rejection rate than the pristine one.

4.4.2.3 Water contact angle after DCMD operation

The water contact angles of contaminated membranes were measured to analyze the effect of DCMD operation in maintaining the membranes' hydrophobicity. Table 16 summarizes these results.

Table 16 – Water contact angle of contaminated PP membranes

		Water Contact Angle (°)	
		Pristine PP	PP 2% PVDF, 6% Sylgard
Before MD		118.92 ± 3.081	142.07 ± 1.67
After MD	Reactive Black Dye	138 ± 0.69	141.26 ± 2.25
	Disperse Black Dye	137.63 ± 2.31	143.63 ± 3.52
	Direct Black Dye	132.73 ± 0.61	142.86 ± 4.71
	Acid Black Dye	138.27 ± 2.35	146.67 ± 7.09

Font: The Author (2021)

The parameter Increment of Surface Contact Angle (ICA) showed an increase in the water contact angle for the pristine PP membrane with all tested dyes (11.61< ICA < 16.27 %), indicating a slight increase in the hydrophobicity of this membrane after de DCMD operation. The non-maintenance of the water contact angle with the pristine PP membrane after DCMD operation was also reported by Ramlow (2018). This phenomenon may indicate dyes depositions on membrane surface that could alter the membrane roughness and may decrease the pore size, increasing the membrane hydrophobicity. The presence of organic compounds on the membrane surface can alter the membrane's overall properties, including the hydrophobicity (GOH *et al*., 2016). In a long-term operation, this deposition can originate the fouling phenomenon, compromising the pristine PP membrane's performance.

On the other hand, this parameter was lesser affected in the modified PP membrane (-0.57 < ICA < 3.24%), indicating a maintenance of the hydrophobicity after the DCMD operation. The modification under the surface seems to become the membrane lesser prone to dye deposition, resulting in a promising MD operation feature. A long-term operation with the modified PP membrane may present a maintenance of permeate flux along the time, once its hydrophobicity was not altered and its surface showed an antifouling property.

4.4.2.4 Morphological and chemical analysis of the contaminated PP membranes after DCMD operation

Alterations on membrane morphology after DCMD tests can be caused due to the dye deposition. For this reason, these alterations are intrinsically related to the chemical characteristics of the dye solutions and their charges. The fouling phenomenon involving dyes can occur in two ways: Concepting a cake or adsorbing into membrane pores. Dyes negatively charged are lesser prone to deposit on the membrane surface. When it occurs, the repulsive forces between the charged dye solution and membrane matrix lead to a dye-dye structure on the membrane surface, known as a cake formation. On the other hand, dyes positively charged are easily adsorbed onto the membrane matrix due to the attractive forces and hydrogen bonding between the dye and the membrane surface. This kind of fouling also affects the membrane porosity and the pore size (LAQBAQBI *et al*., 2019b).

Other morphological alterations could be observed in the modified membranes after the DCMD process, related to the modified layer's degradation on the membrane surface. Thus, after this process, the SEM images become essential no analyze the stability of the proposed modification.

The SEM images obtained after the DCMD operation of PP membranes with the different classes of dyes are shown in Appendix D. Analyzing the pristine PP membranes, a particle deposition is observed for all tested dyes, except the reactive dye. The reactive dyes have azo or anthraquinone as chromogenic groups and are adsorbed to the membrane via sulfonate groups if the membrane has a positive charge (AN *et al*., 2016). As the PP membrane was negatively charged in the reactive dye's pH range, repulsion forces between the membrane and the solution increased, explaining this dye's low deposition on the membrane surface. The same trend was observed for the modified PP membrane (PP 2% PVDF, 6% Sylgard).

Acid dyes, which also present azo as the chromogenic groups and from one to three sulfonate groups (GUARATINI; ZANONI, 2000), develop negative charges in an aqueous solution, which contributed to its low deposition in PP membrane surface. Tests with acid dye solutions in DCMD operation with a hydrophobic membrane were also reported by An *et al*. (2016). A low incidence of fouling was detected in the acid dyes compared with basic dyes.

When dealing with the direct and disperse dye solutions, it becomes possible to observe a higher dye deposition on the membrane surface. As mentioned in the previous section, disperse dyes were more prone to deposit on membrane surface due to their absence of charges in aqueous solution, which did not enable repulsion forces among the solution and the

membrane as much was observed for other classes of dyes. This interaction led to higher permeate fluxes but higher dye deposition. Its potential to deposit on the membrane surface turns this dye class more susceptible to the concentration polarization phenomena. It would compromise the DCMD performance in long-term operations, causing a pore blockage and contamination of the permeate solution (KHUMALO *et al*., 2019b).

Similarly, the EDX analysis of the direct dye (Appendix H) may indicate particle deposition on the membrane surface, where elements beyond carbon were found in membrane surfaces such as silicon, sodium, chloride, and calcium.

Analyzing the modified PP membrane's SEM images after the DCMD operation (Appendix E), it was possible to infer that the operation did not compromise the proposed modification's morphology. It was observed a high roughness drop structure in all microphotographs. The formed structure became harder to detect a dye deposition on the membrane surface. For this reason, the investigation of solid deposition for modified PP membranes was performed through the EDX analysis (Appendix I).

The EDX analysis confirmed the maintenance of the morphological structure presented in the proposed modification once carbon, fluor, silicon, and oxygen were verified on the membrane surface. The PP 2% PVDF, 6% Sylgard membrane after the disperse dye operation presented a chlorine peak, indicating a dye deposition. There were no elements such as sodium and calcium founded in PP membrane after DCMD with disperse dye solution, which may indicate the achievement of an antifouling property of this modified membrane. In the experiments with acid and direct dye, an increment of the silicon peak may indicate solids' deposit on the membrane surface.

The chemical analysis of pristine PP and PP 2% PVDF, 6% Sylgard after DCMD operation was replaced by determining IR spectra of the membranes, shown in Appendix L and M, respectively. Regarding the DCMD experiments with pristine PP membrane, it was observed that the chemical structure was maintained for reactive, acid, and direct black dyes. New peaks on the IR spectra were not found compared with the membrane before MD operation. For these dyes, it is concluded that the dye-membrane interaction was restricted during the dye treatment. On the other hand, upon operation with disperse black dye, the PP membrane presented new peaks on their fingerprint region, at 1265 cm^{-1} and between 1094 and 1000 cm^{-1}. These peaks may correspond to unsaturated aromatics or alkanes, probably originated by the dye's adsorption on the membrane surface. Nonetheless, this interaction did not affect the membrane's functional groups, maintaining its important features linked to them.

The IR spectra of PP 2%PVDF, 6% Sylgard (Appendix M) maintained the membrane's chemical structure after the DCMD operation with reactive and disperse dye. This result appears to be a significant advantage upon the pristine PP membrane, which had its chemical structure affected by the disperse dye solution. However, new peaks at the fingerprint region were added to the membranes after the operation with direct and acid black dye, at 1182 cm^{-1} and between 1085 and 840 cm^{-1}, being more prominent to the direct black dye. These peaks may correspond to aromatic compounds related to the adsorption of these dyes on membrane surfaces. In this sense, the operation did not compromise the overall membrane's chemical structure, maintaining the functional groups and the modified layer proposed in this work.

4.4.3 DCMD tests of modified PA membrane with 2% PVDF, 10% PDMS, 0 or 20% of Si NPs

The modified PA membranes with or without Si NPs, were tested with the reactive black solution, which consists of a common dye employed in the cotton dyeing bath. The modified membrane containing Si NPs, which presented a high contact angle, was also tested with a solution containing an industrial surfactant employed as an additive to the dyeing process (detergent Colorswet). The tests with these classes of membranes are summarized in Table 14. This section will be divided into permeate flux results, rejection rate, and analytical tests after DCMD operation, aiming to provide a better understanding.

4.4.3.1 Permeate flux of PA modified membranes

PA membranes show hydrophilic water behavior due to polar terminations on their surfaces, as the N-H bonds. The commercial membrane employed in this work as the substrate for membrane modification consisted of a dense matrix with much smaller pores than the hydrophobic commercial membranes, leading to a lower permeate flux. For this pristine membrane, the mass transfer phenomenon occurs differently. The diffusion of water across the polymeric matrix occurs because of the smaller diameter of water molecules (0.3 nm, approximately) than the PA membrane pore size (0.68 nm). In this case, the water vapor can cross the membrane pores and the water molecules once the membrane does not present water repellence. The dye molecules are higher than the membrane pores (> 1nm), being retained on the feed side (KHAYET, 2011).

For the modified membranes, the mass transfer phenomenon occurs similarly to the hydrophobic membranes because of the hydrophobic layer addition on the hydrophilic membrane surface. The size limitation occasioned by the difference between the pore size and the dye molecules continues to be a potential agent to increase the rejection rate. The permeate fluxes with distilled water and dye solution obtained to modified and pristine PA membranes are shown in Figure 43.

Figure 43 – Permeate flux with pristine and modified PA membranes with dye solutions

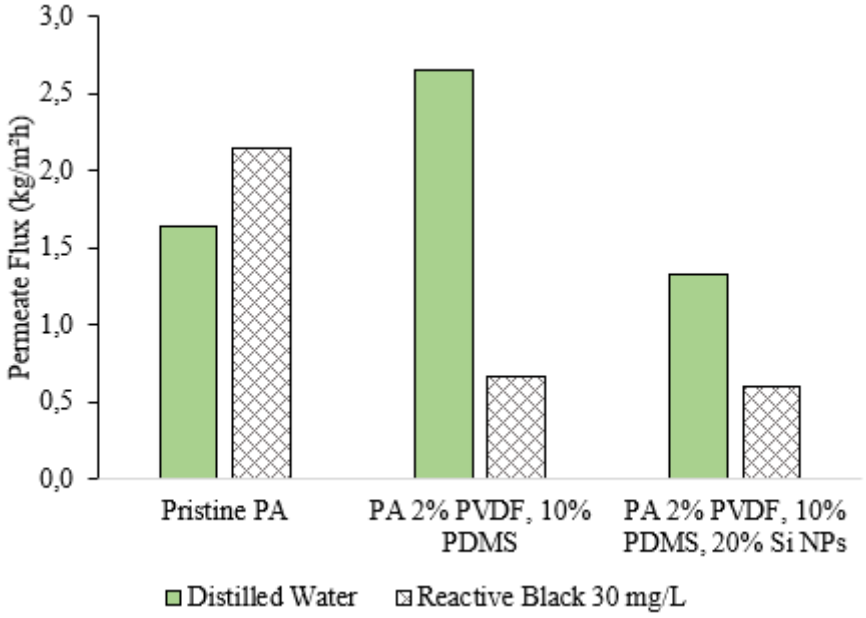

Font: The Author (2021)

Analyzing Figure 43, it was possible to observe that a hydrophobic layer's addition strongly decreased the permeate flux for both proposed modifications. As the substrate consists of a dense membrane, lower permeate fluxes than a porous membrane were expected. Also, the increase in membrane thickness with the modification could increase the mass transfer resistance, despite not negatively affecting the membrane porosity.

The permeate flux with reactive dye solution (2.14 kg m^{-2} h^{-1}) was almost 30% higher than the permeate flux with only water for pristine PA membrane. Among the modified and pristine PA membranes, this trend is only observed for the pristine one. The physicochemical interactions can explain it among the pristine membrane and water, which were strong than these interactions with the membrane and reactive dye solution. Criscuoli *et al*. (2008) also reported these interactions, which explained the higher permeate flux with dyes relating it with

the interaction among the dye and the polymeric structure, leading to the liquid absorption into membrane pores. This interaction becomes higher when dealing with hydrophilic structures.

Although a relation between the permeate flux with the swelling degree for all PA membranes was not observed, there was a strong relationship between the permeate flux and the contact angle with the different solutions for the pristine PA membrane. The strong interaction with the reactive dye solution was remarkable by the smaller contact angle of this membrane with this solution (61.63º). The water contact angle, on the other hand, achieved 75.73º. Therefore, the higher permeate flux of this membrane with reactive black dye is explained by a higher affinity with the membrane surface. Moreover, the hydrophilicity becomes the membrane more prone to the fouling phenomena. The dye deposition on the membrane surface would originate more hydrophilic channels, which might increase the water affinity with the membrane. The fouling phenomenon of all PA membranes is visualized in Figure 44.

Even being the pristine PA membrane a hydrophilic matrix, its zeta potential assumed a negative charge at a neutral pH (-26 mV), according to Figure 33. At this pH, most natural and technical material surfaces assume a negative charge (LUXBACHER, 2014). When polymers' doping (PVDF + PDMS) was incorporated on the membrane surface, the zeta potential decreased its negativity, reaching -23 to -24 mV. This decrease improved the water affinity at a neutral pH, as was the case of distilled water, explaining the higher permeate flux obtained for PA 2% PVDF, 10% PDMS membrane for water, which corresponds to an increase of almost 62%. The increase in permeate flux occurs combined with an increase in this membrane's water contact angle (129.3º).

For the modification using polymers combined with 20% of silica nanoparticles, the zeta potential significantly increased its negativity, upping to -33 to -34 mV. Even though no evidence correlates the zeta potential with the surface roughness (LUXBACHER, 2014), the addition of hydrophobic groups (polymers) combined with Si NPs developed a higher negative zeta potential. It decreased the water affinity for the PA 2% PVDF, 10% PDMS, 20% Si NPs membrane, leading to a lower permeate flux with distilled water. Moreover, the decrease in permeate flux was also related to mass transfer resistance added to the membrane surface through the modification, evidenced by the membrane thickness increment.

Concerning the reactive dye solution, a trend among the modified and pristine PA membranes was observed. The addition of polymers on the PA membrane surface decreased the permeate flux in 1.47 kg m^{-2} h^{-1}, while the modification combining polymers and silica nanoparticles decreased the flux by 1.55 kg m^{-2} h^{-1}. This result can be linked to increased mass

transfer resistance with layers under the membrane surface. In contrast, the fouling phenomenon becomes visually smaller as the modification layers were added, greater for the pristine membrane and lesser for the silica modified membrane (Figure 44). As mentioned previously, the dye deposition can lead to the formation of hydrophilic channels that facilitate water passage by the phenomenon of diffusivity through the membrane, resulting in higher water volumes that can cross the membrane. An in-depth discussion of the fouling phenomenon will be discussed in the following sections. The hydrophobicity was increased with the modifications, inferring the reduction of interactions among the reactive dye with the membrane surface.

Due to the greater contact angle with surfactant solution, the membrane modified with the polymers and Si NPs was chosen to operate with a detergent solution (Colorswet 30 mg L^{-1}). Testing the potential to recover water from solutions containing low surface tension solutes is essential to determine the membrane's capacity to operate with wastewater from a cotton dyeing bath. A pristine PA membrane was also studied with the surfactant solution, aiming to compare the results. The permeate flux results are shown in Figure 45.

Figure 44 – Fouling phenomenon in pristine PA membrane (a), PA 2% PVDF, 10% PDMS (b), and PA 2% PVDF, 10% PDMS, 20% Si NPs (c)

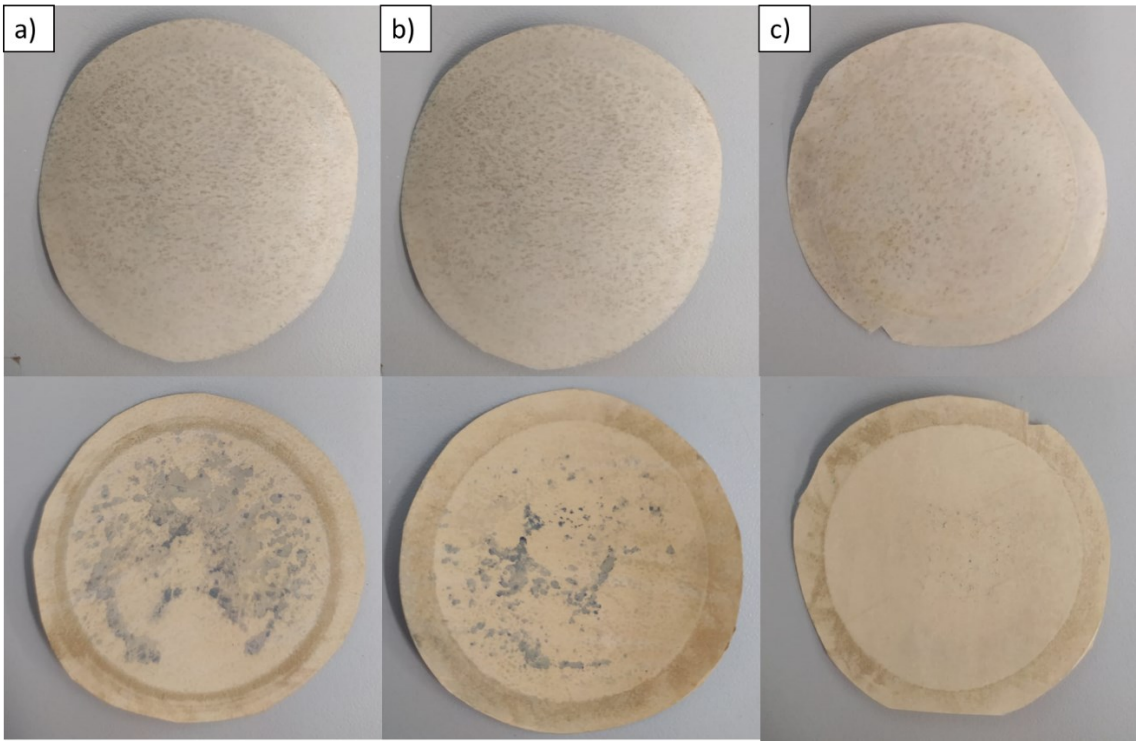

Font: The Author (2021)

Figure 45 – Permeate flux with pristine and modified membrane with surfactant solution

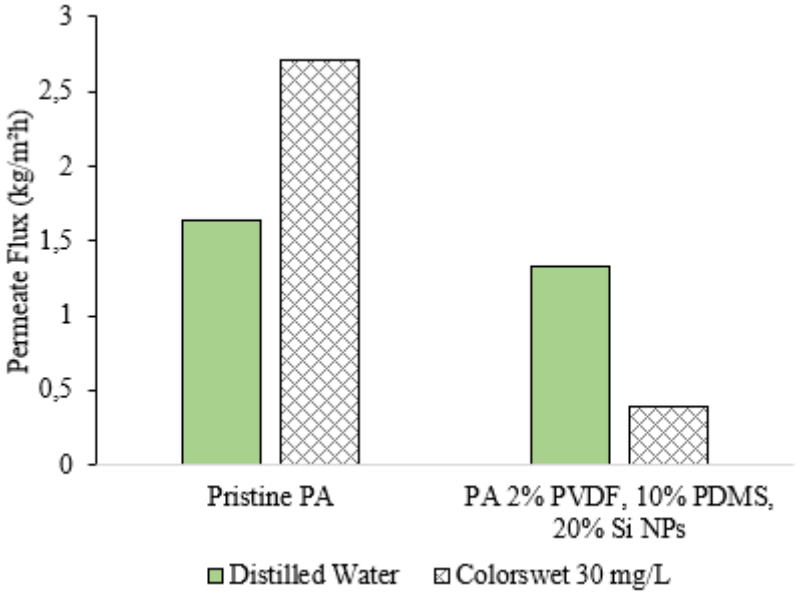

Font: The Author (2021)

As observed for the dye solution, the permeate flux of pristine PA membrane is higher with the surfactant solution than water, mainly due to the higher affinity between the membrane and the surfactant. The pristine PA membrane also presented higher permeate flux with surfactant than the modified membrane (2.71 kg m^{-2} h^{-1}). When analyzing the high pristine membrane's flux values, one wonders about the passage of surfactant molecules to the permeate side, indicating the beginning of wetting phenomena. The same additive at a higher concentration was tested in a DCMD unit by Tolentino Filho (2019). The wetting phenomenon was reached in the first hours of the experiment using a PTFE hydrophobic membrane. Lee, Deka, An (2019) also reported a wetting phenomenon using a hydrophobic PVDF membrane in a DCMD operation with similar concentrations of SDS solution. Regarding a hydrophilic membrane, it was expected that the interactions with the amphiphilic surfactant could be enhanced.

The modified membrane using silica nanoparticles showed the highest contact angle against the surfactant solution (160.5º), along with a significant reduction in the swelling degree comparing with the pristine membrane (41.7% for PA and 25% for modified PA). These results corroborated the increase in low surface tension solutions' repellence, explaining the lower fluxes obtained for this membrane (0.39 kg m^{-2} h^{-1}). The addition of a hydrophobic layer combining PVDF, PDMS, and silica aerogel was reported by Lee, Deka, An (2019). A decrease in the permeate flux was observed as more aerogel was incorporated on the membrane surface.

The increase in the mass transfer resistance by adding the hydrophobic layer may also decrease the permeate flux.

4.4.3.2 Rejection rates of PA modified membranes in DCMD operation

The rejection rates for the DCMD experiments using reactive dye solution (30 mg L^{-1}) were determined using the absorbance curves in the same way as section 6.1.2. The rejection rate was determined using the experiments' superficial tension curves using surfactant (Colorswet 30 mg L^{-1}). The calibration curves allow the correspondence of the superficial tension and concentration of surfactant.

The rejection rates of DCMD experiments using reactive dye solution and surfactant solution are shown in Figure 46.

Figure 46 – Rejection rates of DCMD experiments of PA pristine and modified membranes

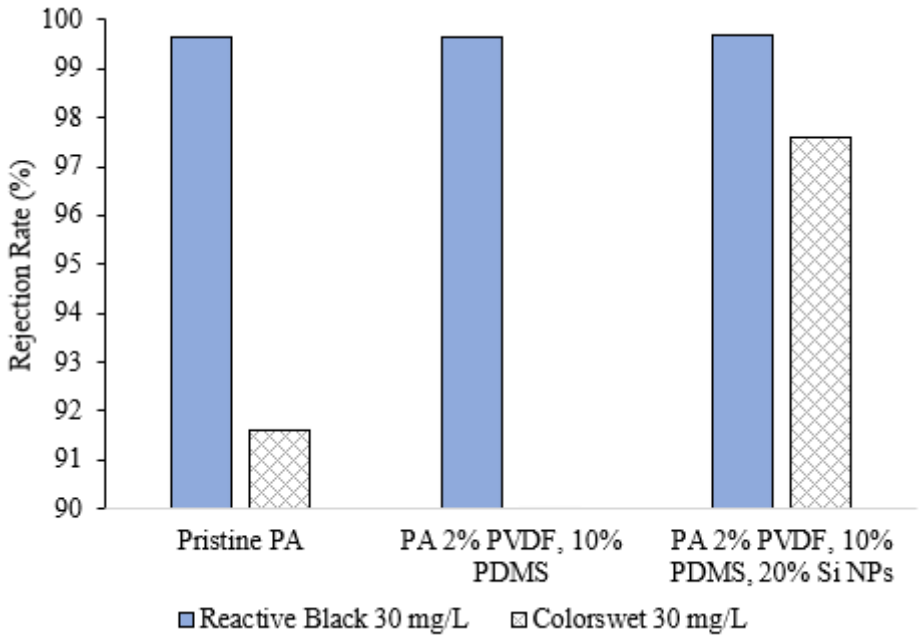

Font: The Author (2021)

Regarding the experiments with reactive dye solutions, all membranes achieved rejection rates higher than 99%, evidencing the high potential to recovery a high-quality permeate from a dye solution. Moreover, the modification layers' addition slightly increased the rejection rate, which reached 99.63% for pristine PA, 99.65% for PA 2% PVDF, 10% PDMS, and 99.69% for PA modified with polymers and silica. High rejection rates using the polyamide membrane

were also reported by Ramlow (2018). According to this author, the high rejection obtained to polyamide membrane is related to the low permeate flux during the DCMD process. The lower water permeation led to fewer water molecules crossing the membrane pores. Moreover, the dye molecules are larger than the membrane pores, causing its retention on the membrane's feed side. These facts explain the high rejection rates obtained even to a hydrophilic membrane.

For modified PA membranes, a small pore size combined with a hydrophobic layer enhanced the rejection rate in DCMD experiments, related to the water repellence properties created on membrane surface and the dye size limitation.

Dealing with the experiments using the surfactant, the rejection rates were enhanced with the proposed modification, achieving 97.61% of rejection to the detriment of 91% of rejection for the pristine PA membrane, probably indicating a beginning of a wetting phenomenon to this membrane. Tolentino Filho (2019) observed a complete wetting in the first 30 min of operation using detergent solutions with a PTFE membrane at a higher detergent concentration. A complete wetting was not observed in the present work due to the lower detergent concentration and the poor time of operation.

The rejection rate results agreed with the contact angle measured for these membranes, which reached up to 160º with surfactant solutions. In the DCMD experiments carried out in this work, there was no monitoring of the rejection rate or the permeate flow overtime. Therefore, there was no way to determine when the wetting phenomena in the pristine PA membrane started, where the surfactant molecules began to cross the membrane's pores. The detergent employed in this work consists of an anionic surfactant that originates negative water solutions charge (CHEW *et al*., 2017). As the modification incorporated hydrophobic coating on the membrane surface, the repellence of negative charges increased, decreasing the surfactant adsorption on membrane pores and resulting in higher rejection rates and high permeate quality.

In the face of the results of permeate fluxes and rejection rate, it can be concluded that the modifications potentially increase the rejection rate dealing with reactive dye solutions, also developing an antifouling property as much as silica nanoparticles were incorporated on the membrane surface. The modified membranes guaranteed high-quality permeate in the process separation, despite their lower permeate fluxes. For the experiment with surfactant, the modified membrane using PVDF, PDMS, and Si NPs can potentially recovery water from low surface tension solutions, with low fluxes but with high rejection rates, avoiding the wetting caused by the surfactant adsorption into membrane pores. In this sense, the PA membrane

modified with 2% PVDF, 10% PDMS, and 20% Si NPs consists of a promisor candidate to recover water from wastewaters from a cotton dyeing bath.

4.4.3.3 Water contact angle after DCMD operation

The water contact angles of contaminated PA membranes were measured to determine the DCMD operation's influence in maintaining the membranes' hydrophobicity (Table 17). It is important to highlight that the measurements were also carried out in the contaminated PA membranes, aiming to compare the results with the modified ones.

Table 17 – Water contact angle of contaminated PA membranes

		Water Contact Angle (°)		
		Pristine PA	PA 2% PVDF, 10% PDMS	PA 2% PVDF, 10% PDMS, 20% Si NPs
Before MD		75.73 ± 3.86	129.3 ± 4.69	167.13 ± 22.29
After MD	Reactive Black Dye	80.93 ± 1.36	141.83 ± 9.06	165.43 ± 12.81
	Detergent	82.46 ± 2.37	-	165.21 ± 11.65

Font: The Author (2021)

The Increment of Surface Contact Angle (ICA) infers about the alteration in membrane hydrophobicity after the DCMD operation. Regarding the operation with reactive dye and detergent, the pristine PA membrane's ICA revealed an increase in the water contact angle in all experiments ($6.87 < ICA < 8.89\%$). Similar results were obtained by Ramlow (2018) applying a pristine PA membrane in a DCMD operation with different classes of dyes and by Alturki *et al*. (2010) in reverse osmosis with a pristine PA membrane operating with effluents. This result corroborated the solute deposition on the membrane surface after DCMD operation. The presence of organic particles can increase the membrane roughness and causes a pore blockage, increasing the contact angle. The same trend was observed for the modified membrane with only PDMS (ICA = 9.67%). An opposite behavior was achieved for the modified PA membrane using PVDF, PDMS, and Si NPs, where the ICA slightly decreased in all the cases ($-1.14 < ICA < -1.02\%$). The decrease in the water contact angle for this membrane can be considered negligible since the measurements' standard deviation embraced it. Therefore, the modified membrane using silica maintained its hydrophobicity after the DCMD

operation with reactive black dye and detergent solutions, evidencing a non-deposition of solute on the membrane surface. Without solids on the membrane surface and non-alterations on membrane chemical composition by a chemical attack, the hydrophobicity was maintained. The results for ICA confirm the promising antifouling property achieved for the modified membrane using Si NPs.

4.4.3.4 Morphological and chemical analysis of the contaminated membranes after DCMD operation

A morphological analysis through SEM microphotographs combined with EDX was carried out to evaluate the MD's effect on the stability of the proposed modification and detect the phenomena involving the MD operation, such as fouling and wetting. All contaminated membranes were analyzed after the DCMD operation. The SEM images of contaminated PA membranes after DCMD operation with reactive black dye (30 mg L^{-1}) and surfactant solution (30 mg L^{-1}) after 4 h of operation are shown in Appendix F and G, respectively.

The operation with Reactive Black solutions led to observing the modified surface's maintenance with the hierarchical drop structure for the PA membrane, evidencing the stability of the proposed modification after the DCMD operation. Deposition of organic matter was founded in the SEM images for pristine PA membrane and visually evidenced by Figure 44. In the 5000x approximation of Appendix x1 for pristine PA membrane, a particle deposition was observed into the membrane fibers, indicating the fouling phenomenon caused by physicochemical interactions among the organic dye and the membrane surface. The DCMD process causes a concentration on the feed solution, related to the vapor passage across the membrane to the permeate side. In a long-term operation, the feed concentration enhanced, resulting in solute deposits under the membrane surface (LU *et al.*, 2017). The fouling phenomenon, combined with the concentration polarization effect, led to increased mass transfer resistance and decreased the permeate flux, even originating the wetting phenomenon. The detection of fouling in a hydrophilic PA membrane was also reported by Ramlow (2018), where it was observed a particle deposition after 3 h of DCMD operation with a reactive black dye solution. According to the author, the particle deposition on the membrane surface is related to the membrane's poor hydrophobicity.

Both modified PA membranes did not present a particle deposition in the SEM images. Figure 44 shows a decrease in dye deposition according to silica nanoparticles' addition on the membrane surface. The incorporation of hydrophilic nanoparticles via electrospinning

modifications on membrane surface was also reported by Hou *et al*. (2018a), Tang *et al*. (2019), Wang *et al*. (2018, 2019a). In these studies, great results in terms of fouling prevention were achieved. This property was attributed to nanoparticles' water-behavior, which avoids the organic fouling due to the inexistence of hydrophobic-hydrophobic attractions between the membrane and the foulant. Moreover, the high roughness occasioned by the incorporation of the nanoparticles also reduces the particle deposition.

The SEM images of contaminated PA membranes after the operation with 30 mg L^{-1} of Colorswet (Appendix G) indicated the stability of the surface structure formed through the electrospray, even after the contact with low surface tension solutions. There were no deposits observed on the surface of the contaminated membranes, indicating no fouling phenomenon.

Aiming to further investigations about modified PA membranes' chemical structure after DCMD operation, EDX and FTIR analyses were carried out. The EDX analysis of PA membranes upon the Reactive Dye and Colorswet treatment are shown in Appendix J and K, respectively. Regarding the experiments with the reactive black dye, the pristine PA membrane showed some contaminants in its surface, evidenced by the sulfur peak in the EDX spectrum. The membrane modified with the polymeric blend showed small traces of sodium, chlorine, and potassium, detriments that its surface may have adsorbed in contact with the dye. There was a decrease in the fluorine and silicon peaks for this membrane compared to that with the pristine membrane.

In contrast, the PA membrane modified with silica showed fluorine, aluminum, and iron peaks in the EDX spectrum. However, the silicon peak was maintained, which may indicate deposits. FTIR analyses of the membranes after the operation with the reactive dye (Appendix N, O, and P) showed a maintenance of the membranes' chemical structure after the operation, leading to conclude that the interaction between the dye and the membrane surface occurs only during the DCMD operation. For the modified membrane using silica (PA 2% PVDF, 10% PDMS, 20% Si), the peak located in 3400 cm^{-1} disappeared, probably related to the change in silica nanoparticles' water behavior during the MD operation.

The surfactant employed in DCMD operation seems to did not cause molecule deposits on the membrane surface, evidenced by the EDX analysis of pristine and modified PA membranes (Appendix K). In this case, the original peaks of fluor and silicon were maintained in the modified membrane after DCMD operation. The FTIR analysis (Appendix P) also confirms the non-alteration of the membrane's chemical structure caused by the operation, even with low surface tension solutions.

5 FINAL CONSIDERATIONS

The hydrophobicity improvement of the modified membranes named PP 2% PVDF, 6% Sylgard, and PA 2% PVDF, 10% PDMS, and 20% Si NPs was achieved in the present work. These membranes also presented stable and satisfactory performances in the DCMD experiments.

The membrane morphology obtained through the electrospraying modification inferred a pattern involving the solution viscosity and the formed drop size. All the dope solutions employed in this work consisted of non-Newtonian fluids, and an improvement in the solution viscosity led to a decrease in the drop size formed on the membrane surface.

Regarding the PP membrane, an improvement in membrane hydrophobicity was not significantly achieved through the first proposed modification using PVDF, PDMS not cured, and silica nanoparticles. The time under the spray did not affect the membrane hydrophobicity. On the other hand, the polymer reticulation of PDMS significantly improved the membrane hydrophobicity. The formed surface also presented a high rough surface with a homogeneous cover, revealed by the morphological analysis. The modification affected the membrane's chemical structure and maintained the pristine PP membrane's thermal resistance.

The modified PP membrane presented a higher contact angle with the four classes of dyes explored in this work (reactive, disperse, direct, and acid at 30 mg L^{-1}) than the pristine one. The modification also decreased the swelling degree for these solutions, except for the reactive black dye. The promising results of contact angle and swelling degree led to choose the PP 2% PVDF, 6% Sylgard membrane to operate with the dye classes. The DCMD performance revealed an improved rejection rate for all tested dyes. The highest rejection rate was obtained for the acid black dye (100%). The increment in the rejection rates was related to reducing zeta potential in the dyes' pH range, which improved the repulsion forces between the membrane and the dye solutions. In contrast, the decrement of physicochemical interactions, combined with the increase in mass transfer resistance due to the added layer, decreased the modified membrane's permeate fluxes, at most 11.6%. This reduction was not observed for the disperse dye. The absence of charges in aqueous solutions led to a high interaction between this dye and the membrane, achieving lower rejection rates and higher permeate fluxes. For this dye, a lesser solid deposition was verified in the chemical analysis compared to the pristine PP membrane. The morphological analysis revealed a maintenance of the roughness structure after the DCMD process, and the water contact angle.

The PA modified membranes using 2% PVDF, 10% PDMS, and 0 or 20% Si NPs revealed the influence of silica nanoparticles on the membrane hydrophobicity for a dense matrix. The membrane modified with 20% Si NPs reached 167.13º of water contact angle, harshly modifying the membrane chemical and morphological surfaces and maintaining the pristine PA membrane's thermal resistance. The modified PA membranes were chosen to operate with the cotton dyeing bath compounds (reactive black dye and detergent). A high superhydrophobic contact angle was obtained for the low surface tension solution (anionic surfactant) (160.5º).

The DCMD operation using PA membranes revealed an antifouling property for the modified PA membranes operating with the reactive black dye solution that increased as much silica was incorporated in the membrane surface. The antifouling property was related to the decrease of the zeta potential achieved through the modification, reducing the physicochemical interactions and solid deposits on the membrane surface. The rejection rates obtained for all PA membranes were higher than 99%. Combined with the particle size limitation, the increase in the contact angle by the proposed modification decreased the water affinity of the membrane, enhancing the rejection rates. However, the increase in the mass transfer resistance of the added layer decreased the permeate fluxes. In dealing with surfactant experiments, a beginning of wetting was observed to the PA membrane, evidenced by the high permeate flux and low rejection rate. The high contact angle and high roughness of the PA 2% PVDF, 10% PDMS, and 20% Si NPs membrane enabled it to operate with low surface tension solutions with high rejection rates, with anti-wetting behavior.

In a general way, this work contributed to the mitigation of the inherent phenomenon of the DCMD process, such as wetting and fouling, related to the water recuperation from textile wastewater. The proposed modifications enabled the PP membrane to operate with enhanced performances with different dye classes. The modified PA membrane was able to recover water with high quality from cotton dyeing bath compounds, with anti-fouling and anti-wetting properties.

Although the great results obtained from the proposed modifications, some further studies are needed to become feasible the scale-up of the MD process, focusing on water recuperation from textile wastewater. Some suggestions of future studies are described as follow:

a) Investigate the conductivity, mechanical resistance, and LEP value of modified membranes.

b) Long-term operation tests with the modified membranes with the tested solutions, aiming to verify the maintenance of chemical and morphological structure along with the time. Moreover, to verify the maintenance of antifouling and anti-wetting properties;
c) Develop cleaning strategies for the modified PP membranes for the direct dye solutions, where the fouling was detected;
d) Explore the modified membrane with other dyeing additives, such as dispersants, salts, and acids, to verify the DM performances against other chemical compounds;
e) Operate the modified membrane with real effluents from textile dyeing bath, to visualize the compounds' interaction in the membrane's performance.
f) Analyze the economic viability of the DM process with the modified membranes to water recovery from textile wastewater.

REFERENCES

AGARWAL, S.; GREINER, A.; WENDORFF, J. H. Functional materials by electrospinning of polymers. **Progress in Polymer Science**, v. 38, n. 6, p. 963–991, 2013.

AL-FURAIJI, M. *et al*. Triple-Layer Nanofiber Membranes for Treating High Salinity Brines Using Direct Contact Membrane Distillation. **Membranes**, v. 9, n. 5, p. 60, 2019.

ALAM, M. N.; CHRISTOPHER, L. P. A novel, cost-effective and eco-friendly method for preparation of textile fibers from cellulosic pulps. **Carbohydrate Polymers**, v. 173, p. 253–258, 2017.

ALKHUDHIRI, A.; DARWISH, N.; HILAL, N. Membrane distillation: A comprehensive review. **Desalination**, v. 287, p. 2–18, 2012.

ALKLAIBI, A. M.; LIOR, N. Membrane-distillation desalination: Status and potential. **Desalination**, v. 171, n. 2, p. 111–131, 2005.

ALSAADI, A. S. *et al*. Experimental and theoretical analyses of temperature polarization effect in vacuum membrane distillation. **Journal of Membrane Science**, v. 471, p. 138–148, 2014.

ALTURKI, A. A. *et al*. Combining MBR and NF/RO membrane filtration for the removal of trace organics in indirect potable water reuse applications. **Journal of Membrane Science**, v. 365, n. 1–2, p. 206–215, 2010.

AMDA, A. M. DE D. DO M. A. **Indústria têxtil consome 93 bilhões de metros cúbicos de água por ano**. Disponível em: <https://www.amda.org.br/index.php/comunicacao/informacoes-ambientais/5240-industria-textil-consome-93-bilhoes-de-metros-cubicos-de-agua-por-ano>. Acesso em: 26 jun. 2019.

AN, A. K. *et al*. High flux and antifouling properties of negatively charged membrane for dyeing wastewater treatment by membrane distillation. **Water Research**, v. 103, p. 362–371, 2016.

ATTIA, H. *et al*. Robust superhydrophobic electrospun membrane fabricated by combination of electrospinning and electrospraying techniques for air gap membrane distillation. **Desalination**, v. 446, n. June, p. 70–82, 2018a.

ATTIA, H. *et al*. Robust superhydrophobic electrospun membrane fabricated by combination of electrospinning and electrospraying techniques for air gap membrane distillation. **Desalination**, v. 446, n. June, p. 70–82, 2018b.

BASTIAN, E. Y. O. *et al*. **Guia técnico ambiental da indústria têxtil - Série P + L.** [s.l: s.n.].

BATISTA, M. M. **Tratamento eletroquímico de efluentes têxteis**. [s.l.] Universidade da Beira Interior, 2015.

BELLINCANTA, T. *et al*. Preparação e caracterização de membranas poliméricas a partir da blenda polisulfona/poliuretano. **Polimeros**, v. 21, n. 3, p. 229–232, 2011.

BELTRAME, L. T. C. **Caracterização de Efluente Têxtil e Proposta de Tratamento**. [s.l.]

Universidade Federal do Rio Grande do Norte, 2000.

BERGNA, G.; BIANCHI, R.; MALPEI, F. GAC adsorption of ozonated secondary textile effluents for industrial water reuse. **Water Science and Technology**, v. 40, n. 4–5, p. 435–442, 1999.

BHARDWAJ, N.; KUNDU, S. C. Electrospinning: A fascinating fiber fabrication technique. **Biotechnology Advances**, v. 28, n. 3, p. 325–347, 2010.

BILIŃSKA, L. *et al*. Coupling of electrocoagulation and ozone treatment for textile wastewater reuse. **Chemical Engineering Journal**, v. 358, n. July 2018, p. 992–1001, 2019.

BORETTI, A.; ROSA, L. Reassessing the projections of the World Water Development Report. **npj Clean Water**, v. 2, n. 1, p. 15, 2019.

BOUBAKRI, A.; HAFIANE, A.; BOUGUECHA, S. A. T. Direct contact membrane distillation: Capability to desalt raw water. **Arabian Journal of Chemistry**, v. 10, p. S3475–S3481, 2017.

BRAILE, P. .; CAVALCANTI, J. E. W. . **Manual de Tratamento de Águas Residuárias Industriais**. São Paulo: CETESB, 1993.

CAMACHO, L. M. *et al*. Advances in membrane distillation for water desalination and purification applications. **Water (Switzerland)**, v. 5, n. 1, p. 94–196, 2013a.

CAMACHO, L. M. *et al*. Advances in Membrane Distillation for Water Desalination and Purification Applications. **Water**, p. 103, 2013b.

CANEVAROLO JR, S. V. **Técnicas de caracterização de polímeros**. São Paulo - SP: Artliber Editora, 2003.

CETESB - COMPANHIA AMBIENTAL DO ESTADO DE SÃO PAULO. **Águas Interiores 2020- O problema da escasez de água no mundo**. Disponível em: <https://cetesb.sp.gov.br/aguas-interiores/informacoes-basicas/tpos-de-agua/o-problema-da-escasez-de-agua-no-mundo/>. Acesso em: 1 abr. 2020.

CHEN, X. *et al*. Tubular hydrophobic ceramic membrane with asymmetric structure for water desalination via vacuum membrane distillation process. **Desalination**, v. 443, p. 212–220, 2018.

CHEN, X. *et al*. Ceramic nanofiltration and membrane distillation hybrid membrane processes for the purification and recycling of boric acid from simulative radioactive waste water. **Journal of Membrane Science**, v. 579, p. 294–301, 2019.

CHEW, N. G. P. *et al*. Surfactant effects on water recovery from produced water via direct-contact membrane distillation. **Journal of Membrane Science**, v. 528, n. January, p. 126–134, 2017.

CHOUDHURY, M. R. *et al*. PT. **Advances in Colloid and Interface Science**, 2019.

CINPERI, N. C. *et al*. Treatment of woolen textile wastewater using membrane bioreactor, nanofiltration and reverse osmosis for reuse in production processes. **Journal of Cleaner**

Production, v. 223, p. 837–848, 2019.

COUTO, C. F. *et al*. Effect of humic acid concentration on pharmaceutically active compounds (PhACs) rejection by direct contact membrane distillation (DCMD). **Separation and Purification Technology**, v. 212, p. 920–928, 2019.

CRISCUOLI, A.; DRIOLI, E. Vacuum membrane distillation for the treatment of coffee products. **Separation and Purification Technology**, v. 209, p. 990–996, 2019.

CUI, Z.; DRIOLI, E.; LEE, Y. M. Recent progress in fluoropolymers for membranes. **Progress in Polymer Science**, v. 39, n. 1, p. 164–198, 2014.

DAMTIE, M. M. *et al*. Membrane distillation for industrial wastewater treatment: Studying the effects of membrane parameters on the wetting performance. **Chemosphere**, v. 206, p. 793–801, 2018.

DE SOUSA SILVA, R. **CONDIÇÕES ÓTIMAS PARA TRATAMENTO DE EFLUENTE TÊXTIL USANDO DESTILAÇÃO POR MEMBRANA POR CONTATO DIRETO**. [s.l.] Universidade Federal de Santa Catarina, 2019.

DE SOUSA SILVA, R. *et al*. Steady state evaluation with different operating times in the direct contact membrane distillation process applied to water recovery from dyeing wastewater. **Separation and Purification Technology**, v. 230, p. 115892, 2020.

DEKA, B. J. *et al*. Omniphobic re-entrant PVDF membrane with ZnO nanoparticles composite for desalination of low surface tension oily seawater. **Water Research**, v. 165, p. 114982, 2019.

DENG, L. *et al*. Robust superhydrophobic dual layer nanofibrous composite membranes with a hierarchically structured amorphous polypropylene skin for membrane distillation. **Journal of Materials Chemistry A**, v. 7, n. 18, p. 11282–11297, 2019.

DESA, A. L. *et al*. Industrial textile wastewater treatment via membrane photocatalytic reactor (MPR) in the presence of ZnO-PEG nanoparticles and tight ultrafiltration. **Journal of Water Process Engineering**, v. 31, n. June, p. 100872, 2019.

DONG, B.-B. *et al*. Polymer-derived porous SiOC ceramic membranes for efficient oil-water separation and membrane distillation. **Journal of Membrane Science**, v. 579, p. 111–119, 2019.

DRIOLI, E.; ALI, A.; MACEDONIO, F. Membrane distillation: Recent developments and perspectives. **Desalination**, v. 356, p. 56–84, 2015.

DUONG, H. *et al*. **MEMBRANE DISTILLATION FOR SEAWATER DESALINATION APPLICATIONS IN VIETNAM: POTENTIAL AND CHALLENGES**. [s.l: s.n.]. v. 55

DUONG, H. C. *et al*. Membrane Distillation for Seawater Desalination Applications in Vietnam: Potential and Challenges. **Vietnam Journal of Science and Technology**, v. 55, n. 6, p. 659, 2017b.

EYKENS, L. *et al*. Membrane synthesis for membrane distillation: A review. **Separation and Purification Technology**, v. 182, p. 36–51, 2017a.

EYKENS, L. *et al*. Membrane synthesis for membrane distillation: A review. **Separation and Purification Technology**, v. 182, n. March, p. 36–51, 2017b.

FENG, C. *et al*. Production of drinking water from saline water by air-gap membrane distillation using polyvinylidene fluoride nanofiber membrane. **Journal of Membrane Science**, v. 311, n. 1–2, p. 1–6, 2008.

FENG, S. *et al*. Progress and perspectives in PTFE membrane: Preparation, modification, and applications. **Journal of Membrane Science**, v. 549, n. October 2017, p. 332–349, 2018.

FÊNIX - FABRIL INDÚSTRIA E COMÉRCIO. **Tingimento Têxtil**. Disponível em: <https://www.fenixfabril.com.br/noticia/10/tinturaria/tingimento-textil>. Acesso em: 28 jun. 2019.

FILHO, C. M. T. *et al*. **Membrane distillation for recovery of textile wastewaters: Determination of operational conditions with PTFE membrane and high dye concentrations**. AIP Conference Proceedings. **Anais**...2020

GARCÍA, J. V. *et al*. Membrane distillation trial on textile wastewater containing surfactants using hydrophobic and hydrophilic-coated polytetrafluoroethylene (PTFE) membranes. **Membranes**, v. 8, n. 2, 2018.

GOH, P. S. *et al*. Recent trends in membranes and membrane processes for desalination. **Desalination**, v. 391, p. 43–60, 2016.

GOMES DE ARAÚJO, R. **Análise Das Propriedades Micro E Macroscópicas De Blendas De Poliamida 4,6/Poliamida 6**. [s.l.] Federal University of Santa Catarina, 2002.

GOMES, R. **Tingimento e Ultimação I - Curso Química da Qualidade**. [s.l: s.n.].

GONZÁLEZ, D.; AMIGO, J.; SUÁREZ, F. Membrane distillation: Perspectives for sustainable and improved desalination. **Renewable and Sustainable Energy Reviews**, v. 80, p. 238–259, 2017.

GUAN, G. *et al*. Evaluation of heat utilization in membrane distillation desalination system integrated with heat recovery. **Desalination**, v. 366, p. 80–93, 2015.

GUARATINI, C. C. I.; ZANONI, M. V. B. Corantes têxteis. **Química Nova**, v. 23, n. 1, p. 71–78, 2000.

HABERT, A. C.; BORGES, C. P.; NOBREGA, R. **Processos de Separação com Membranas**. Rio de Janeiro: [s.n.].

HAMMAMI, M. A. *et al*. Engineering hydrophobic organosilica nanoparticle-doped nanofibers for enhanced and fouling resistant membrane distillation. **ACS Applied Materials and Interfaces**, v. 9, n. 2, p. 1737–1745, 2017.

HOLKAR, C. R. *et al*. A critical review on textile wastewater treatments: Possible approaches. **Journal of Environmental Management**, v. 182, p. 351–366, 2016.

HOU, D. *et al*. Fabrication and characterization of electrospun superhydrophobic PVDF-HFP/SiNPs hybrid membrane for membrane distillation. **Separation and Purification**

Technology, v. 189, p. 82–89, 2017.

HOU, D. *et al*. Composite membrane with electrospun multiscale-textured surface for robust oil-fouling resistance in membrane distillation. **Journal of Membrane Science**, v. 546, n. April 2017, p. 179–187, 2018a.

HOU, D. *et al*. A novel dual-layer composite membrane with underwater-superoleophobic/hydrophobic asymmetric wettability for robust oil-fouling resistance in membrane distillation desalination. **Desalination**, v. 428, n. August 2017, p. 240–249, 2018b.

HOU, D. *et al*. Electrospun nanofibrous omniphobic membrane for anti-surfactant-wetting membrane distillation desalination. **Desalination**, v. 468, n. August 2018, p. 114068, 2019a.

HOU, D. *et al*. Electrospun nanofibrous omniphobic membrane for anti-surfactant-wetting membrane distillation desalination. **Desalination**, v. 468, n. August 2018, p. 114068, 2019b.

HUBADILLAH, S. K. *et al*. Hydrophobic ceramic membrane for membrane distillation: A mini review on preparation, characterization, and applications. **Separation and Purification Technology**, v. 217, p. 71–84, 2019.

JIA, W. *et al*. Superhydrophobic membrane by hierarchically structured PDMS-POSS electrospray coating with cauliflower-shaped beads for enhanced MD performance. **Journal of Membrane Science**, n. August, p. 117638, 2019.

JUNG, J. W. *et al*. Electrospun nanofibers as a platform for advanced secondary batteries: A comprehensive review. **Journal of Materials Chemistry A**, v. 4, n. 3, p. 703–750, 2016.

KHAN, A. A. *et al*. Hybrid organic-inorganic functionalized polyethersulfone membrane for hyper-saline feed with humic acid in direct contact membrane distillation. **Separation and Purification Technology**, v. 210, p. 20–28, 2019.

KHAYET, M. Membranes and theoretical modeling of membrane distillation: A review. **Advances in Colloid and Interface Science**, v. 164, n. 1–2, p. 56–88, 2011.

KHAYET, M.; GARCÍA-PAYO, C.; MATSUURA, T. Superhydrophobic nanofibers electrospun by surface segregating fluorinated amphiphilic additive for membrane distillation. **Journal of Membrane Science**, v. 588, n. April, p. 117215, 2019a.

KHAYET, M.; GARCÍA-PAYO, C.; MATSUURA, T. Superhydrophobic nanofibers electrospun by surface segregating fluorinated amphiphilic additive for membrane distillation. **Journal of Membrane Science**, v. 588, n. April, p. 117215, 2019b.

KHUMALO, N. P. *et al*. Congo red dye removal by direct membrane distillation using PVDF/PTFE membrane. **Separation and Purification Technology**, v. 211, p. 578–586, 2019a.

KHUMALO, N. P. *et al*. Congo red dye removal by direct membrane distillation using PVDF/PTFE membrane. **Separation and Purification Technology**, v. 211, n. October 2018, p. 578–586, 2019b.

KUNZ, A. *et al*. Novas tendências no tratamento de efluentes têxteis. **Quimica Nova**, v. 25, n. 1, p. 78–82, 2002.

LADCHUMANANANDASIVAM, R. **Processos químicos têxteis**. 2. ed. Natal, RN- Brasil: Curso de Engenharia Têxtil, 2008. v. III

LAFI, R. *et al*. Treatment of textile wastewater by a hybrid ultrafiltration/electrodialysis process. **Chemical Engineering and Processing - Process Intensification**, v. 132, n. August, p. 105–113, 2018.

LAQBAQBI, M. *et al*. Application of direct contact membrane distillation for textile wastewater treatment and fouling study. **Separation and Purification Technology**, v. 209, n. August 2018, p. 815–825, 2019a.

LAQBAQBI, M. *et al*. Application of direct contact membrane distillation for textile wastewater treatment and fouling study. **Separation and Purification Technology**, v. 209, p. 815–825, 2019b.

LEAPER, S. *et al*. Air-gap membrane distillation as a one-step process for textile wastewater treatment. **Chemical Engineering Journal**, v. 360, p. 1330–1340, 2019.

LEE, E. J. *et al*. Engineering the Re-Entrant Hierarchy and Surface Energy of PDMS-PVDF Membrane for Membrane Distillation Using a Facile and Benign Microsphere Coating. **Environmental Science and Technology**, v. 51, n. 17, p. 10117–10126, 2017.

LEE, E. J.; DEKA, B. J.; AN, A. K. Reinforced superhydrophobic membrane coated with aerogel-assisted polymeric microspheres for membrane distillation. **Journal of Membrane Science**, v. 573, n. September 2018, p. 570–578, 2019a.

LEE, E. J.; DEKA, B. J.; AN, A. K. Reinforced superhydrophobic membrane coated with aerogel-assisted polymeric microspheres for membrane distillation. **Journal of Membrane Science**, v. 573, n. September 2018, p. 570–578, 2019b.

LI, H. *et al*. Improved desalination properties of hydrophobic GO-incorporated PVDF electrospun nanofibrous composites for vacuum membrane distillation. **Separation and Purification Technology**, v. 230, n. August 2019, p. 115889, 2019a.

LI, K. *et al*. Fabrication of PVDF nanofibrous hydrophobic composite membranes reinforced with fabric substrates via electrospinning for membrane distillation desalination. **Journal of Environmental Sciences (China)**, v. 75, p. 277–288, 2019b.

LI, Q. *et al*. An integrated, solar-driven membrane distillation system for water purification and energy generation. **Applied Energy**, v. 237, p. 534–548, 2019c.

LIN, P. J. *et al*. Prevention of surfactant wetting with agarose hydrogel layer for direct contact membrane distillation used in dyeing wastewater treatment. **Journal of Membrane Science**, v. 475, p. 511–520, 2015.

LIN, P. J. *et al*. Polyvinylidene fluoride membrane modification via oxidant-induced dopamine polymerization for sustainable direct-contact membrane distillation. **Journal of Membrane Science**, v. 443, n. May, p. 31–42, 2018.

LIU, Q. *et al*. Functional materials by electrospinning of polymers. **Progress in Polymer Science**, v. 38, n. 6, p. 963–991, 2013.

LIU, Y. *et al*. Controlling numbers and sizes of beads in electrospun nanofibers. **Polymer International**, v. 57, n. 4, 2007.

LOKARE, O. R. *et al*. Concentration polarization in membrane distillation: I. Development of a laser-based spectrophotometric method for in-situ characterization. **Journal of Membrane Science**, 2019.

LOULERGUE, P. *et al*. Air-gap membrane distillation for the separation of bioethanol from algal-based fermentation broth. **Separation and Purification Technology**, v. 213, p. 255–263, 2019.

LU, X. *et al*. Anti-fouling membranes by manipulating surface wettability and their anti-fouling mechanism. **Desalination**, v. 413, p. 127–135, 2017.

LUXBACHER, T. **The ZETA Guide**. 1ª ed. Austria: Anton Paar GmbH, 2014.

MADALOSSO, H. B. *et al*. Modeling and experimental validation of direct contact membrane distillation applied to synthetic dye solutions. **Journal of Chemical Technology and Biotechnology**, 2020.

MADALOSSO, H. B. *et al*. Membrane Surface Modification by Electrospinning, Coating, and Plasma for Membrane Distillation Applications: A State-of-the-Art Review. **Advanced Engineering Materials**, v. 2001456, 2021.

MARTÍNEZ-DÍEZ, L.; VÁZQUEZ-GONZÁLEZ, M. I. Temperature and concentration polarization in membrane distillation of aqueous salt solutions. **Journal of Membrane Science**, v. 156, n. 2, p. 265–273, 1999.

MENDEZ, D. L. M. *et al*. Improved performances of vacuum membrane distillation for desalination applications: Materials vs process engineering potentialities. **Desalination**, v. 452, p. 208–218, 2019.

MILNITZ, D.; LUNA, M. M. M. CARACTERIZAÇÃO DA INDÚSTRIA TÊXTIL E DE CONFECÇÕES DO ESTADO DE SANTA CATARINA: PRINCIPAIS ELOS, PARCEIROS E PRODUTOS COMERCIALIZADOS. **Revista da UNIFEBE**, v. 1, p. 166–181, 2017.

MOKHTAR, N. M. *et al*. The potential of direct contact membrane distillation for industrial textile wastewater treatment using PVDF-Cloisite 15A nanocomposite membrane. **Chemical Engineering Research and Design**, v. 111, p. 284–293, 2016.

NIU, B. *et al*. Rheological aspects in fabricating pullulan-whey protein isolate emulsion suitable for electrospraying: Application in improving β-carotene stability. **Lwt**, v. 129, n. February, p. 109581, 2020.

NÚÑEZ, J. *et al*. Application of electrocoagulation for the efficient pollutants removal to reuse the treated wastewater in the dyeing process of the textile industry. **Journal of Hazardous Materials**, v. 371, n. November 2018, p. 705–711, 2019.

PURKAIT, M. K. *et al*. Introduction to Membranes. In: **Interface Science and Technology**. [s.l: s.n.]. v. 25p. 1–37.

RAMLOW, H. **DESTILAÇÃO POR MEMBRANA APLICADA AO TRATAMENTO DE**

ÁGUAS RESIDUAIS DA INDÚSTRIA TÊXTIL. [s.l.] Universidade Federal de Santa Catarina (UFSC), 2018.

RAMLOW, H. *et al*. Dye synthetic solution treatment by direct contact membrane distillation using commercial membranes. **Environmental Technology (United Kingdom)**, v. 0, n. 0, p. 1–39, 2019a.

RAMLOW, H. *et al*. Influence of dye class on the comparison of direct contact and vacuum membrane distillation applied to remediation of dyeing wastewater. **Journal of Environmental Science and Health, Part A**, v. 54, n. 13, p. 1337–1347, 2019b.

RAMLOW, H. *et al*. Intensification of water reclamation from textile dyeing wastewater using thermal membrane technologies – Performance comparison of vacuum membrane distillation and thermopervaporation. **Chemical Engineering and Processing - Process Intensification**, v. 146, n. October, p. 107695, 2019c.

RAMLOW, H.; FILHO, C. M. T.; ANDRADE, K. L. **Potencialidade de uma membrana plana comercial de PVDF aplicada à recuperação de água do efluente do tingimento têxtil contendo corante disperso no processo de destilação por membrana**. 15º Congresso Brasileiro de Polímeros (15 CBPOL). **Anais**...Bento Golçalves - RS: 2019

RAMLOW, H.; MACHADO, R. A. F.; MARANGONI, C. Direct contact membrane distillation for textile wastewater treatment: A state of the art review. **Water Science and Technology**, v. 76, n. 10, p. 2565–2579, 2017.

RAY, S. S. *et al*. Poly(vinyl alcohol) incorporated with surfactant based electrospun nanofibrous layer onto polypropylene mat for improved desalination by using membrane distillation. **Desalination**, v. 414, p. 18–27, 2017a.

RAY, S. S. *et al*. Uniform hydrophobic electrospun nanofibrous layer composed of polysulfone and sodium dodecyl sulfate for improved desalination performance. **Separation and Purification Technology**, v. 186, p. 352–365, 2017b.

RAY, S. S. *et al*. Casting of a superhydrophobic membrane composed of polysulfone/Cera flava for improved desalination using a membrane distillation process. **RSC Advances**, v. 8, n. 4, p. 1808–1819, 2018.

REZAEI, M. *et al*. Wetting phenomena in membrane distillation: Mechanisms, reversal, and prevention. **Water Research**, v. 139, p. 329–352, 2018.

SANTORO, S. *et al*. A non-invasive optical method for mapping temperature polarization in direct contact membrane distillation. **Journal of Membrane Science**, v. 536, n. October 2016, p. 156–166, 2017.

SHARMA, A. *et al*. Adsorption of textile wastewater on alkali-activated sand. **Journal of Cleaner Production**, v. 220, p. 23–32, 2019.

SHOUKAT, R.; KHAN, S. J.; JAMAL, Y. Hybrid anaerobic-aerobic biological treatment for real textile wastewater. **Journal of Water Process Engineering**, v. 29, n. July 2018, p. 100804, 2019.

SILVA, T. L. S. *et al*. Desalination and removal of organic micropollutants and microorganisms

by membrane distillation. **Desalination**, v. 437, p. 121–132, 2018.

SISSOM, L. E.; PITTS, D. R. **Fenômenos de Transporte**. Rio de Janeiro: Guanabara Dois, 1979.

SIYAL, M. I. *et al*. Surface modification of glass fiber membranes by fluorographite coating for desalination of concentrated saline water with humic acid in direct-contact membrane distillation. **Separation and Purification Technology**, v. 205, n. May, p. 284–292, 2018.

TAI, Z. S. *et al*. An Overview of Membrane Distillation. In: ISMAIL, A. *et al*. (Eds.). . **Membrane Separation Principles and Applications**. 1st. ed. [s.l.] Elsevier, 2018. p. 251–281.

TANG, M. *et al*. Anti-oil-fouling hydrophobic-superoleophobic composite membranes for robust membrane distillation performance. **Science of The Total Environment**, v. 696, p. 133883, 2019.

TIJING, L. D. *et al*. Fouling and its control in membrane distillation-A review. **Journal of Membrane Science**, v. 475, p. 215–244, 2015.

TOLENTINO FILHO, C. M. **Influência da composição de águas residuais de tingimento de fibras têxteis no desempenho do processo de destilação por membranas**. [s.l.] Universidade Federal de Santa Catarina, 2019.

TWARDOKUS, R. G. **Reuso de água no processo de tingimento da Indústria Têxtil**. [s.l.] Universidade Federal de Santa Catarina, 2004.

VAN DER BRUGGEN, B.; CURCIO, E.; DRIOLI, E. Process intensification in the textile industry: The role of membrane technology. **Journal of Environmental Management**, v. 73, n. 3, p. 267–274, 2004.

VELOSO, L. DE A. **Corantes e PigmentosServiço Brasileiro de Resposta Técnica**. [s.l: s.n.]. Disponível em: <http://www.crq4.org.br/quimicaviva_corantespigmentos>.

WANG, K. *et al*. Hydrophilic surface coating on hydrophobic PTFE membrane for robust anti-oil-fouling membrane distillation. **Applied Surface Science**, v. 450, p. 57–65, 2018.

WANG, K. *et al*. Development of a composite membrane with underwater-oleophobic fibrous surface for robust anti-oil-fouling membrane distillation. **Journal of Colloid and Interface Science**, v. 537, p. 375–383, 2019a.

WANG, K. *et al*. Development of a composite membrane with underwater-oleophobic fibrous surface for robust anti-oil-fouling membrane distillation. **Journal of Colloid and Interface Science**, v. 537, p. 375–383, 2019b.

WANG, P.; CHUNG, T.-S. Recent advances in membrane distillation processes: Membrane development, configuration design and application exploring. **Journal of Membrane Science**, v. 474, p. 39–56, 2015.

WARSINGER, D. M. *et al*. Scaling and fouling in membrane distillation for desalination applications: A review. **Desalination**, v. 356, p. 294–313, 2015.

WEILER, D. K. **Caracterização e Otimização do reuso de águas na Indústria Têxtil**. [s.l.] Universidade Federal de Santa Catarina (UFSC), 2005.

YE, Y. *et al*. Microbubble aeration enhances performance of vacuum membrane distillation desalination by alleviating membrane scaling. **Water Research**, v. 149, p. 588–595, 2019.

ZAZOU, H. *et al*. Treatment of textile industry wastewater by electrocoagulation coupled with electrochemical advanced oxidation process. **Journal of Water Process Engineering**, v. 28, n. February, p. 214–221, 2019.

ZHAO, L. *et al*. Activated carbon enhanced hydrophobic/hydrophilic dual-layer nanofiber composite membranes for high-performance direct contact membrane distillation. **Desalination**, v. 446, n. August, p. 59–69, 2018a.

ZHAO, L. *et al*. Activated carbon enhanced hydrophobic/hydrophilic dual-layer nanofiber composite membranes for high-performance direct contact membrane distillation. **Desalination**, v. 446, n. August, p. 59–69, 2018b.

APPENDIX A – EDX analysis of pristine PP membrane (a), modified PP membrane with 2% PVDF, 10% PDMS 20% Si (b), and modified PP membrane with 2% PVDF, 6% Sylgard (c)

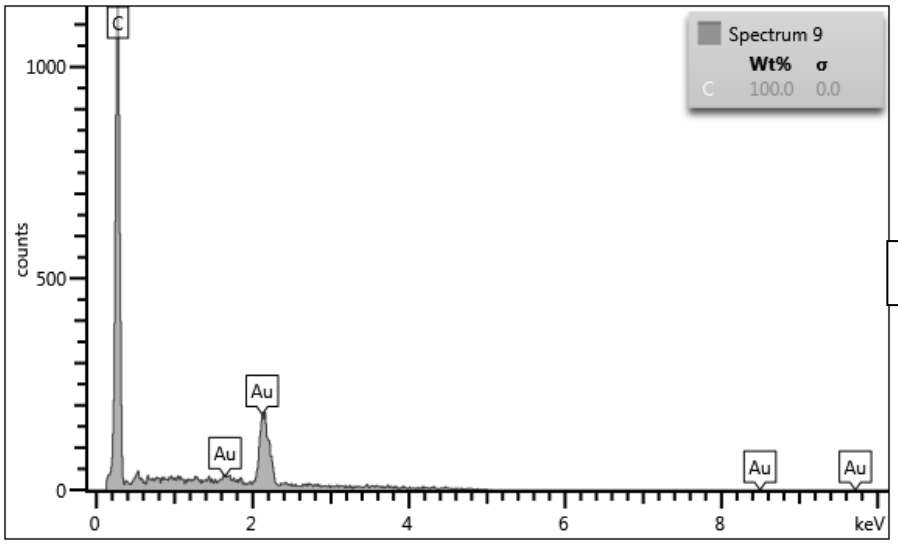

(a)

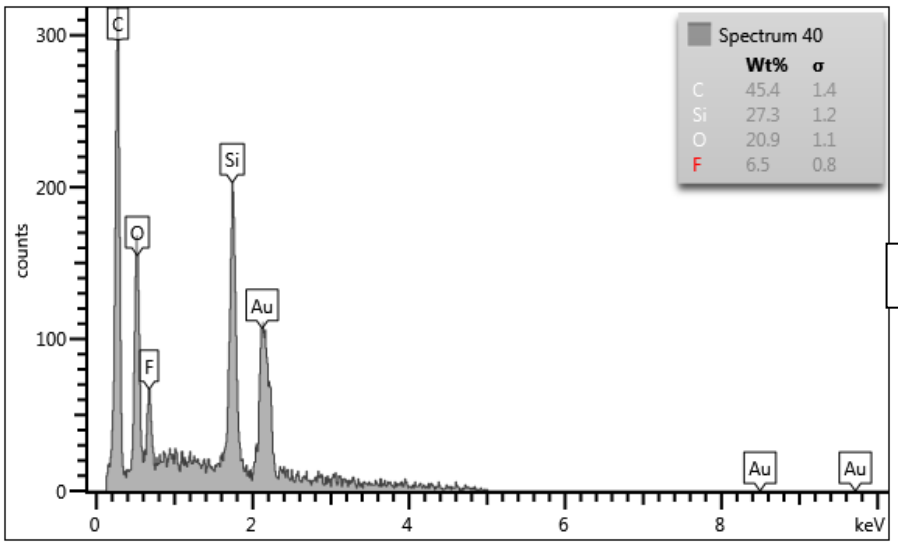

(b)

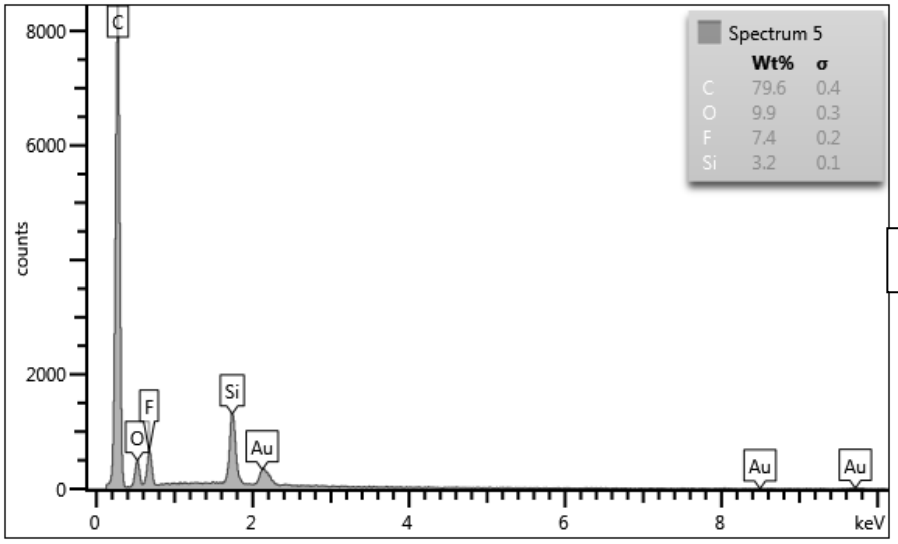

(c)

APPENDIX B – EDX analysis of pristine PA membrane (a), and modified PA membranes with 2% PVDF, 10% PDMS (b), and 2% PVDF, 10% PDMS, 20% Si (c)

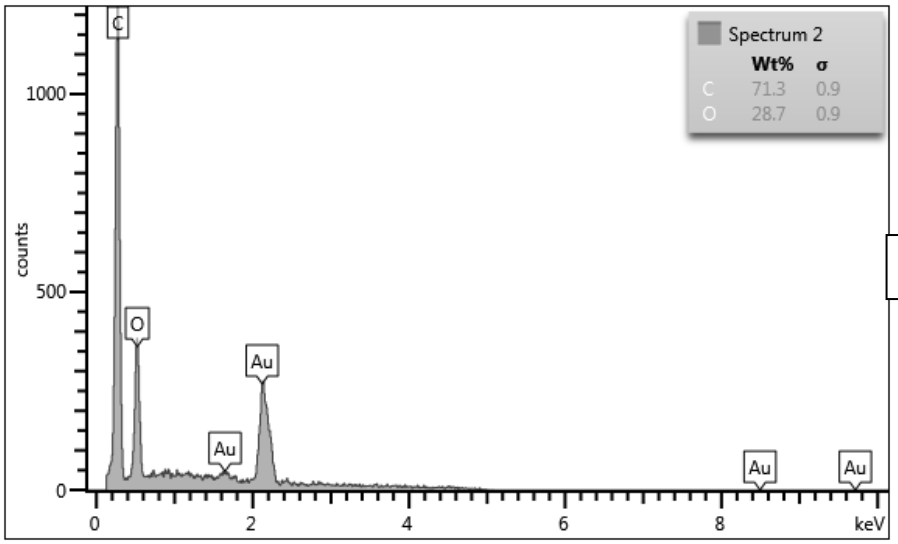

(a)

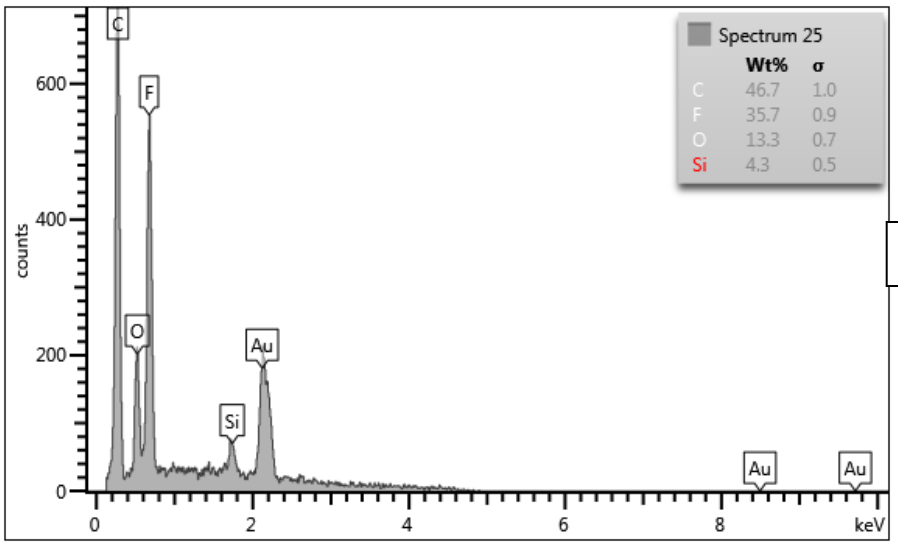

(b)

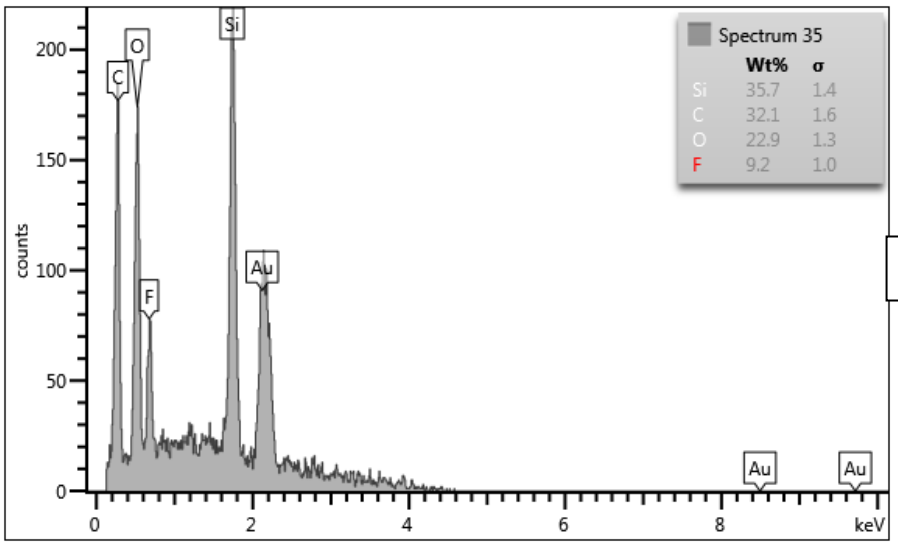

(c)

APPENDIX C – Contact angle measurements of selected membranes with all tested solutions

	Contact Angle					
Membrane	Water	Reactive Black	Disperse Black	Direct Black	Acid Black	Surfactant (Detergent)
Pristine PP	118.92 ± 3.26	132.13 ± 1.17	132.6 ± 0.79	133.03 ± 2.91	132.93 ± 0.76	130.23 ± 2.75
PP 2% PVDF, 6% Sylgard	142.07 ± 1.67	132.87 ± 0.51	133.33 ± 0.91	148.38 ± 12.36	151.5 ± 6.18	142.6 ± 4.27
Pristine PA	75.73 ± 3.86	61.63 ± 3.57	68.33 ± 2.35	62.23 ± 0.61	66.30 ± 0.56	61.13 ± 1.37
PA 2% PVDF, 10% PDMS	129.3 ± 4.69	76.67 ± 2.38	93.20 ± 0.72	96.9 ± 8.92	98.03 ± 2.9	78.13 ± 10.32
PA 2% PVDF, 10% PDMS, 20% SiNPs	167.13 ± 22.28	-	-	-	-	160.5 ± 2.6

APPENDIX D – SEM analysis of pristine PP membrane after DCMD operation with reactive black (a), disperse black (b), direct black (c), and acid black (d) solutions, in concentration of 30 mg L^{-1}, amplified in 1.000, 3.000 and 5.000 times.

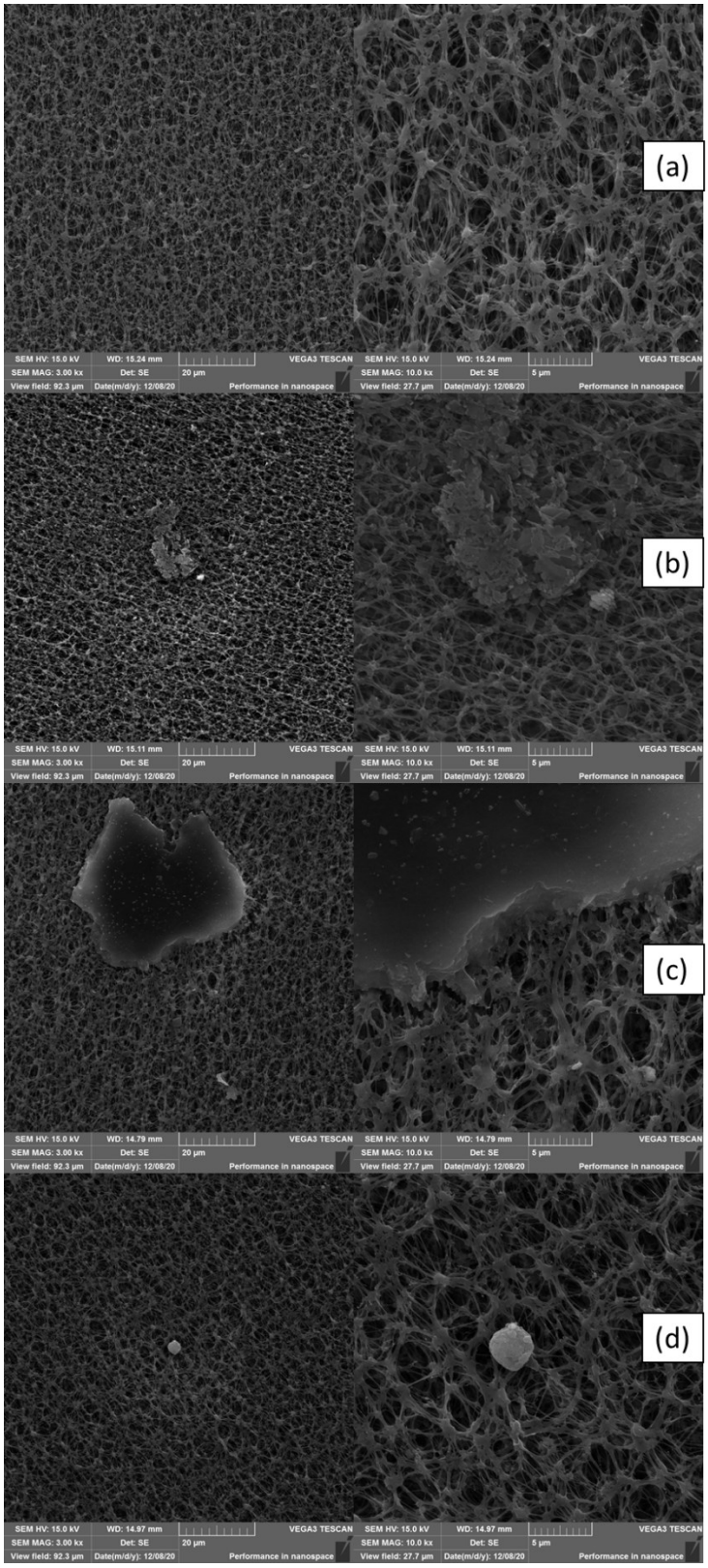

APPENDIX E – SEM analysis of PP 2% PVDF, 6% Sylgard membrane after DCMD operation with reactive black (a), disperse black (b), direct black (c), and acid black (d) solutions, in concentration of 30 mg L^{-1}, amplified in 1.000, 3.000 and 5.000 times.

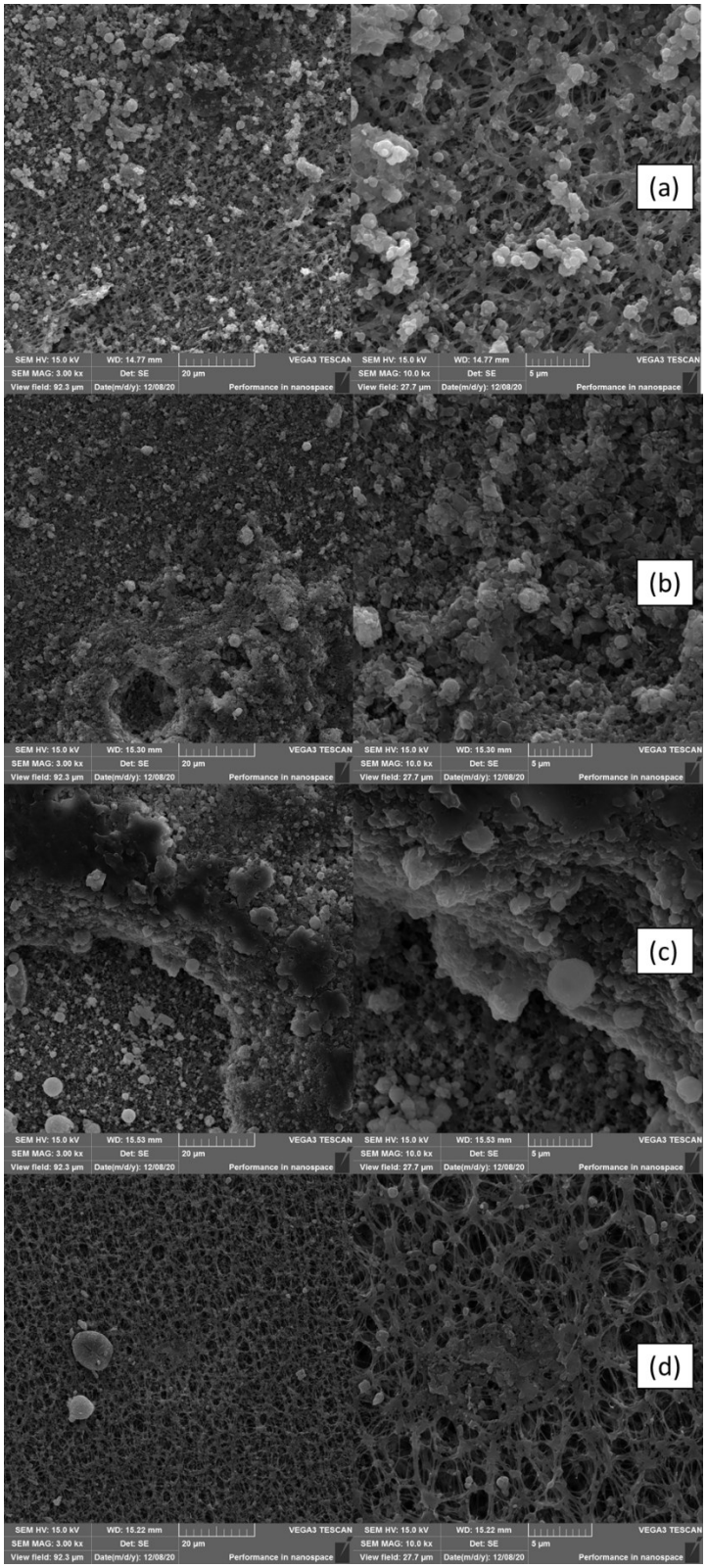

APPENDIX F – SEM analysis of pristine PA membrane (a), and modified PA membrane with 2% PVDF, 10% PDMS, and 0% Si NPs (b) or 20% Si NPs (c) after DCMD operation with reactive black solution (30 mg L^{-1}), amplified in 1.000, 3.000 and 5.000 times.

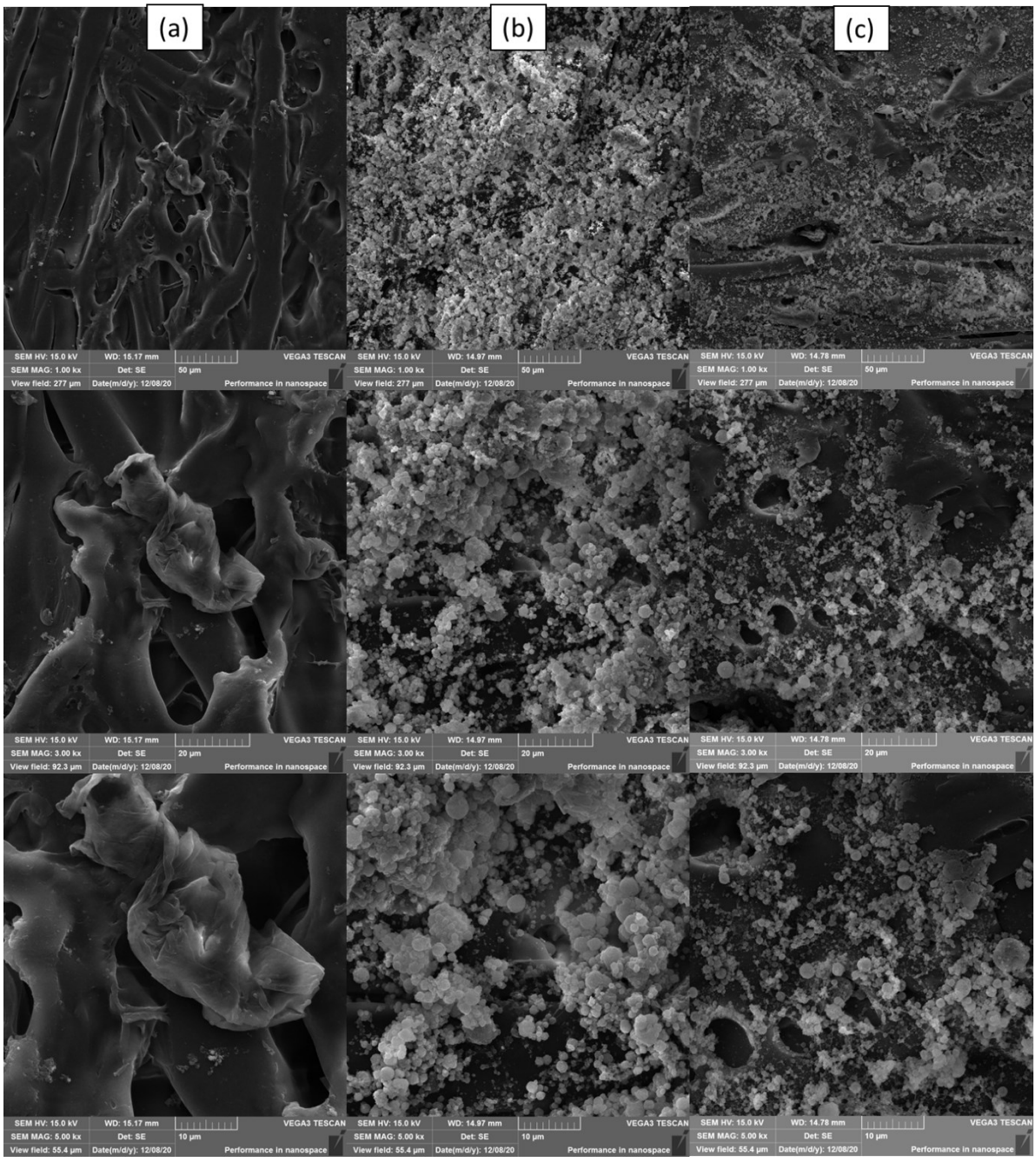

APPENDIX G – SEM analysis of pristine PA membrane (a), and modified PA membrane with 2% PVDF, 10% PDMS, and 20% Si NPs (b) after DCMD operation with Colorswet solution (30 mg L^{-1}), amplified in 1.000, 3.000 and 5.000 times.

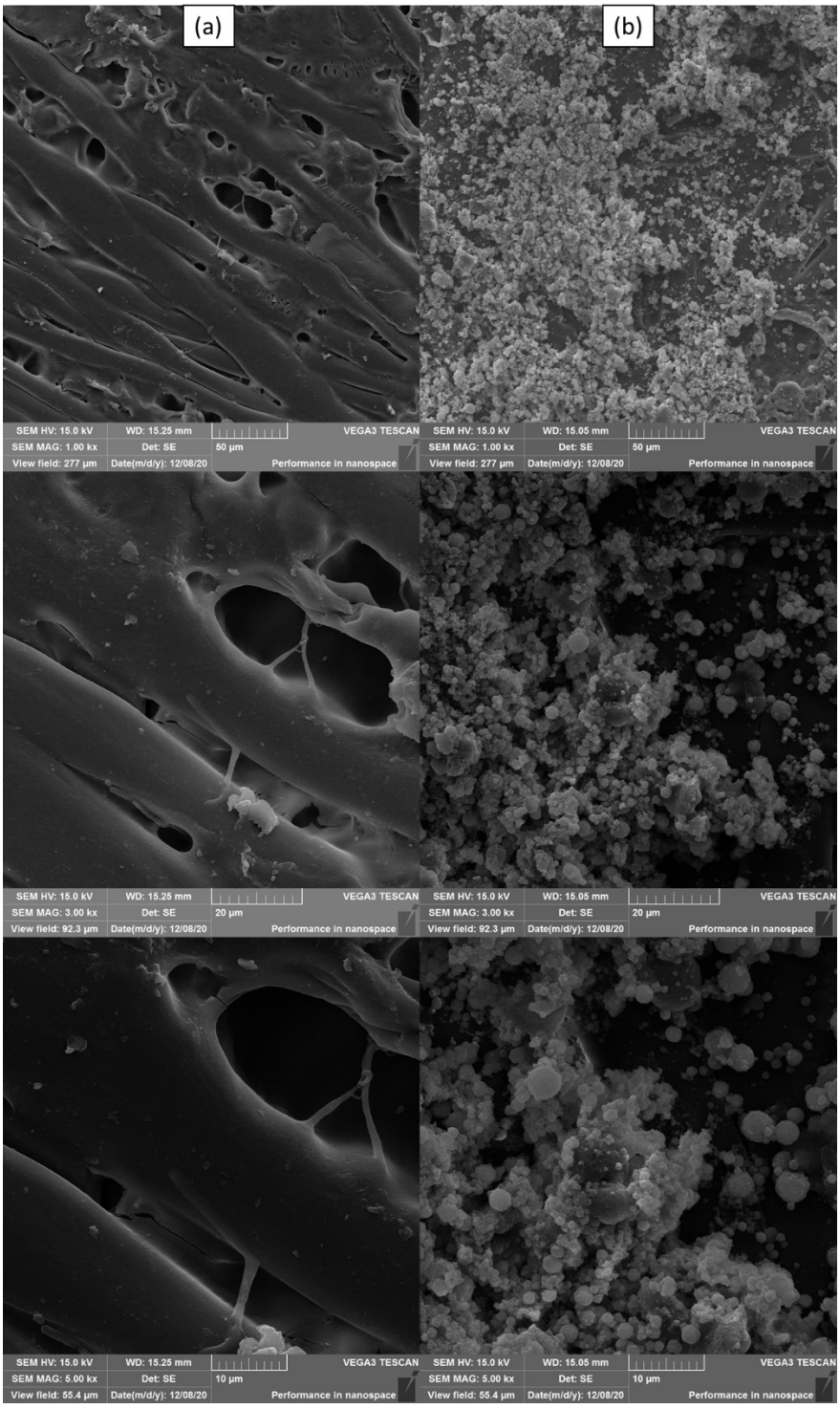

APPENDIX H – EDX analysis of pristine PP membrane after DCMD operation with Reactive Black (a), Disperse Black (b), Direct Black (c), and Acid Black (d) solutions, in concentration of 30 mg L^{-1}

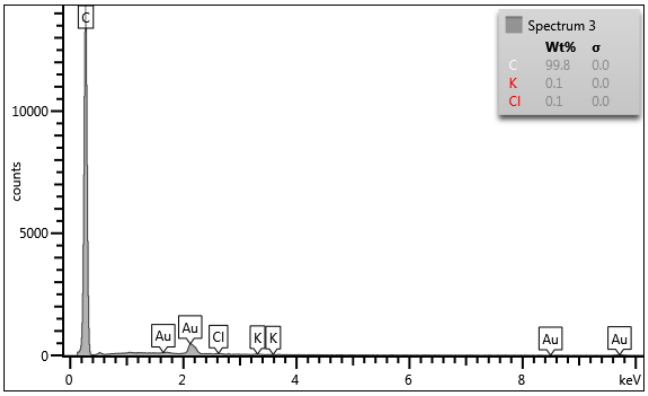

(a)

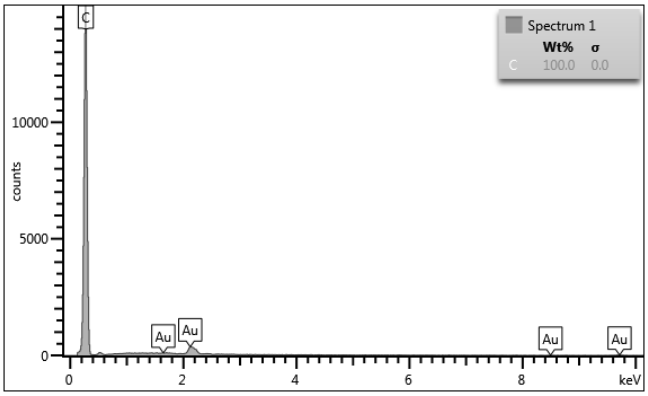

(b)

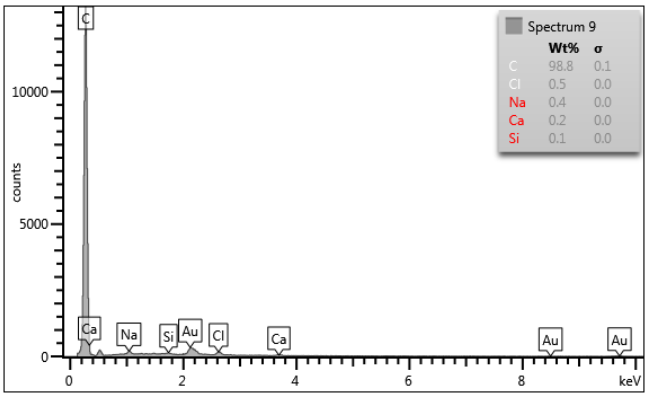

(c)

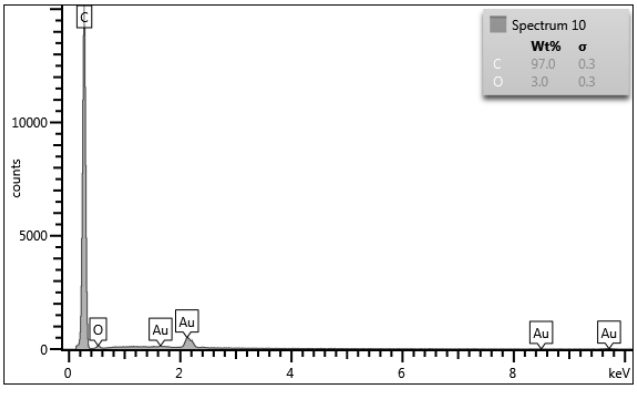

(d)

APPENDIX I – EDX analysis of PP 2% PVDF, 6% Sylgard membrane after DCMD operation with reactive black (a), disperse black (b), direct black (c), and acid black (d) solutions, in concentration of 30 mg L^{-1}

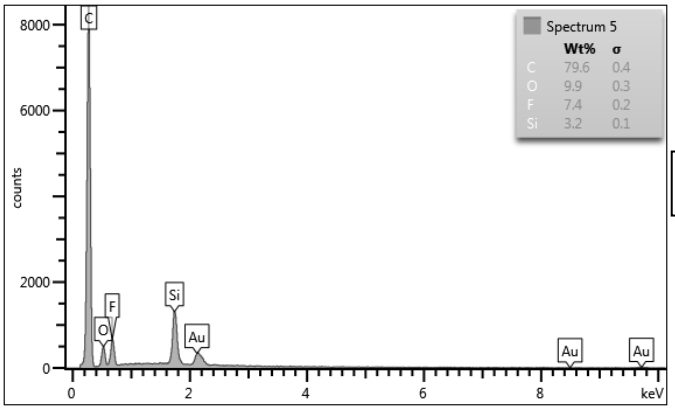

(a)

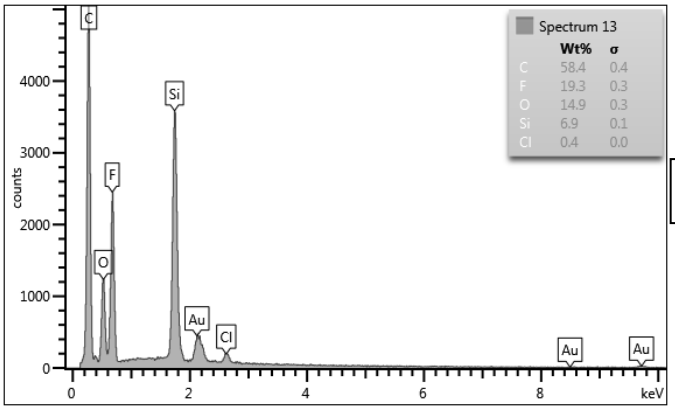

(b)

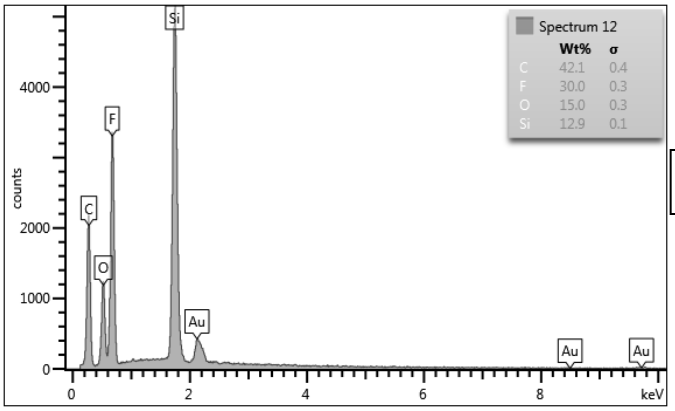

(c)

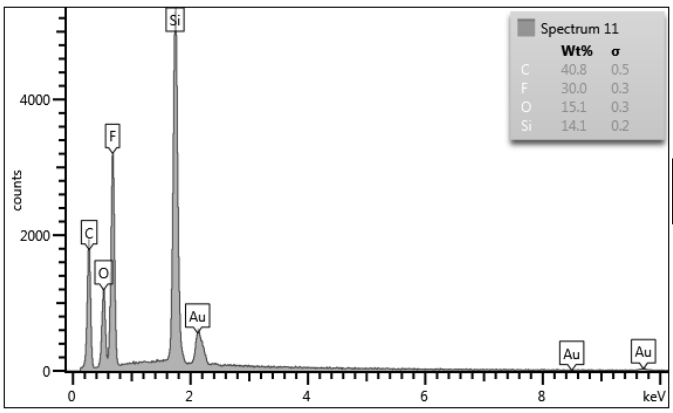

(d)

APPENDIX J – EDX analysis of pristine PA membrane (a), and modified PA membrane with 2% PVDF, 10% PDMS, and 0% Si NPs (b) or 20% Si NPs (c) after DCMD operation with Reactive Black solution (30 mg L^{-1}).

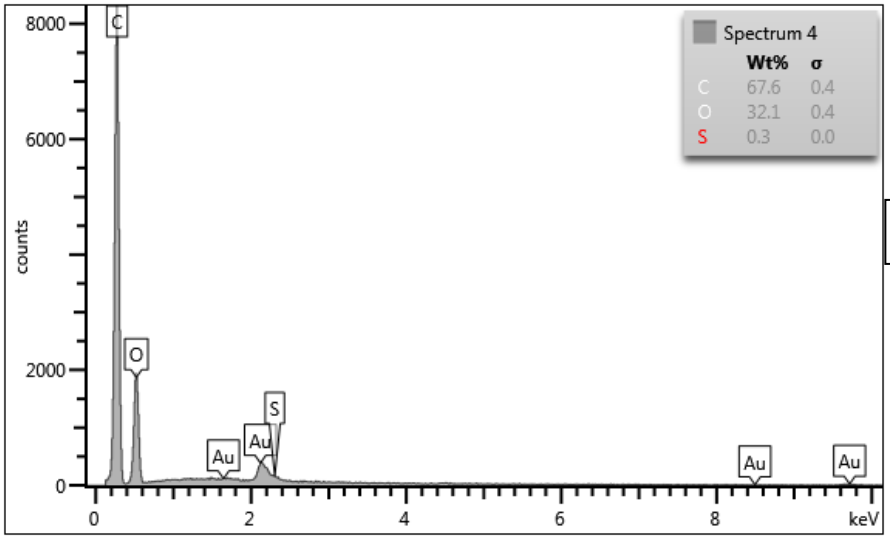

(a)

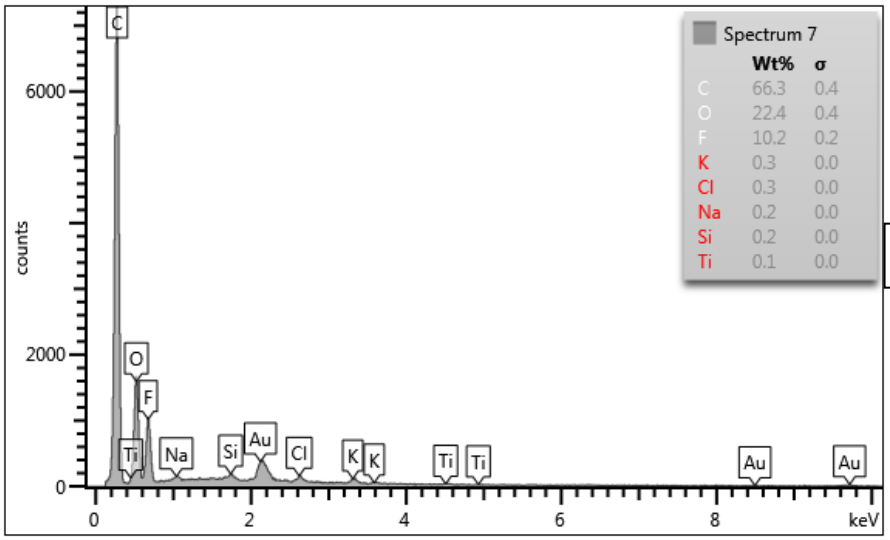

(b)

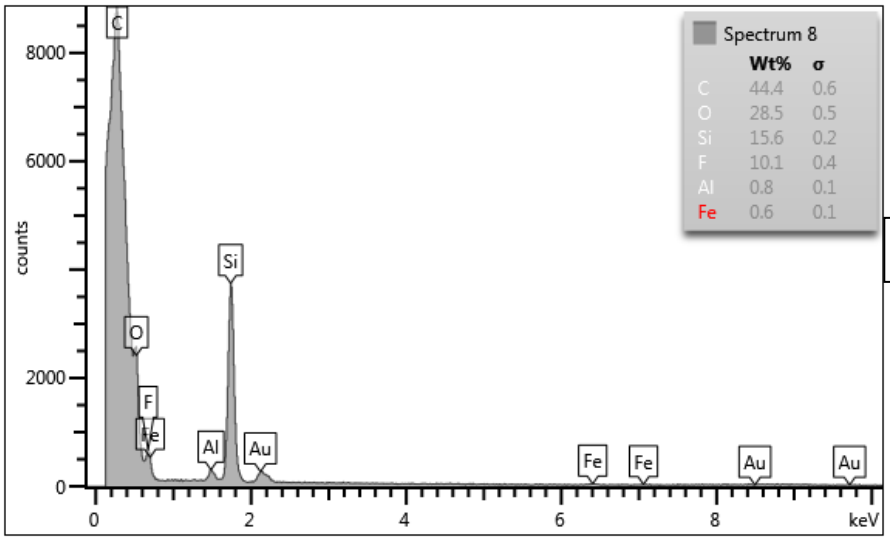

(c)

APPENDIX K – EDX analysis of pristine PA membrane (a), and modified PA membrane with 2% PVDF, 10% PDMS, and 20% Si NPs (b) after DCMD operation with Colorswet solution (30 mg L^{-1}).

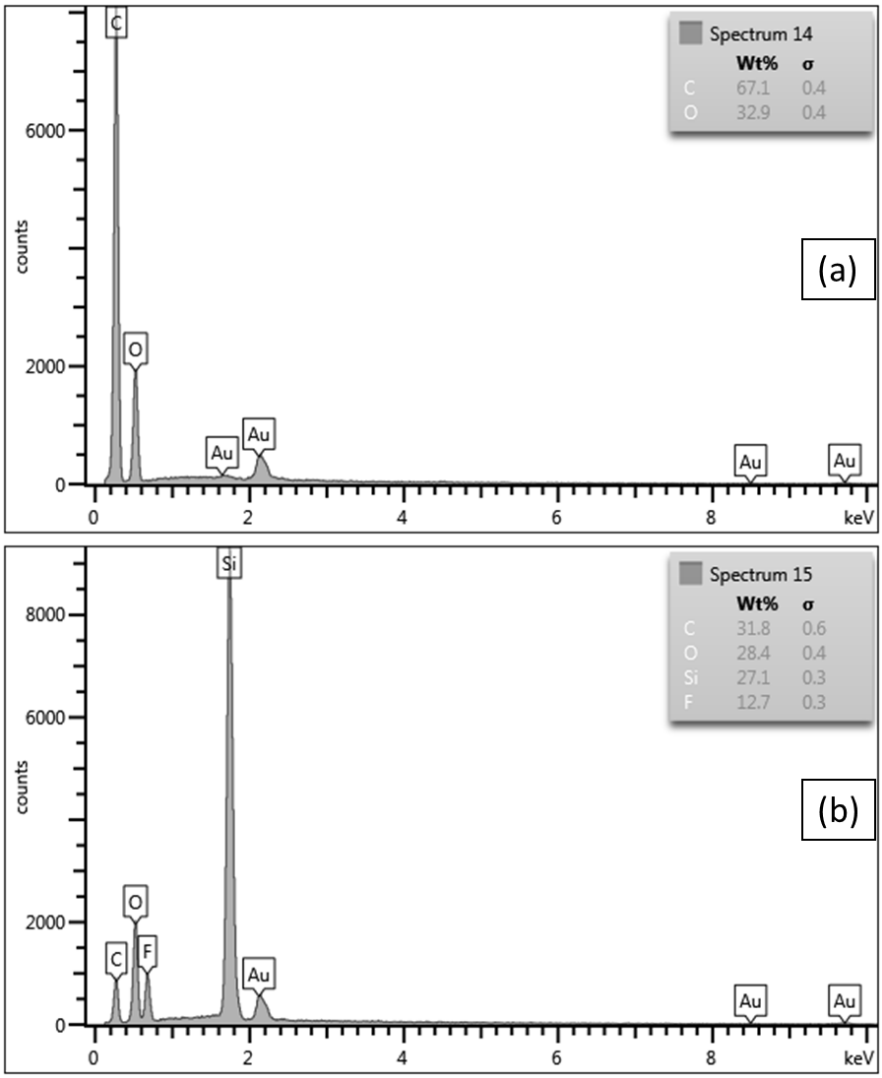

APPENDIX L – IR spectra of pristine PP membrane (a) and PP membrane after DCMD operation with Reactive Black Dye (b), Disperse Black Dye (c), Direct Black Dye (d) and Acid Black Dye (e) solutions, in a concentration of 30 mg L^{-1}

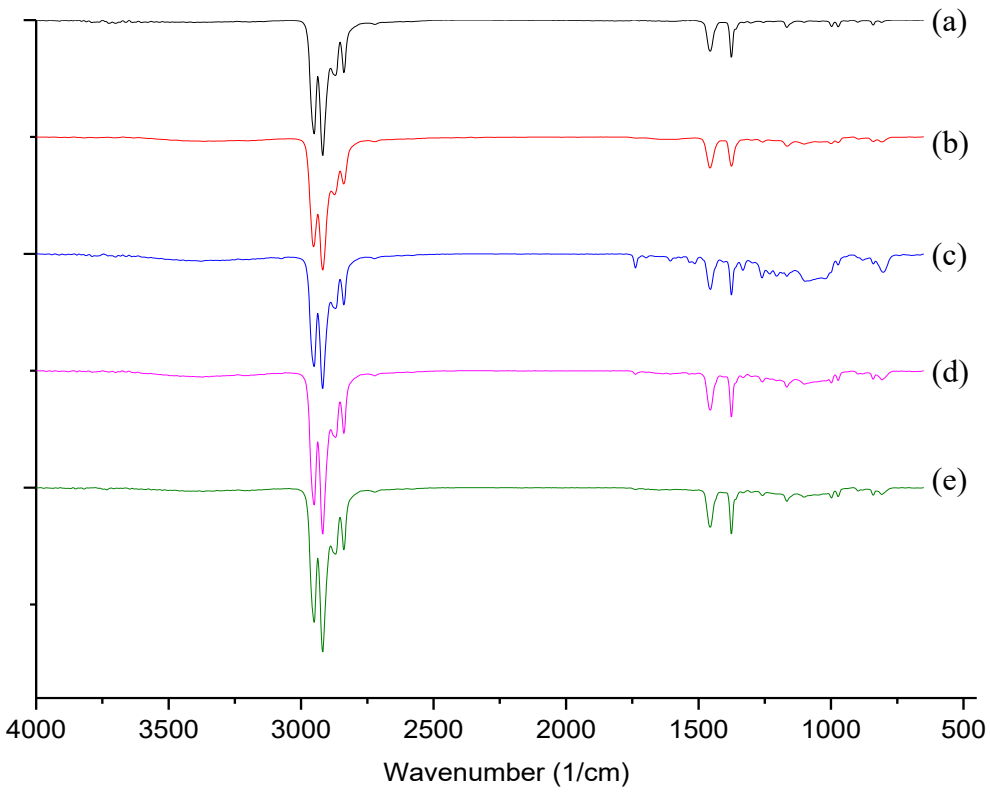

APPENDIX M – IR spectra of pristine PP 2% PVDF, 6% Sylgard membrane (a) and PP 2% PVDF, 6% Sylgard membrane after DCMD operation with Reactive Black Dye (b), Disperse Black Dye (c), Direct Black Dye (d) and Acid Black Dye (e) solutions, in a concentration of 30 mg L^{-1}

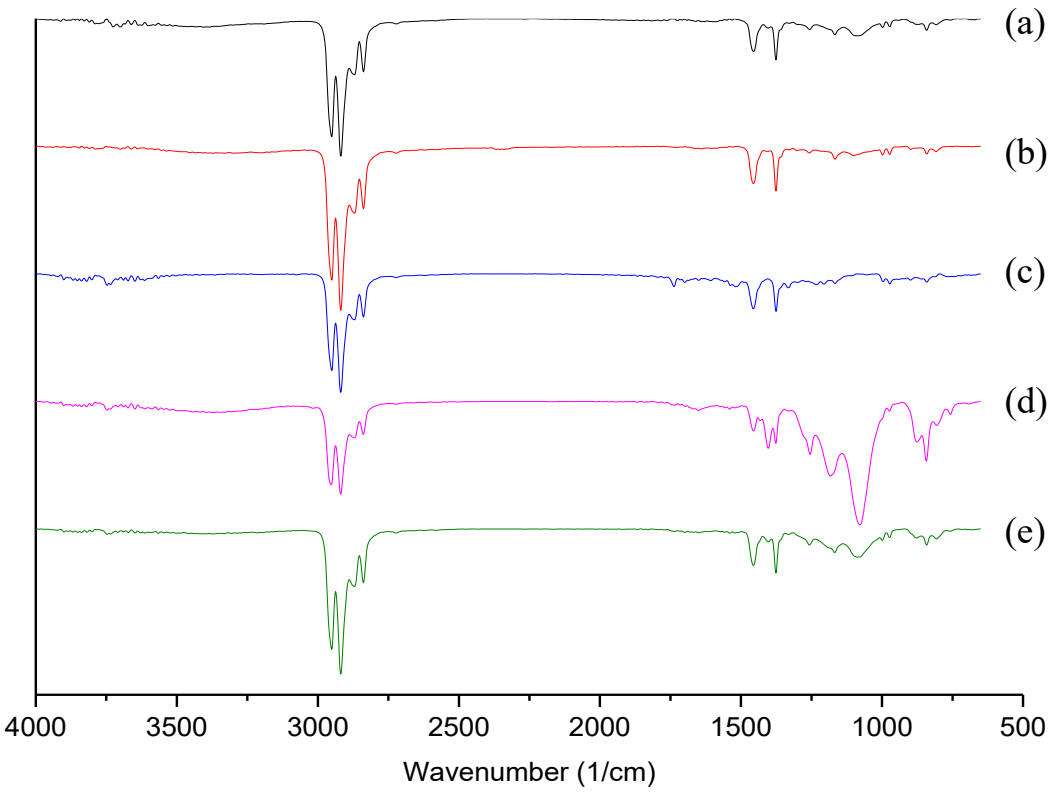

APPENDIX N – IR spectra of pristine PA membrane (a) and PA membrane after DCMD operation with Reactive Black Dye (b), and Colorswet (c) in a concentration of 30 mg L^{-1}

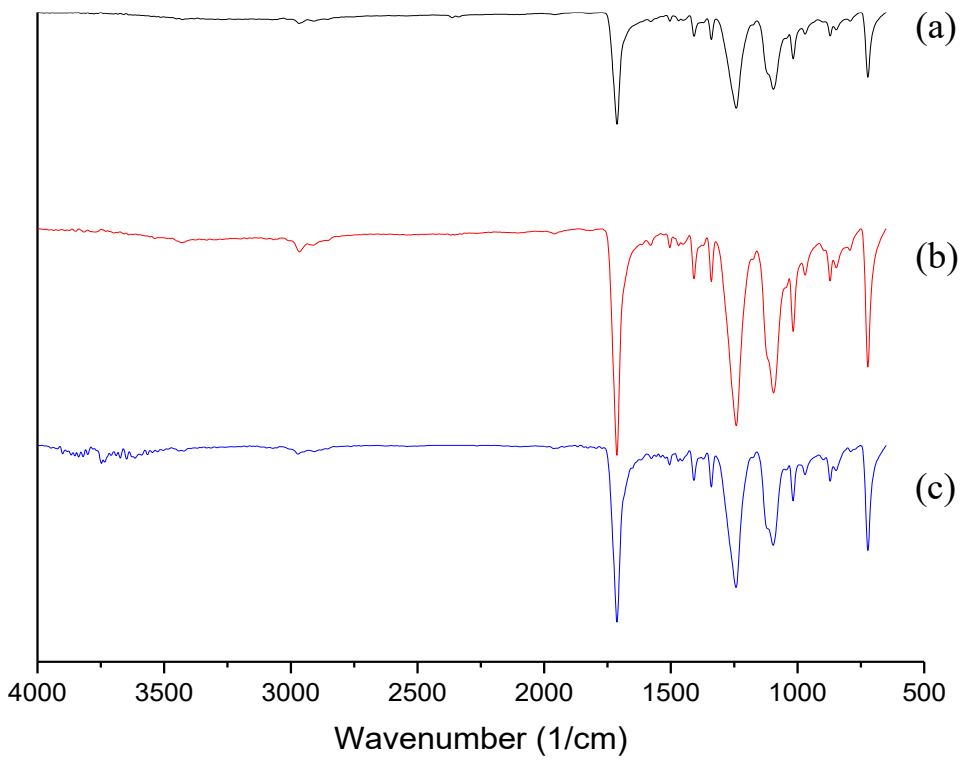

APPENDIX O – IR spectra of pristine PA 2% PVDF, 10% PDMS membrane (a) and PA 2% PVDF, 10% PDMS after DCMD operation with Reactive Black Dye (b) in a concentration of 30 mg L^{-1}

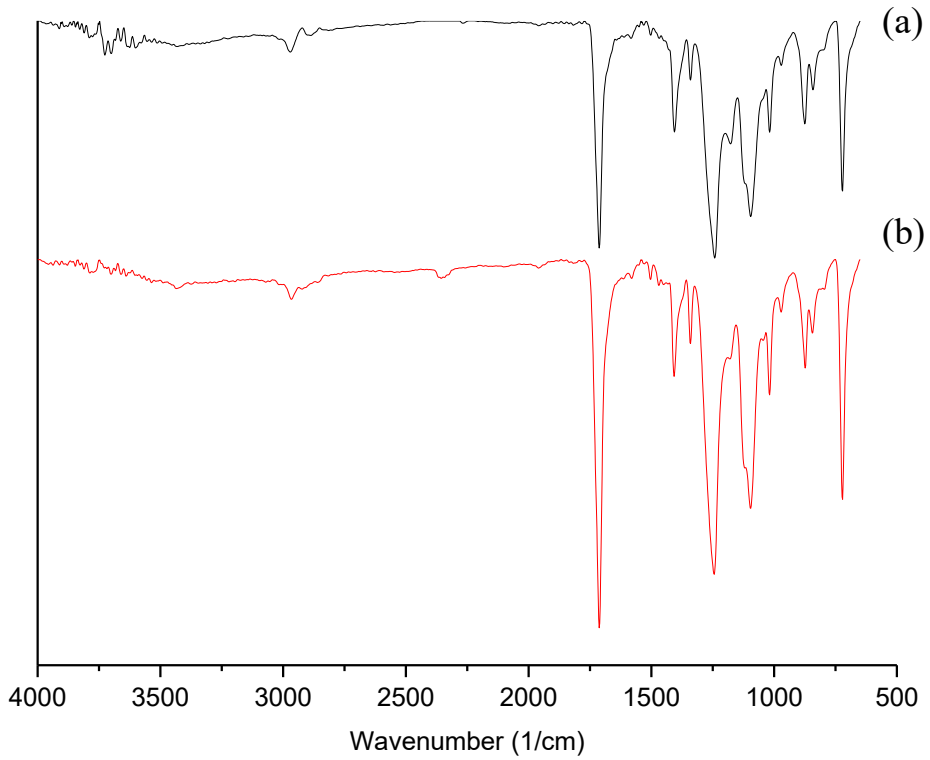

APPENDIX P – IR spectra of pristine PA 2% PVDF, 10% PDMS, 20% Si NPs membrane (a) and PA 2% PVDF, 10% PDMS, 20% Si after DCMD operation with Reactive Black Dye (b), and Colorswet (c) in a concentration of 30 mg L^{-1}

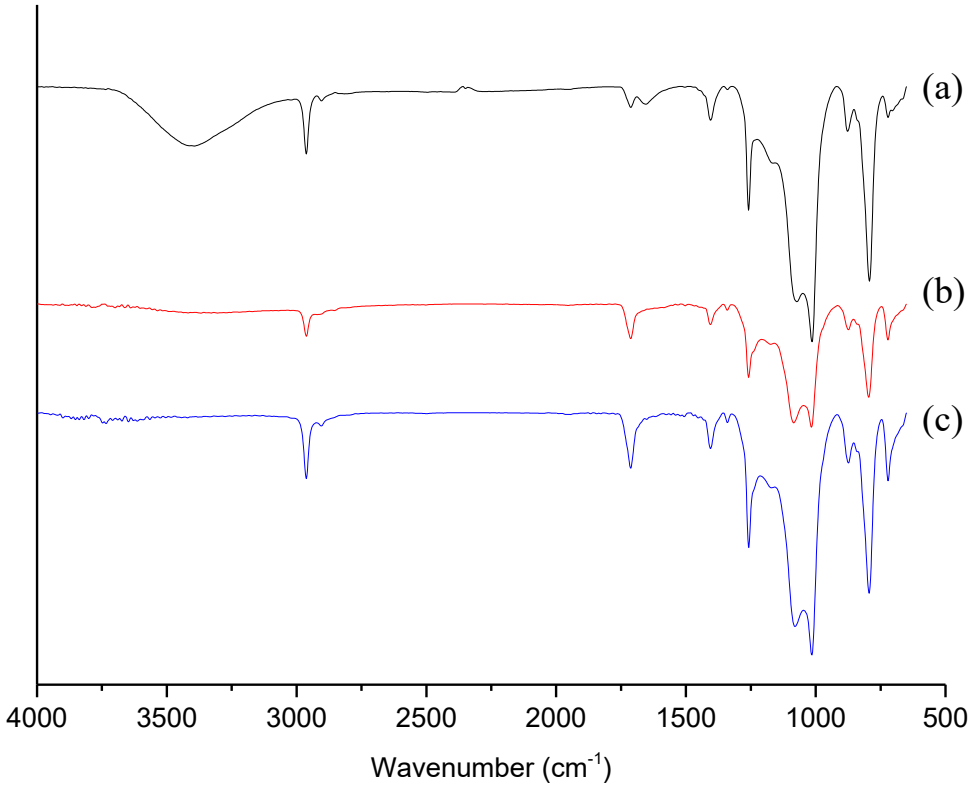

APPENDIX Q – Tuckey test of water contact angle measurements for PP 2% PVDF, 6 or 10% PDMS, 0, 10, 20 or 30% Si, at 30, 60 and 90 min.

	Pristine PP	6_0-30	6_0-60	6_0-90	6_10-30	6_10-60	6_10-90	6_20-30	6_20-60	6_20-90	6_30-30	6_30-60	6_30-90	10_0-30	10_0-60	10_0-90	10_10-30	10_10-60	10_10-90	10_20-30	10_20-60	10_20-90	10_30-30	10_30-60	10_30-90
Pristine PP		1	1	1	1	0,986	0,09295	1	0,997	1	0,6074	0,9926	0,8781	1	0,9977	1	1	1	1	1	0,8928	0,9733	0,09543	1	1
6_0-30	1,25		1	1	1	1	0,5532	1	0,7304	1	0,9883	1	0,9998	1	1	1	1	0,9999	1	1	0,3165	0,5121	0,5607	0,9646	0,9794
6_0-60	0,6734	0,5763		1	1	0,9998	0,28	1	0,9339	1	0,8969	1	0,9902	1	1	1	1	1	1	1	0,6	0,7973	0,2856	0,9982	0,9993
6_0-90	0,3548	1,604	1,028		1	0,9414	0,04662	1	0,9998	0,9991	0,4249	0,9626	0,7359	1	0,9836	1	1	1	1	1	0,9669	0,9954	0,04799	1	1
6_10-30	0,8547	0,395	0,1813	1,209		1	0,3569	1	0,887	1	0,9409	1	0,9964	1	1	1	1	1	1	1	0,5054	0,7149	0,3634	0,9945	0,9975
6_10-60	2,486	1,237	1,813	2,841	1,632		0,9798	0,9963	0,1743	1	1	1	1	0,9991	1	0,9913	0,9305	0,9031	1	0,9998	0,03645	0,08217	0,9811	0,4827	0,5505
6_10-90	5,052	3,802	4,378	5,406	4,197	2,565		0,1442	0,000556	0,7651	1	0,966	0,9994	0,203	0,932	0,1107	0,04192	0,03331	0,3551	0,2659	5,55E-05	0,0001739	1	0,003865	0,005325
6_20-30	0,2473	1,002	0,426	0,6021	0,6073	2,239	4,804		0,9882	1	0,7316	0,9983	0,9416	1	0,9996	1	1	1	1	1	0,8048	0,9336	0,1477	0,9999	1
6_20-60	2,204	3,454	2,877	1,849	3,059	4,69	7,256	2,451		0,5141	0,01604	0,2126	0,05876	0,9698	0,2836	0,9947	0,9999	1	0,8881	0,9414	1	1	0,0005776	1	1
6_20-90	1,673	0,4234	0,9997	2,028	0,8184	0,8132	3,379	1,426	3,877		0,9991	1	1	1	1	1	0,9987	0,9973	1	1	0,1681	0,31	0,7715	0,8657	0,9056
6_30-30	3,698	2,449	3,025	4,053	2,844	1,212	1,353	3,451	5,902	2,025		1	1	0,8231	1	0,6569	0,3997	0,3487	0,9401	0,8862	0,002148	0,005905	1	0,07728	0,09865
6_30-60	2,361	1,111	1,687	2,716	1,506	0,1256	2,691	2,113	4,565	0,6876	1,338		1	0,9997	1	0,9957	0,9547	0,9339	1	0,9999	0,04724	0,1037	0,9679	0,5478	0,6162
6_30-90	3,087	1,838	2,414	3,442	2,232	0,6009	1,964	2,84	5,291	1,414	0,6112	0,7265		0,9734	1	0,9063	0,7111	0,6562	0,9963	0,9882	0,009579	0,02413	0,9995	0,2212	0,2684
10_0-30	0,4571	0,7925	0,2163	0,8119	0,3975	2,029	4,594	0,2098	2,661	1,216	3,241	1,904	2,63		0,9999	1	1	1	1	1	0,7099	0,8777	0,2076	0,9996	0,9999
10_0-60	2,165	0,9155	1,492	2,52	1,31	0,3211	2,886	1,918	4,369	0,4921	1,533	0,1955	0,922	1,708		0,9988	0,9793	0,9672	1	1	0,06963	0,1461	0,935	0,6496	0,7149
10_0-90	0,09583	1,154	0,5775	0,4506	0,7588	2,39	4,956	0,1515	2,3	1,577	3,603	2,265	2,991	0,3613	2,069		1	1	1	1	0,8622	0,9609	0,1135	1	1
10_10-30	0,4066	1,656	1,08	0,0518	1,261	2,893	5,458	0,6539	1,797	2,08	4,105	2,767	3,494	0,8637	2,572	0,5024		1	1	1	0,9731	0,9966	0,04317	1	1
10_10-60	0,5167	1,766	1,19	0,1619	1,371	3,003	5,568	0,764	1,687	2,19	4,215	2,877	3,604	0,9738	2,682	0,6125	0,1101		1	1	0,9834	0,9983	0,03433	1	1
10_10-90	0,8508	0,3988	0,1774	1,206	0,003885	1,636	4,201	0,6034	3,055	0,8223	2,848	1,51	2,236	0,3937	1,314	0,755	1,257	1,367		1	0,5074	0,7168	0,3616	0,9946	0,9976
10_20-30	0,6371	0,6125	0,03626	0,9919	0,2176	1,849	4,414	0,3898	2,841	1,036	3,061	1,724	2,45	0,18	1,528	0,5413	1,044	1,154	0,2137		0,6189	0,8122	0,2714	0,9986	0,9995
10_20-60	3,039	4,289	3,713	2,684	3,894	5,526	8,091	3,287	0,8352	4,712	6,738	5,4	6,126	3,496	5,204	3,135	2,633	2,523	3,89	3,676		1	5,78E-05	1	0,9999
10_20-90	2,631	3,881	3,305	2,277	3,486	5,118	7,683	2,879	0,4273	4,304	6,33	4,992	5,718	3,088	4,796	2,727	2,225	2,115	3,482	3,268	0,4079		0,0001809	1	1
10_30-30	5,037	3,788	4,364	5,392	4,183	2,551	0,01424	4,79	7,241	3,364	1,339	2,677	1,95	4,58	2,872	4,942	5,444	5,554	4,187	4,4	8,077	7,669		0,004003	0,005512
10_30-60	1,452	2,701	2,125	1,097	2,306	3,938	6,503	1,699	0,7524	3,125	5,15	3,812	4,539	1,909	3,617	1,547	1,045	0,935	2,302	2,089	1,588	1,18	6,489		1
10_30-90	1,321	2,57	1,994	0,966	2,176	3,807	6,372	1,568	0,8832	2,994	5,019	3,682	4,408	1,778	3,486	1,417	0,9142	0,8042	2,172	1,958	1,718	1,31	6,358	0,1308	

Legend: First number: Polymer concentration (6 or 10) _ Second number: Si NPs concentration (0, 10, 20, 30) – Third number: Time (30, 60, 90).

Red color: Water contact angles that presents significantly difference.